



LSA: LARGE SOUTHERN ARRAY

Combined Report
April 1997

An
IRAM-ESO-OSO-NFRA
Study Project

Table of Contents

Introduction	1
A Large Millimeter Array with 10000 m² Collecting Area	3
<i>D. Downes</i>	
Millimeter versus Sub-mm Arrays	12
<i>S. Guilloteau</i>	
System Temperatures and Design Parameters	18
<i>S. Guilloteau</i>	
Site Testing for the LSA Project	22
<i>A. Otárola, G. Delgado, L-Å. Nyman, D. Hofstadt, P. Shaver, R. Booth</i>	
Site Selection: Global Characteristics Concerning the Atacama Area	29
<i>M. Sarazin</i>	
Site selection: Summary of Problems Encountered in Working at High Altitudes	36
<i>R. Roach</i>	
Phase Calibration Strategies	39
<i>Edited by S. Guilloteau with inputs from the IRAM staff</i>	
LSA Telescopes	44
<i>D. Plathner</i>	
Millimetre Receiver Technology for a Large Array	61
<i>J.W. Lamb</i>	

Receivers for the LSA	70
<i>B. Lazareff</i>	
Transmission of Interferometer Signals in the Future	76
<i>M. Torres</i>	
Correlator Developments for (Sub)Millimeter Telescopes	78
<i>A. van Ardenne, A. Bos</i>	
LSA-Correlator Study: Starting Point for a Dedicated Workprogram	85
<i>A. van Ardenne, A. Bos</i>	

Introduction: A European Study Project for a Southern Millimetre Array

1 Background

Since 1991 European astronomers have been discussing a large millimetre-wavelength array for the southern hemisphere, the “large Southern Array” or LSA. This instrument will be a true ‘next generation’ millimetre telescope, capable of opening up new directions in millimetre science as well as extending the exciting recent developments in the field. It will have very high sensitivity (an order of magnitude improvement in sensitivity over today’s major instruments) and angular resolution (0.1 arcsec at a wavelength of 3 mm). In terms of both performance and science drivers, the LSA is seen as a millimetre counterpart to both the VLT and HST.

In order to refine this concept, to explore possible sites and to investigate the technology required, the Institute de Radio Astronomie Millimétrique (IRAM), the European Southern Observatory (ESO), the Onsala Space Observatory (OSO) and the Netherlands Foundation for Research in Astronomy (NFRA) agreed to pool their resources in a joint European study. A Memorandum of Understanding was signed in April 1995, with the goal of producing a report within two years which could be discussed by the community and serve as the basis for further studies.

A document outlining the LSA concept and scientific objectives was produced in October 1995 (“LSA: Large Southern Array”; ed. D. Downes). A workshop was held in December 1995 to discuss the wide range of science that the LSA would make possible, and the proceedings of that workshop were published in 1996 (“Science with Large Millimetre Arrays”, ESO Astrophysics Symposia, Springer; ed. P. Shaver). Several meetings of the Study Project were held, with participation from astronomers and engineers from a variety of countries and institutes, listed below. Here we present the Combined Report, which summarizes the status of several individual technical studies.

2 Current Status

The current concept of the LSA is basically that proposed in the October 1995 document: high sensitivity, to be achieved through a collecting area of 10,000 m², requiring some 50 × 16m or 100 × 11m antennas; high angular resolution (0.1 arcsec at 3 mm), requiring baselines of 10 km; and a high quality site, above 3,000 m in the Atacama desert. The reports by Downes and Guilloteau provide arguments for placing emphasis on millimetre wavelengths. The LSA workshop clearly demonstrated that a very wide range of exciting science would be possible with such an array, and the main science drivers would include the origins of galaxies, stars, and planets.

Several apparently excellent, accessible sites have been identified in the Chilean Andes, in particular a site near Pampa San Eulogio, at an altitude of nearly 3800 m (see the report by Otarola *et al.*). This should be an excellent choice both scientifically and logistically, and site monitoring measurements are underway. The site study team has also used its local knowledge to help the Japanese and US projects with their site work, and all three groups are collaborating closely and sharing data.

Technical studies have included key items like antennas, receivers and correlators. For the main frequency range of the LSA, today's state of the art receivers are almost as good as is possible, although they do require SIS technology which involves 3K coolers. Nevertheless reliable cryostats are available as well. The antenna study by D. Plathner is very encouraging; more detailed studies (including industrial) are now required. More work is required to fully specify the correlator concept but there is agreement that a 60 station correlator is feasible - again an industrial study is appropriate. Finally, phase compensation studies at IRAM have given promising results on a method to calibrate the array based on continuum measurements at 1.3 mm. In all areas it appears likely that the required technology will be available.

3 Future Development

This report gives the results of a two year study, conducted with very limited funds. The next phase of study and design work will require an increased level of support. At the same time, organizational issues must now be addressed in order to fully define the project. If these steps can be taken soon, it should be possible to realize the LSA within the next decade.

M. Grewing, IRAM
P. Shaver, ESO
R. Booth, OSO (chair)
H. Butcher, NFRA

Participants in LSA Study Project meetings and activities include the following: T. Andersen (ESO Garching), P. Andreani (Univ. di Padova), L. Bååth (Halmstad Univ.), A. Bos (NFRA, Dwingeloo), L. Bronfman (Univ. de Chile, Santiago), G. Delgado (SEST, La Silla), P. Dewdney (DRAO, Penticton), D. Downes (IRAM, Grenoble), P. Encrenaz (Obs. de Paris), S. Guilloteau (IRAM, Grenoble), R. Hills (MRAO, Cambridge), D. Hofstadt (ESO, Santiago), F. Israel (Leiden Obs.), J. Lamb (IRAM and Caltech), K. Menten (MPIfR, Bonn), L.-A. Nyman (SEST, La Silla), A. Otárola (ESO, Chile), D. Plathner (IRAM, Grenoble), R. Roach (CMRC, Copenhagen), M. Sarazin (ESO, Garching), G. Tofani (Oss. di Arcetri, Florence), M. Torres (IRAM, Grenoble), A. van Ardenne (NFRA Dwingeloo), E. van Dishoeck (Leiden Obs.), F. Viallefond (Obs. de Paris), R. Wielebinski (MPIfR, Bonn), J. Whiteoak (ATNF, Narrabri), C. Wilson (McMaster, Canada), T. Wilson (MPIfR, Bonn)

A Large Millimeter Array with 10000 m² Collecting Area

D. Downes

Institut de Radio Astronomie Millimétrique, Grenoble, France

Abstract

The Large Millimeter Array should have a collecting area of 10000 m², a resolution of 0.1'' at 3 mm, and at least 1000 simultaneous baselines. The aim is to have a collecting area and resolution 10 times better than available so far. This new mm array should be on a site above 3000 m that allows 10 km baselines. Design goals should be reliability, robustness, and simplicity. Combinations that would give a 10000 m² area would be 50 × 16 m or 100 × 11 m dishes.

1 Introduction: Millimeter vs. Sub-Millimeter

To avoid confusion, we should specify right at the start that these specifications are for a **millimeter** array, not a sub-millimeter array. We wish to have antennas that are nearly perfect up to 345 GHz (0.87 mm), but we allow the efficiency to degrade at higher frequencies.

The reasons for this are as follows:

- The two regimes are different, in respect to atmospheric transparency, altitude required, phase fluctuations, maximum usable baselines, field of view and consequences for the size of antennas, precision required for pointing, focus control, antenna surface accuracy, and beam optics. All of these factors make big differences in the total cost. It is probably cheaper in the long run to build two separate instruments for the two regimes than to try to make one instrument do everything.
- Experience in other bands shows that the best quality is obtained when an instrument is dedicated to working in a limited range rather than trying to cover everything. The world's best infrared telescopes, the IRTF and the UKIRT, are dedicated to mid-infrared observing, and do not try to do optical observing as well. This is because the IR has different requirements than the optical, and both the IRTF and the UKIRT are especially designed for those requirements (very small subreflectors to minimize thermal radiation, very fast chopping, highly accurate pointing and tracking because there are often no guide stars, very massive mounts, refrigerated primaries, etc.)
- One of the daunting challenges in designing a large millimeter array is the spectral-line system. It already seems clear that with the large number of baselines, it will not

Table 1: 10-Sigma Sensitivity at 230 GHz in 1^{hr} with $T_{\text{sys}} = 100$ K and Area = 10^4 m².

max. baseline	230 GHz beam	Galactic		Extragalactic		Continuum 10 σ at $\delta\nu$ = 2 GHz
		resolution at 10 kpc	10 σ at $\delta\nu$ = 2 km/s	resolution at 10 Mpc	10 σ at $\delta\nu$ = 20 km/s	
0.3 km	1''	$5.0 \cdot 10^{-2}$ pc	0.1 K	50 pc	0.04 K	0.2 mJy
1.0 km	0.3''	$1.5 \cdot 10^{-2}$ pc	1 K	15 pc	0.4 K	0.2 mJy
3.0 km	0.1''	$5.0 \cdot 10^{-3}$ pc	10 K	5 pc	4 K	0.2 mJy
10. km	0.03''	$1.5 \cdot 10^{-3}$ pc	100 K	1.5 pc	40 K	0.2 mJy

be possible to observe all frequencies simultaneously. That is, it will not be possible to cover the sub-mm bands simultaneously with all the mm bands. In this respect, it will be quite inefficient to try to combine a sub-mm array and a mm-array in one and the same instrument.

– Because of the factor of ten difference in wavelength, and hence in phase errors, the “long baselines” for sub-mm astronomy will actually be the “short baselines” for mm astronomy. The best time of year to do sub-mm astronomy will be the winter. But this will also be the best time of year to do the really long baselines for mm astronomy. It will be operationally very inefficient, if not impossible, to re-configure the array from the extended configuration for mm astronomy to the compact configuration for sub-mm astronomy in a short time. This will guarantee fights for priority and will waste the best time of the year.

These overriding operational considerations mean it would be better to design two separate, dedicated instruments, one mainly for sub-mm, and one mainly for millimeter – just like the dedicated telescopes for the mid-IR and the visible ranges.

Because we know there are thousands of sources to study in the millimeter range, and because the signals are strong, because we know the project is feasible, and because there are not any working sub-mm arrays yet, we have chosen to start with the millimeter array first. Depending on the success or lack of success of the Smithsonian sub-mm array on Mauna Kea, and the funding of the MMA project at a 5000-m altitude site in Chile, we may or may not propose our own dedicated sub-mm array at a later date.

For the time being, we are concentrating on the millimeter array. Perhaps to avoid confusion, we should even re-name our project the LMA – Large Millimeter Array. This makes it clear what we are working on, and it does not have any conflict with the US or Japanese project names.

The rest of these specifications are for this millimeter array.

2 Sensitivity Goals at 230 GHz

A feasible goal for a 21st century array is a collecting area of 10000 m². The resolution, now $\sim 1''$ with existing mm interferometers, should also be improved by a factor of 10, which implies baselines of 5 to 10 km. The interrelated goals of collecting area, sensitivity, and resolution could be attained with an array of 50 \times 16 m antennas, or 100 \times 11 m antennas.

The brightness temperature sensitivity of a large array varies as

$$\Delta T_b \propto \frac{\lambda^{2.5} T_{\text{sys}} B_{\text{max}}^2}{n D^2 (t \Delta V)^{0.5}} \quad (1)$$

where λ is wavelength, T_{sys} is system temperature, B_{max} is maximum baseline, n is number of dishes, D is their diameter, t is integration time, and ΔV is velocity resolution. Expected sensitivities of the LMA are summarized in Table 1. There is very interesting science to be done with sub-arcsecond beams, but because maximum usable baseline is related to collecting area, this science can only become accessible if a new large mm array has a collecting area of $\sim 10000 \text{ m}^2$.

3 Characteristics of a Next-Generation MM Array

To make a major impact in astrophysics, the interferometer must have:

- **A capability to open up new fields of science.** An obvious domain is cosmology and the epoch of galaxy formation. A powerful array such as proposed here will also revolutionize research on protoplanetary disks around nearby stars, the formation of protostars, the structure and chemistry of circumstellar envelopes, and molecular gas in nearby galaxies.
- **For research on star formation and evolution, a capability to see across the Galaxy** all the objects — outflows, young stars, old stars, molecular clouds — that we now study in detail at 1 kpc distance.
- **For research on galaxy evolution, a capability to see across the universe,** i.e., enough sensitivity and resolution to detect dust and gas in galaxies at $z > 2$. These criteria imply a factor of 10 improvement over present telescopes. This is feasible with current technology, and can be achieved with:
 - **An angular resolution of $0.1''$ at a wavelength of 3 mm.** An important requirement for early universe studies is angular resolution. To study objects at $z > 2$, we need $0.1''$ resolution at 3 mm and $0.05''$ at 1.3 mm. This implies baselines of 5 to 10 km. For a given system temperature, the noise in Jy is the same on all baselines, but the noise in brightness temperature varies as baseline squared (eq.1). This noise can rapidly dominate the signal, which is limited to a few tens of K by the emission physics. Thus we cannot use long baselines (10 km) unless we have plenty of sensitivity. Most mm astronomy is spectroscopy, with bandwidths governed by the linewidths, not the receivers. Furthermore, in some of the mm windows, receiver performance is close to the atmospheric noise limits. *So for much of the spectral line research, the only way to increase sensitivity is to increase the collecting area.* In particular, we can only reach angular resolutions of $\leq 0.1''$ for thermal lines if we increase the collecting area by an order of magnitude over current values.
- **A collecting area of 10000 m^2 .** The 1000 m^2 area of present mm telescopes allows us to detect some high- z galaxies, but only gas-rich and gravitationally-lensed galaxies like IRAS F10214+4724 and H1413+117 at $z = 2.5$. What is needed for further advances at high z is the next factor of 10 step in collecting area. In mm astronomy we've gone from

the 10 m class to the 30–45 m class, but must now take the next step — another factor of ten in collecting area, to a mm telescope with the same collecting area as the VLA, about 10000 m², equivalent to ten times the IRAM interferometer. The requirements of a factor of ten increase in collecting area and a site with enough room to exploit the sensitivity and give 0.1'' resolution imply:

- **Many antennas:** 10000 m² = 50 × 16 m dishes, or 100 × 11 m dishes.
- **A large number of baselines** (≥ 1000) for high-quality, fast images.
- **A site with 10 × 10 km** of flat terrain above an altitude of 3000 m in a dry climate.

Field of View: If the antennas are 16 m dishes, their field of view at 3 mm will be about 50'', which is sometimes felt to be too small for the type of interferometry done in the 1980's and 1990's. These considerations will be less important in 2010 to 2040, when scientific interest will have shifted to objects at greater distances or more compact than those studied today. Relevant points will be:

- For studies of faint, distant, and compact objects for which we want 0.1'' beams, **calibration** will be crucial. This includes the per-baseline sensitivity on calibrator sources, the number of usable calibrator sources on the sky, their separation from the source being observed, and the number of objects on which self-calibration can be used. Calibration is easier with large (16 m) dishes, and for a 21st-century array, may outweigh considerations about field of view.
- High z source sizes will be a few arcsec or less. The fields of view provided by 16 m dishes will be more than adequate.
- The ratio of field of view to beamsize will be greatly improved over present day mm arrays. The field of view of 16 m dishes will be more than adequate for most projects. With the long baselines made possible by a big collecting area, the ratio of field of view to resolution (baseline to dish size) will be the same as in cm astronomy: a 0.1'' beam in a 55'' field of view means 300,000 beam areas per field of view, not the present 750 beam areas with 2'' beams.
- Mosaicing is now a standard technique of mm arrays and ongoing improvements to the software have made wide-field mapping rather routine.
- If needed, field of view could also be increased by use of multi-beam receivers. In the electronics, there might be a choice between simultaneous multi-frequencies at a single position, or simultaneous multi-fields at a single frequency.

A Zero-Order Cost Estimate: For a collecting area of 10000 m², we adopt a model array of 50 × 16 m dishes and assume costs can be scaled to those of current IRAM dishes. The 1995 price of 4M Ecu per IRAM dish includes the cost of a built-in transporter for each antenna; it would be lower if the dishes were fixed or moved by an independent transporter. Based on the experience with the 6 antennas built by IRAM, we expect a 25% cost reduction due to a simplified design, and another 20% reduction for a large production run like 50 × 16 m. To benefit from such economies of scale, we must obtain approval for the whole project, rather than partial funding for the array at widely-spaced epochs. We also extrapolated from IRAM receiver costs and the per-baseline cost of correlators and

IFs. We estimated costs of control and assembly buildings on site and a headquarters in a city, to obtain the following investment costs (in M Ecu): 150 for antennas, 75 for electronics, 18 for infrastructure, 2.5 for management, 24.5 for contingency, all for a total of 270 M Ecu (1995). Experience suggests a new large mm array will need a staff of 150. The laboratory for computer, receiver and electronic engineers should be within 2 hours' drive of the site. There should be ≥ 20 people on-site on work days. If the array were in northern Chile, most of the staff's families might live in Santiago, and personnel might fly in for weekly shifts at the observatory. A staff of 150 means an operating budget of ≥ 30 M Ecu/yr (1995), depending on the site. In sum, the project will approach the cost of the VLT or a scientific satellite. The investment cost is 0.1 Space Telescope, and the running cost will be less than 5%/yr of the Space Telescope running costs.

4 Design Study

Many tasks of the design phase could be done by a consortium of existing institutes. The study could use the IRAM array to test new correlators, IF systems, and one or more prototype antennas. One of the most difficult tasks will be the IF processing and phase tracking system, which defines interfaces for receivers and correlators, and hence requires excellent coordination.

Antennas: To minimize repairs and maintenance on a spread-out, remote site, a design goal should be reliability of all components. The dishes should be simple and robust, and able to keep their mm-quality surface without any active corrections. The goal should be to have strong antennas which can survive in the outdoors, without astrodomes, and without active optics. The design study should consider a low-maintenance, fault-tolerant antenna with a minimum of serviceable parts; possibly no receiver cabin; receivers in a compact, plug-in, cryogenic module instead; new antenna mounts; simpler designs; a robust reflector, possibly without an enclosed back structure; a subreflector support that is stable under wind gusts and thermal changes; a minimum number of parts to assemble; and improved pointing accuracy and pointing stability. Because of the small beamwidths at mm wavelengths, strong efforts should be made to improve pointing and focussing accuracy. Thermal effects dominate the precision of pointing and focussing. The study should be aimed at keeping pointing precision and focus stability even when part of the antenna structure is in sunlight, and part in shadow. The dishes should be heavy enough to keep their pointing accuracy in winds up to 20 m/s. **The telescope pointing deserves strong engineering efforts.** It may be desirable, in the late 1990's, to try out one or more prototypes of improved antennas with the IRAM array before starting a production run for a next-generation mm array. These prototypes might then be re-integrated into the new instrument when it is built.

Receivers should be designed to be tunerless, maintenance-free, have a minimum of moving parts, and require no helium filling. Operation on a remote, spread-out site will require upgrades in current receivers to maximize robustness and reliability and minimize maintenance. The receiver box must hold ≥ 6 different mixers, as observing in several frequency bands simultaneously would give higher scientific throughput and better capability to correct for atmospheric phase variations. The design study must evaluate the impact

on sensitivity of simultaneous frequency operation, given the additional optics required and the difference in the primary beams. Closed-cycle cryo-generators for the receivers must be maintenance-free for long periods, and possibly installable in modular form. The modular concept must be evaluated relative to other designs optimized for system noise. Work on higher-temperature superconducting junctions would be of great interest, especially if these components make cryo-generators cheaper and easier to maintain. Testing of prototypes is needed to see whether SIS receivers can be replaced by HEMT receivers, at least at 3 mm.

IF stages need further development to cover large bandwidths, i.e., several GHz for simultaneous observing at different frequencies. Larger IF bandwidths than those used at present are needed to increase spectral-line observing efficiency and continuum sensitivity. Bandwidth requirements are particularly demanding for extragalactic observing at 1.3 mm. Detailed work is needed on optical fiber transport of the IF signals and the L.O. phase reference. Cost comparisons are needed for transport of digital vs. analog signals by optical fibers. Study and prototype testing is needed for development of integrated IF filters and low-cost LO systems. Phase stability of the electronics is a challenge. Over 1 to 100 second intervals, the electrical length variations over 10 km baselines must be kept to less than $10 \mu\text{m}$, or equivalently the timing precision must be better than 0.04 picoseconds per 1 - 100 sec interval for operation at 300 GHz. Even more stringent accuracy is needed if sub-mm operation is planned.

Correlators must be developed to cover broad bandwidths and to work for long periods without chip failures. Engineers should consider dedicated broad and narrow-band correlators, possibly of different types. A broad band correlator might cover 2 to 8 GHz at 5 to 10 MHz resolution for continuum and extra-galactic work, and a narrow band correlator might have ten windows each 10 to 160 MHz wide, at 50 kHz to 1 MHz resolution, for lines in Galactic sources or in nearer, strong-line galaxies. Ultra-fast samplers must be developed and tested to evaluate the technological possibilities and reliability of ultra-fast chips vs. many units of slower chips. Work must be done on the control of timing for mm array electronics over several kilometers. Is it possible to make the phase switching that separates the sidebands an option, depending on whether the dominant noise is instrumental or atmospheric?

Software needs a large effort, to develop the ability to handle multi-frequency spectral-line operation on ≥ 1000 baselines. Data cubes will be much larger than those produced by mm arrays so far, or by the VLA. Because of the long baselines, the array will operate partly in a multi-speckle regime, and new software strategies may be needed to overcome atmospheric fluctuations.

Phase Correction: A critical development will be a method to correct interferometer phases for atmospheric fluctuations. This development will have implications for site selection, frequency coverage, computing needs, mode of operation, baseline lengths, and array configurations. At cm wavelengths, the signal-to-noise ratio permits many VLA programs to use self-calibration and correct for instrumental and atmospheric phase errors. A similar procedure is used in the modeling and global fringe fitting in VLBI. To do this, the signal to noise ratio must be > 3 in integration times of a few seconds. However, most sources of interest for mm interferometry are weak, thermal sources, requiring coherent

integration times of many hours ! If there are no corrections to the phase fluctuations, the atmospheric seeing limit for mm interferometers is about $0.5''$, independent of frequency. Hence the maximum usable baseline, without phase corrections, would be about 450 m at 3 mm, to within a factor of two. One way to correct the phase is to use the variations of sky brightness temperature, which are proportional to the water vapor variations within a primary beam. This method requires receivers stable to one part in 10^5 . Current IRAM results show a radiative correction method does indeed work in clear sky conditions. Whatever the method finally adopted, large dishes, e.g., 16 m dishes instead of 8 m dishes, are important to increase the signal-to-noise ratio per baseline, and to maximize the number of sources usable for self-calibration. *A workable method of phase correction will be essential before a large new mm array can be built.* We intend to refine this method with the IRAM array in the coming years.

Interferometer Configuration: The antennas might be in a ring or in a Gaussian random pattern, so natural weighting would yield a gaussian beam with low sidelobes. Some ideas on configurations to optimize the u, v coverage are given by Cornwell (1987, 1988) and Keto (1992). Servicing might be done with an elevator platform on a truck. This solution must be weighed against the ease of assembling antennas in a hall, and bringing them back for maintenance and upgrades. However, for ≥ 50 dishes, it may be better to build antennas in the open air. It would be feasible to construct 10 dishes per year. One could imagine two work crews, with one crane, with each team finishing a dish every two months. A separate team would do cabling and equip the dishes with a receiver package. With such an assembly, the configuration needs careful thought so the new array can start working progressively. Since construction will extend over several years, it would be good to start doing science as soon as 10 dishes are on site, and then exploit the full instrument several years later when all antennas are operating. The first 10 dishes would operate with a maximum baseline ≤ 1 km. The next 10 dishes could then be used of baselines twice as long as the first group, and so on, up to the final group of 10 antennas allowing the longest baselines. In this schedule, there might be 30 antennas within a core ~ 1 km in diameter. This 1-km core might contain half the total collecting area and form a sensitive compact array for initial detections without serious phase problems. The best telescopes, with the best panels from a large production run, might all be put in the inner compact group for observing at 345 GHz or in the sub-mm windows, while the outer antennas might be mainly used for 3 and 1.3 mm. While construction of the complete array might take 5 years, some observing might be able to start after the first year of assembly. When could such a mm array enter into full operation? For large facilities like the VLA, IRAM, and the VLT, the time from initial designs to initial operation was 10 to 20 years, So if serious planning starts in 1997, a large new mm array could be in a productive phase around 2010.

5 Conclusions

- The LSA, a Large Southern millimeter Array with a collecting area of 10000m^2 , ten times greater than available at present, would open new directions in astrophysics and greatly enhance the rich harvest of results already obtained from this unique part of the electromagnetic spectrum.

- The mm array could consist of 50×16 m dishes or 100×11 m dishes with pointing accuracy $1''$ r.m.s., above 3000 m altitude on a site allowing baselines of 5 to 10 km. With the larger dishes, The global surface accuracy might be $50 \mu\text{m}$ r.m.s. with the larger dishes or $25 \mu\text{m}$ with the smaller dishes. The goal is to synthesize a $0.1''$ beam at 3 mm.

- Receivers should cover, in first priority, **the 3 mm and 1.3 mm windows**. These are likely to be the two windows where most of the science will be done. It would also be desirable to equip the antennas in the other mm windows (2 mm, 7 mm, and 0.8 mm), and depending on the site chosen and the dish surface accuracy, possibly the sub-mm windows as well.

- The main requirements could be met with existing technology, but to optimize this technology and minimize operating costs, design studies are needed:

- For the antennas: low production costs; robust, open-air antennas that can be assembled easily, and that need minimal maintenance. For antennas up to 16 m diameter, operating in the mm ranges, **the surface accuracy is not the problem. The problem is the pointing accuracy.** The antenna structures must be thermally stable, giving good pointing and focus stability, even when part of the structure is shadowed.

- For the receivers: low production costs, robust modules, broad bandwidths, no tuning, no helium filling, with simultaneous multi-frequency operation.

- For the IF system: broad-band IFs, fiber optic transport of analog or digital IF signals and local oscillator phase reference, analog or digital delay lines; excellent instrumental phase stability.

- For the correlators: broad-bandwidths; low chip failure rates; ultra-fast samplers, evaluate ultra-fast chips vs. many units with slower chips; evaluate the need for separate correlators for continuum and spectroscopy.

- Investment and operating costs would be ~ 270 M Ecu (1995) and 30 M Ecu/yr, respectively. A staff of ~ 150 persons would be needed. On the likely sites, staff may have to be flown in weekly from a large city.

- Incorporation of one or more prototype antennas in the IRAM array would be an important intermediate step before starting large-scale industrial production for a new large mm array. This would allow testing of new antenna and receiver technology, help to develop methods to correct for atmospheric phase fluctuations, and would be scientifically rewarding as well.

Finally, we emphasize how this proposal differs from other programs to extend the existing mm arrays of BIMA, OVRO, NRO, or IRAM, or to build new arrays such as the Smithsonian sub-mm array, the MMA proposed by NRAO, or the large mm/sub-mm array proposed by Nobeyama: **The main point is the huge collecting area.** The aim is to achieve the maximum feasible sensitivity and resolution, and to concentrate on compact mm sources, rather than extended ones. Two scientific domains in which this telescope will excel will be detection of gas and dust in galaxies at high redshifts and the detection of accretion disks and proto-planetary disks around young stellar objects in our Galaxy.

The second point is the wavelength range. We put our highest priority on a **millimeter** interferometer, that will operate mainly at 3 mm and 1.3 mm. While it is difficult to predict discoveries in advance, the relative richness of the different mm windows in molecular lines and the seeing limits on usable baselines both suggest that the scientific productivity will be greatest in the 3 mm and 1.3 mm windows. Although the inner parts of the instrument might have the best antennas, allowing operation to 0.8 mm or even shorter in some seasons, the main goal would be to have access to the rich spectrum of molecular emission in the millimeter ranges. Hence, in contrast to other proposed new arrays, the goal of the Large Southern Array is to attain the collecting area and resolving power needed to explore the universe in the very productive millimeter bands.

Millimeter versus Sub-mm Arrays

S. Guilloteau

Institut de RadioAstronomie Millimétrique, 300 rue de la Piscine,
F-38406 Saint-Martin D'Hères, France

Abstract

I evaluate the relative performance of the mm and sub-mm window from the point of view of the trade-off between sensitivity and angular resolution. Both the spectral line and continuum cases are considered.

These estimates clearly demonstrate that the sub-mm windows provide little advantage over the 200-300 GHz window except under exceptional circumstances, even when a suitable molecular line can be found.

This shows that, although sub-mm interferometers can be justified on a specific scientific argumentation, the 1-1.5 mm window is the best choice for a "general purpose" high angular resolution instrument.

1 Background

It is often believed that high angular resolution is easier at high frequencies, because with antennas of a given size, beam dilution decreases with increasing frequencies. To evaluate the validity of this statement, let us perform a "thought" experiment in which we assume we can observe a given source at an arbitrary frequency between say 10 and 1000 GHz, with an array of antennas of a given (arbitrary) size and surface accuracy. We now ask the following question:

What is the optimum frequency (in terms of sensitivity) for such an observation if we want to reach 1" angular resolution over a given field of view?

The answer depends on four parameters: the effective system temperature of the array, after correction for atmospheric extinction, the antenna efficiencies as a function of frequency, the spectrum of the source, and the field of view.

2 Practical Cases

2.1 Perfect Antennas, Small Field of View

In a first step, let us treat the spectral line case. The source intensity (in terms of flux density) is that of a blackbody multiplied by an opacity factor. Let us assume we can arbitrarily select a suitable spectral line so that this factor is 0.5 (still optically thin, but not too weak) at any frequency. The line flux density of the source goes as ν^2 . However, the effective bandwidth over which we can integrate for a given velocity resolution goes

as ν , since Doppler broadening is the dominant process in most astronomical sources. Accordingly, the effective signal-to-noise in a given time goes as $T_{sys}(\nu) \times \nu^{2.5}$.

Figure 1 illustrates the dependence of signal-to-noise with frequency (using 100 GHz as an arbitrary reference). The system temperatures were computed using the standard atmospheric model ATM from J.Cernicharo and the receiver temperatures were assumed to be 0.1 K per GHz. 3 curves were computed, for 0.5, 1 and 2 mm of precipitable water vapor. These values are close to the Cerro Chajnantor quartiles (0.55, 0.85 and 1.4 mm respectively). The antenna efficiency is assumed to be independent of the frequency.

Under such conditions, Figure 1 shows that the 900 GHz window becomes better than the 1-mm band for water vapor content less than 1.2 mm (or about 60% of the time), and that the 600 GHz window is better than the 1-mm band for water vapor content less than 0.7 mm (about 35% of the time). The 350 and 460 GHz window are only marginally better than the 1-mm window even in the best conditions.

For continuum work, the spectral index can be anything between -1.5 (e.g. quasars) and 4 (dust in galaxies). For continuum data, the bandwidth does no longer depend on frequency, but is set by the correlator. Hence, for sources with spectral index $\simeq 2.5$ (e.g. circumstellar dust disks), Figure 1 can be used directly. Sources with higher spectral index will be preferentially observable at higher frequencies. However, the optically thick regime will be ultimately reached.

2.2 Perfect Antennas, Large Field of View

The above estimates were valid for observation of a single primary beam. If the field to be imaged exceeds the antenna primary beam, the situation changes. Let us treat the case in which mosaicing is required at all frequencies. The number of primary beams to be imaged is then proportional to ν^2 . Hence the integration time for each field goes as ν^{-2} . Accordingly, the effective signal-to-noise goes only as $T_{sys}(\nu) \times \nu^{1.5}$ (for spectral lines). Figure 2 illustrates this case. It can now be seen that even in the best weather conditions, the 1-mm window is the optimum frequency band.

2.3 Good Antennas (but not Perfect), Small Field of View

If we introduce a "realistic" antenna, for example a 25 μm surface accuracy, the high frequency band becomes more difficult. It can be seen from Figure 3 that even in the "small field of view" case, there is no sensitivity gain in going at high frequencies, despite the very good performance assumed for the antennas. On the other hand, below 300 GHz, antennas with 50 μm rms surface accuracy essentially produce the same performances.

2.4 Comparison of two Arrays

Finally, let us compare two different arrays. Array 1 follows the LSA concept, with 50 16-m antennas of surface accuracy 50 μm . Array 2 follows the MMA concept, with 40 8-m antennas of 25 μm surface accuracy. Figure 4 compares their respective sensitivities for a given angular resolution for spectral line observations and field of view limited to the primary beam. This figure clearly demonstrates that the high frequency capability of the proposed MMA does not compensate for the smaller collecting area compared to the LSA concept.

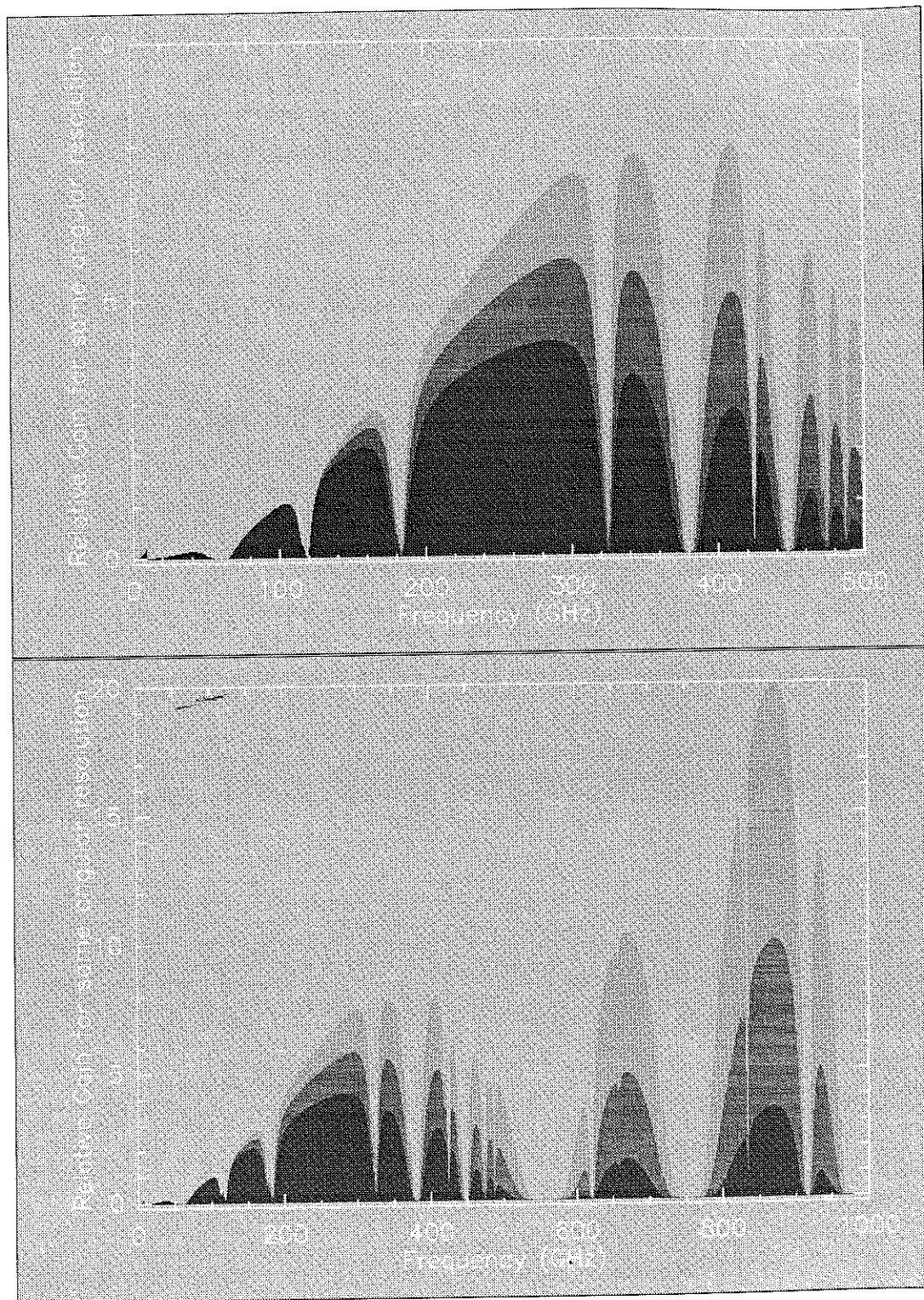


Figure 1: Relative signal-to-noise ratio as function of frequency for a perfect antenna: 10-500 GHz range (top) and 10-1000 GHz range (bottom). The 3 curves are given for 0.5, 1 and 2 mm of H₂O, from lighter to darker

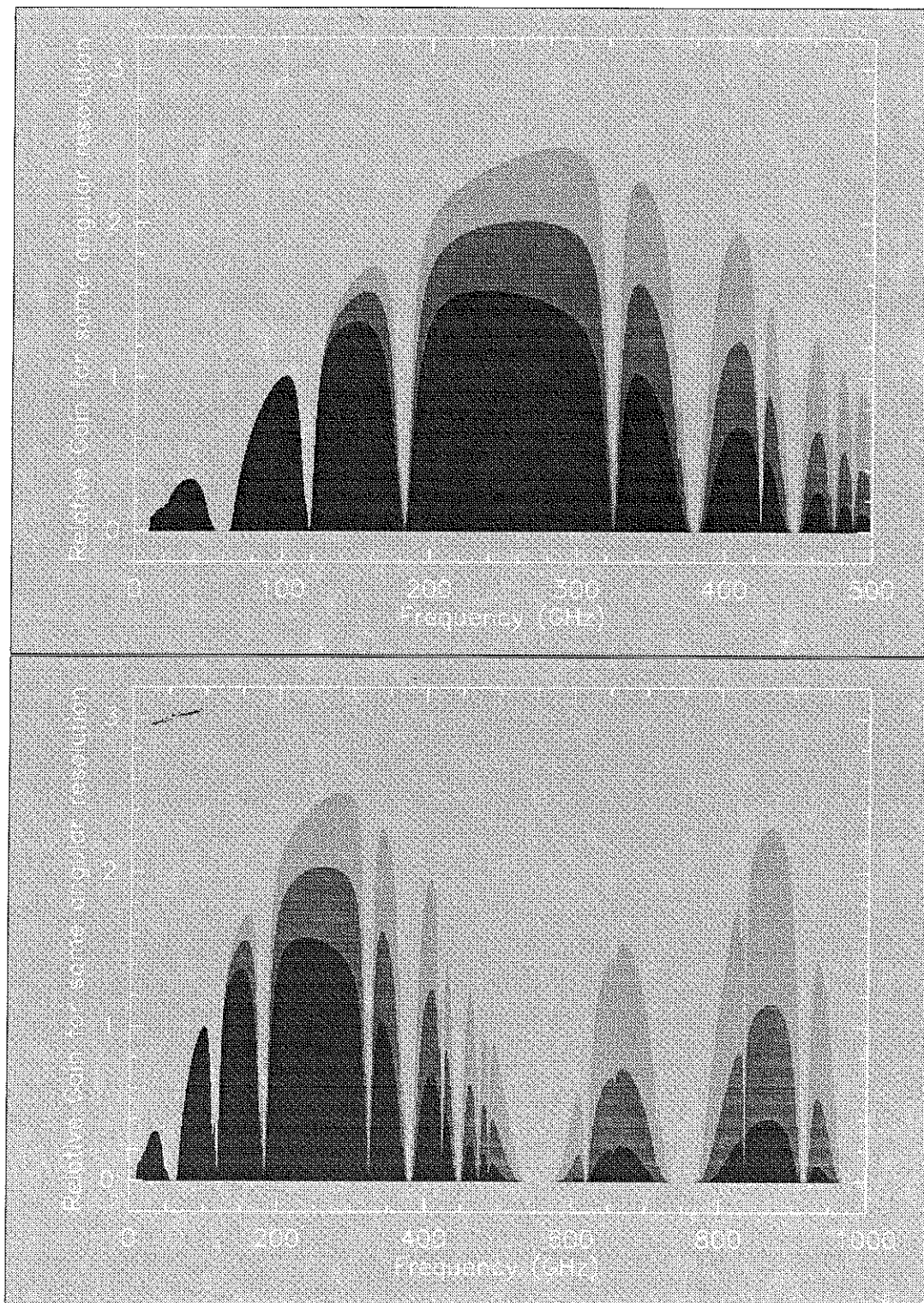


Figure 2: Relative signal-to-noise ratio as function of frequency for the mosaicing case: 10-500 GHz range (top) and 10-1000 GHz range (bottom). The 3 curves are given for 0.5, 1 and 2 mm of H₂O, from lighter to darker

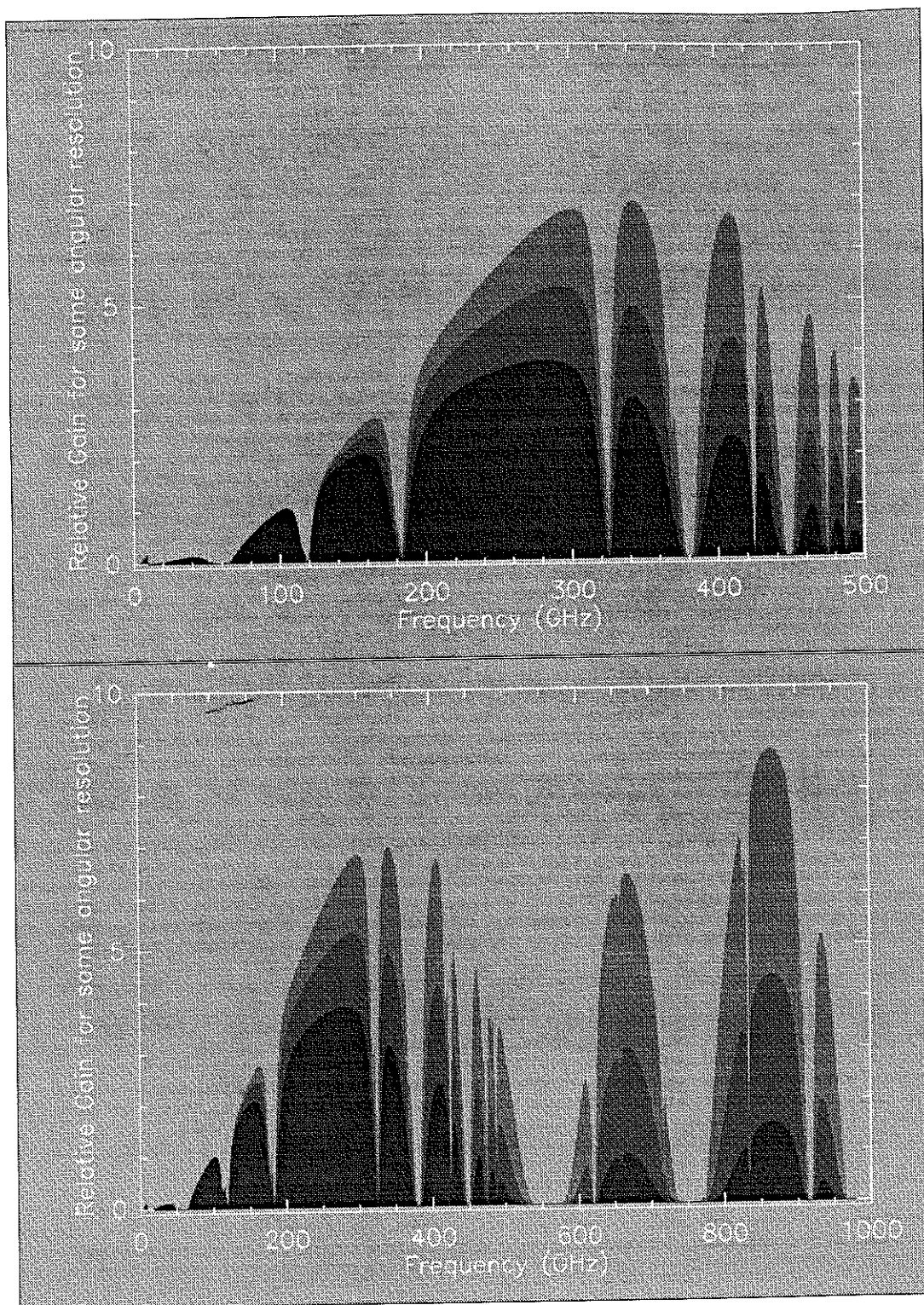


Figure 3: Relative signal-to-noise ratio as function of frequency for a $25 \mu\text{m}$ rms surface accuracy: 10-500 GHz range (top) and 10-1000 GHz range (bottom). The 3 curves are given for 0.5, 1 and 2 mm of H_2O , from lighter to darker

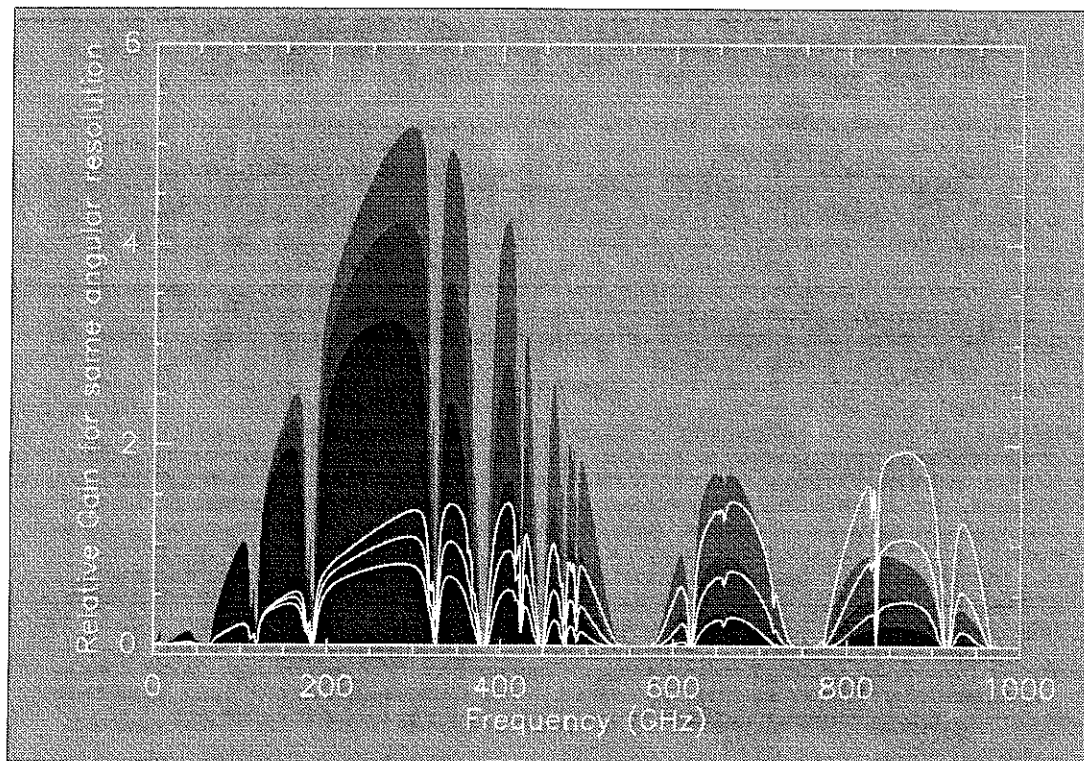


Figure 4: Relative signal-to-noise ratio as function of frequency for the LSA and the MMA. The 3 grey-scaled curves are for the LSA, for 0.5, 1 and 2 mm of H₂O, from lighter to darker. The 3 white curves are for the MMA

3 Conclusion

From a strict point of view of sensitivity for a given angular resolution, the sub-mm window provides no advantage over the 200-300 GHz band, even when using very optimistic figures for the antenna accuracy. Moreover, it is difficult to find suitable “probe” (e.g. molecular line) in the sub-mm range for many astrophysical sources. At low temperatures (e.g. <20 K), only lower excitation lines are accessible.

Accordingly, I conclude that the sub-mm domain cannot be justified on the basis of high angular resolution only. The justification for sub-mm can only reside in specific spectral lines and study of very optically thin “relative high” temperature regions (> 200 K). The 1-mm window is *in essentially all cases* the **best window** for high angular resolution.

Finally, it should be stressed that the good sub-mm windows are the 900 GHz band and to a lesser extent, the 600 GHz band. Obtaining performant antennas for these windows impose to *double* the accuracy specifications: surface precision, tracking and pointing accuracy, focus and nodal point stability. Such a large change in antenna specifications has a considerable impact on the antenna cost.

System Temperatures and Design Parameters

S. Guilloteau

Institut de RadioAstronomie Millimétrique, 300 rue de la Piscine,
F-38406 Saint-Martin D'Hères, France

Abstract

System temperature which can be expected for the LSA are estimated, and the principal limiting factors described. It is shown that for the expected sites, Oxygen absorption alone is the dominant factor below 130 GHz, and water vapor becomes dominant only at higher frequencies. A reasonable extrapolation of the water vapor content from the site survey performed at Cerro Chajnantol (elevation 5500 m) shows that for a 3500 m elevation site, the system temperature is approximately given by $T_{sys} = 15 + 0.25 \times \nu$ for ν between 20 and 300 GHz. Strongly reduced sensitivity occurs near the Oxygen lines (50-70 GHz, 115-121 GHz) and near the 183 GHz line of H₂O. A higher elevation site is not justified if less than 50% of the observing time is spent at frequencies higher than 150 GHz.

These estimate clearly demonstrate that increasing the collecting area is the **only** way to improve the sensitivity for spectral line observations.

1 Background: Atmospheric Opacity

Figure 1 presents the atmospheric opacity of the two major constituents of the atmosphere: O₂ and H₂O. The curves have been computed for parameters relevant to Cerro Chajnantol, where extensive site survey has been performed for the MMA. The opacity distribution measured at 225 GHz during the site survey is consistent with precipitable H₂O content of less than 0.55 mm for 25% of the time, less than 0.85 mm for 50% of the time and less than 1.4 mm for 75% of the time.

An essential point which stands out from Figure 1 is that, for water vapor content around 1mm, the opacity is totally dominated by Oxygen at frequencies below about 130 GHz. Moreover, because of the strong line near 60 GHz, this opacity does not decrease with decreasing frequency as the water vapor contribution.

Assuming the scale height of the water vapor is about 2 km, a site at 3500 m elevation would be expected to have a mean water vapor content of 1.7 mm, with less than 1 mm 25 % of the time. However, it has not yet been demonstrated that a scale height distribution is applicable. Since the general air flow runs West to East over the Chilean Andes, we might expect that the same air layers smoothly drift across the Andes with an almost frozen water vapor content because it hardly ever rains in this area. Accordingly, the above estimate may be pessimistic.

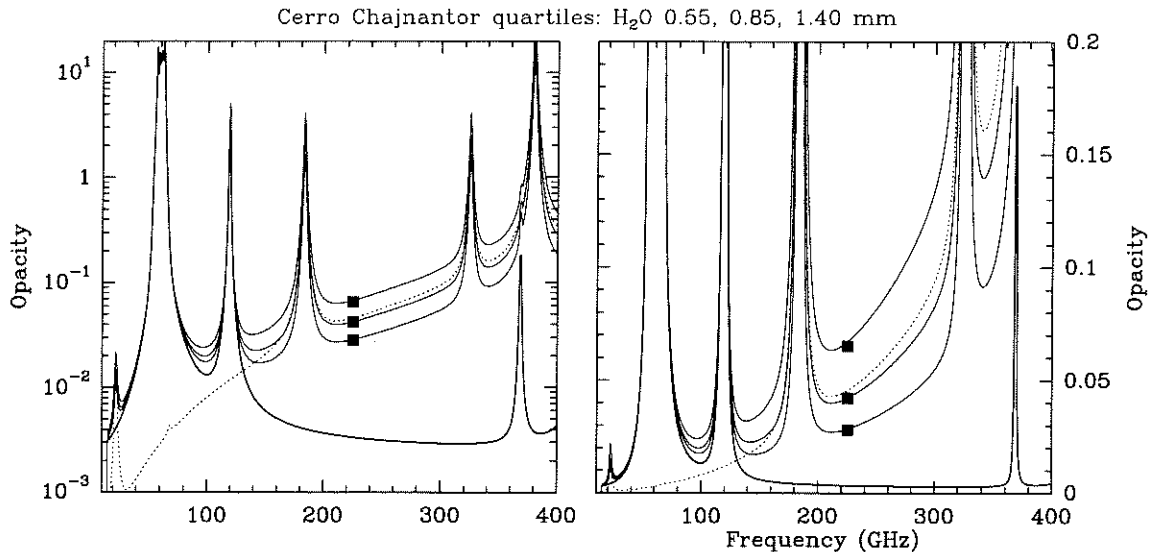


Figure 1: Dotted line: zenith opacity due to 1mm of precipitable water vapor. Thick line: zenith opacity due to O₂ alone at 5500 m altitude. Thin lines: total atmospheric opacity for 0.55, 0.85 and 1.4 mm of precipitable water vapor respectively. The black squares indicate the 25%, 50% and 75% quartiles of *measured* opacities at 225 GHz from a 6 month period of site survey.

2 Estimate of T_{sys} for the LSA

Based on the above derivation, I have studied the influence of various instrumental or environmental parameters on the expected system temperatures. The results are summarized in Figure 2, and the behaviour can be understood as follows. A “standard” curve was computed with the following mean parameter values: local temperature 0°C, site elevation 3500 m, precipitable water 1mm, forward efficiency of the antenna 0.95, receiver temperature $2h\nu/k$, and image sideband rejection by 20 dB. A single parameter has been varied each time. The system temperature is given for SSB observations, as relevant for spectroscopy, and for a source elevation of 45°.

- Dependence on altitude

The amount of precipitable water was fixed to 1mm. The altitude effect is thus essentially due to the pressure difference. It can be seen that this is a relatively minor effect. Significant differences only appear above 320 GHz.
- Dependence on outside temperature

The dependence comes essentially from the emissivity of the lower layers of the atmosphere, and is even weaker than that of the site altitude.
- Precipitable water vapor

Above 130 GHz, the effect is quite significant and a drier site offers a significant advantage in the 1 to 2mm window. However, below 130 GHz, the system temperature becomes practically independent of the water vapor content, provided this content is less than 2mm.

Temperature 0°C, Altitude 3.5 km, H₂O 1 mm
 $F_{\text{eff}} 0.95$, $T_{\text{rec}} 2h\nu/K$, Rejection 20 dB

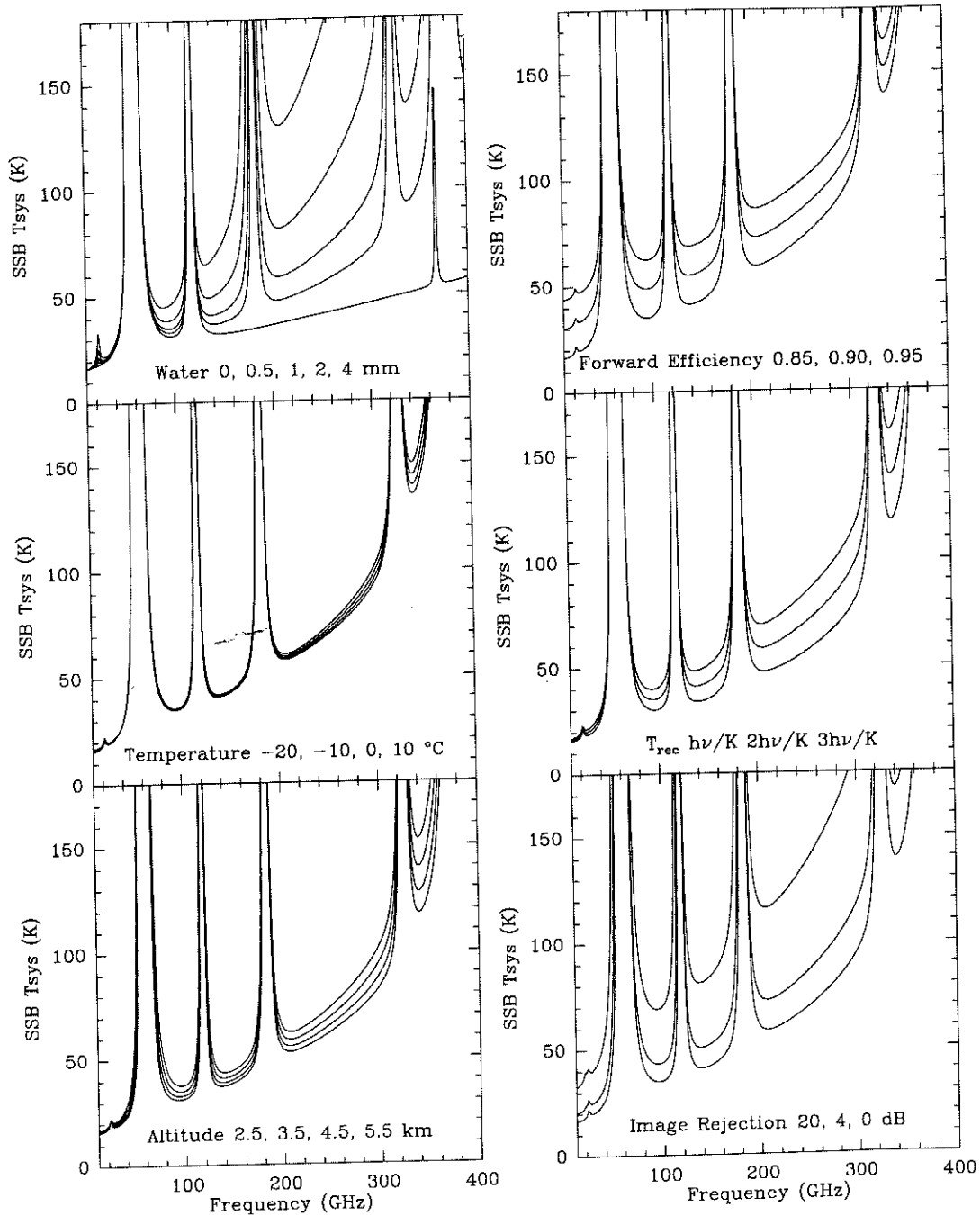


Figure 2: Influence of various parameters on the Single-Sideband system temperature curves as a function of observing frequency. Top left: influence of precipitable water vapor content. Middle left: influence of the outside temperature Bottom left: influence of the site altitude. Top right: influence of the forward efficiency. Middle right: influence of the receiver temperature (including optics). Bottom right: influence of the image rejection.

- Forward efficiency
Minimizing losses is absolutely essential. This must be kept as a major goal in the antenna design.
- Receiver temperature
A goal of $2h\nu/k$ seems realistic. Note that below 120 GHz, the dependence is relatively weak.
- Image rejection
This is essential. The curve was computed for an IF of 1.5 GHz and should be redone for better accuracy. This will in general degrade further the DSB case.

Except in frequency ranges close to some O₂ or H₂O line, the typical T_{sys} obtained for the “mean” set of parameters is well estimated by

$$T_{sys}(K) = 15 + 0.25\nu(\text{GHz}) \quad (1)$$

3 Discussion

From the previous plots, we may conclude the following:

- The altitude brings a sensitivity gain **only if** the water vapor changes.
- Single sideband design of the receivers is essential.
- Antenna losses should be kept to a minimum.
- If the 1.3mm band is to be used less than 50% of the time, there is no need to go to a significantly higher altitude. The higher (and thus presumably drier) sites are only justified for submm observations if our guess of 1mm precipitable water vapor is correct.
- Should there be any emphasize for frequencies close to some oxygen line, such as CO J=1-0, the advantage of the high altitude site is even more limited.

A proper estimate of the mean water vapor content of anticipated sites is required for further progress.

Site Testing for the LSA Project

A. Otárola¹, G. Delgado¹, L-Å. Nyman¹, D. Hofstadt¹, P. Shaver², R. Booth³

¹ European Southern Observatory, Casilla 19001, Santiago 19, Chile

² European Southern Observatory, Karl-Schwarzschild-Str. 2,
D-85748 Garching bei München, Germany

³ Onsala Space Observatory, S-439 92 Onsala, Sweden

Abstract

In this paper we give a description of the present status of the site survey for the LSA project (First Phase), as well as the plan of activities for the installation of the equipment (Second Phase.) A detailed description of the necessary resources in manpower and budget are also included.

1 Introduction

The main goals for the LSA project have been defined in the document "*LSA: Large Southern Array*", compiled by D. Downes [1]:

1. An angular resolution of 0.1" at a wavelength of 3 mm
2. Collecting area of 10.000 m²
3. Frequency range between 43 GHz and 350 GHz
4. Large number of baselines configurations for high quality images and excellent capability for *fast* imaging
5. Flat terrain in a dry climate, preferably near a city or pre-existing infrastructure

These goals define the characteristics of the candidate sites to be monitored:

1. A large flat area allowing baselines up to 10 km
2. High altitude and dry site, preferable above 3.500 m, to guarantee low water vapour content and minimize oxygen opacity
3. Good overall meteorological parameters in order to maximize the throughput of the array
4. Good access to roads and power lines

Based on data gathered in surveys by the Smithsonian Astrophysical Observatory [2] and Nobeyama Radio Observatory [3] indicating that sites on the western slopes of the Andes are very suitable for millimeter wave radio astronomy (together with the fact that the Atacama desert is the driest place on earth), we conducted an exploration of candidate sites for the LSA project in northern Chile. The results of this exploration were summarised in the report *Site Survey for a Large Southern Array* by Otárola *et al* [4].

We selected a site called *Pampa San Eulogio* which is located in the foothills of the Andes Mountain range about 200 km SE from Antofagasta and almost at same latitude as *Cerro Paranal* where ESO's VLT project is being built. *Pampa San Eulogio* is an exceptionally flat area of 20×20 km with an average altitude of 3.750 m. Based on available meteorological data this site should present low precipitable water vapour, in the range of 2 mm, and conditions to achieve a high phase stability for the planned array. The site is located on an area exhibiting an annual precipitation lower than 10 mm (see Fig. 1).

2 Phase 1: Present Status and Achievements to Date in the Site Testing for the LSA Project

In April 1996 the site testing group suggested *Pampa San Eulogio* as the best candidate site for the LSA project, and a global strategy for the site measurements was decided. At the same time a research was conducted to find out the legal status of the land concerning mining rights and ownership of the land surface.

2.1 Preliminary Study of Global Meteorological Conditions

Once the potential site was selected available meteorological data was collected from different sources in the area in order to obtain a first idea of the weather conditions. The data was analyzed, at our request, by Dr. Fuenzalida from the Geophysics Department of *Universidad de Chile* [5]. From his report we show the extrapolated daily cycles of values for wind speed (Fig. 2) and specific (absolute) humidity (Fig. 3), indicating that the site is suitable for the LSA.

2.2 Status of the Site Testing Equipment

The site test equipment on *Pampa San Eulogio* will measure the following parameters:

1. Weather parameters (Temperature, atmospheric pressure, wind direction and speed, sun radiation, relative humidity)
2. Precipitable water vapour content
3. Phase stability

The weather parameters are going to be measured by three autonomous weather stations deployed on the area. These stations have already been purchased and are stored in Antofagasta.

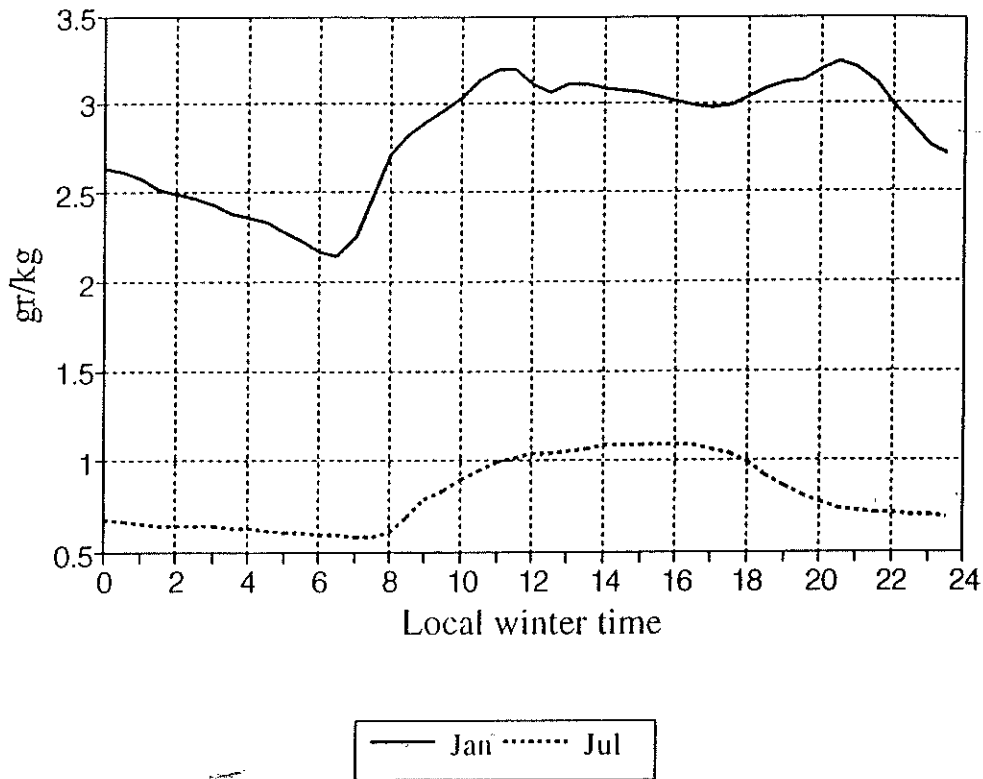


Figure 3: Daily absolute humidity cycle

A container with solar panels will provide power and housing to the computers, radiometer and interferometer. This container is a commercial unit bought in the USA. Right now it is stored in Santiago ready to be moved as soon as the installation phase is started.

Additional techniques for the site survey will be the launching of radiosonde balloons to obtain a vertical profile of the atmosphere to validate models. New techniques including the use of remote sensing satellites in the infrared regime will be explored.

3 Phase 2: Future Site Testing Activities

The highest priority presently is to install the site test equipment on the site, and to start the data collecting phase as soon as possible. This work should take place during the first quarter of 1997.

4 Resources

This section includes information about available and required manpower and funding for the two years period 1997-1998.

4.1 Manpower

Today the site testing team in Chile consists of one fully dedicated ESO staff (A. Otárola) with support from two SEST team members (G. Delgado and L-Å. Nyman). D. Hofstadt, Director of ESO-Chile, acts as the overall coordinator of the Chilean side of the project and conducts most of the contacts with government authorities. Valuable support is provided by M. Sarazin who leads the site testing group of ESO's VLT project. Also the support of ESO staff J. Navarrete has been offered. The presently available staff is considered enough for the next two years of operation.

4.2 Funding

In the following table a breakdown of the necessary funds is presented. These are needed for the next two years of operation of the site test, and some of these funds are already available in the 1997 budget.

Item	Cost [DM]	Comment
Installation of equipment	60.000	Only once
Logistic	5.000	Only once during installation
Contracts	120.000	Radiosonde and IR remote sensing if required
Site operation	35.000	Vehicles and fuel
Manpower	100.000	
Radiometer	75.000	
Travel	63.000	
Miscellaneous	10.000	
Total	468.000	

5 Conclusions

After one year of work of the site survey team, with the allocated budget, we have selected *Pampa San Eulogio* in northern Chile as a good potential site for the LSA project. Most of the equipment is ready to be installed during the first quarter of 1997. Regarding manpower we conclude that the actual availability is enough for the operation during the next two years of survey.

References

- [1] LSA: Large Southern Array, D. Downes Ed., An IRAM-ESO-OSO-NFRA Study Project, 1995
- [2] P. Raffin and A. Kusunoki, Searching for Submm Interferometer Sites in Chile, Submillimeter Array Technical Memorandum, Smithsonian Astrophysical Observatory, 1992

- [3] K. Kono, R. Kawabe, M. Ishiguro, T. Kato, A. Otárola, R. Booth, and L. Bronfman, Preliminary result of Site Testing in Northern Chile with a Portable 220 GHz Radiometer, NRO Technical Report No. 42, 1995
- [4] A. Otárola, G. Delgado, and L. Bååth, Site Survey for a Large Southern Array, Science with Large Millimetre Arrays, P. Shaver Ed., Proceedings of the ESO-IRAM-NFRA-Onsala Workshop, pp. 358-364, 1996 90-2, 1990
- [5] H. Fuenzalida, Preliminary Report: Climate Near Salar de Punta Negra, Internal Report, 1996
- [6] S. Radford, G. Reiland, and B. Shillue, Site Test Interferometer, Publications of the Astronomical Society of the Pacific, pp. 441-445, 1996

Site Selection: Global Characteristics Concerning the Atacama Area

M. Sarazin

European Southern Observatory
Karl-Schwarzschild-Str. 2
D-85748 Garching bei München, Germany

1 Steps Towards Global Retrospective Site Surveys

1.1 Introduction

Among the challenges of traditional site surveys is the long term required for accumulating a consistent database about one given geographical location and the limitations in the surveyed area due to the amount of necessary investment per surveyed site.

It would be ideally more efficient to preselect candidate sites on the basis of a retrospective analysis long enough to reveal climatic trends. However, it is also of interest to extend backwards the database for the LSA site currently under investigation and to assess at the lowest cost its relative merit with respect to neighbouring areas (eg. Argentinian side of the boarder). Finally, the potentialities of global surveys extend beyond the site selection process because they offer a forecast ability which can boost the efficiency of an observing facility operated in the flexible scheduling mode.

Although the Atacama area benefits from a very stable climate, considerable changes took place in the far past ([Grenon 90]). Middle term cycles are also noticeable at ESO observatories with regards to cloud cover as shown on Figure 1. The lower amplitude of the climatic fluctuations above Paranal agree with the initial assumption of a better stability of the Northern Atacama area. Although the global figures did not change compared to 10 years ago, the differential performance shown on Figure 2 shows that a shorter site survey conducted at a non-representative period (1988-1990) would have led to a 50% underestimate of the superiority of Paranal with respect to La Silla.

1.2 Available Database

Databases covering several years are available from radiosoundings, global atmospheric model analyses and satellite images.

Radiosondes are launched twice a day from ground stations (only once a day from Antofagasta) and move horizontally with the wind by several tens of kilometers during ascent, they are thus representative of average conditions over a 100 km area around the launching site.

Global models such as the ECMWF (European Center for Medium Range Forecast) atmospheric model produce routine global analyses for the four main synoptic hours 00,

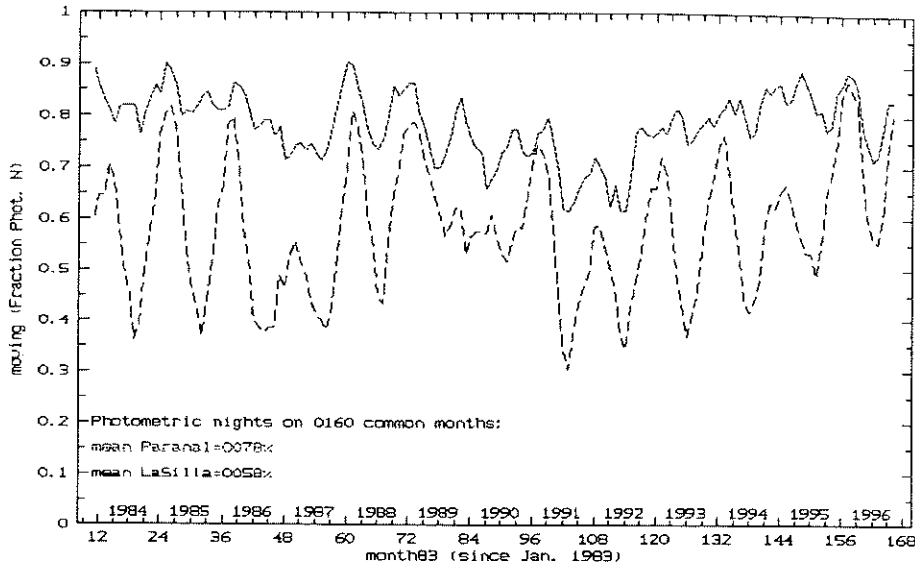


Figure 1: Monthly percentage of photometric nights at Paranal and La Silla (filtered with a 5 month wide window) from 1983 to 1996

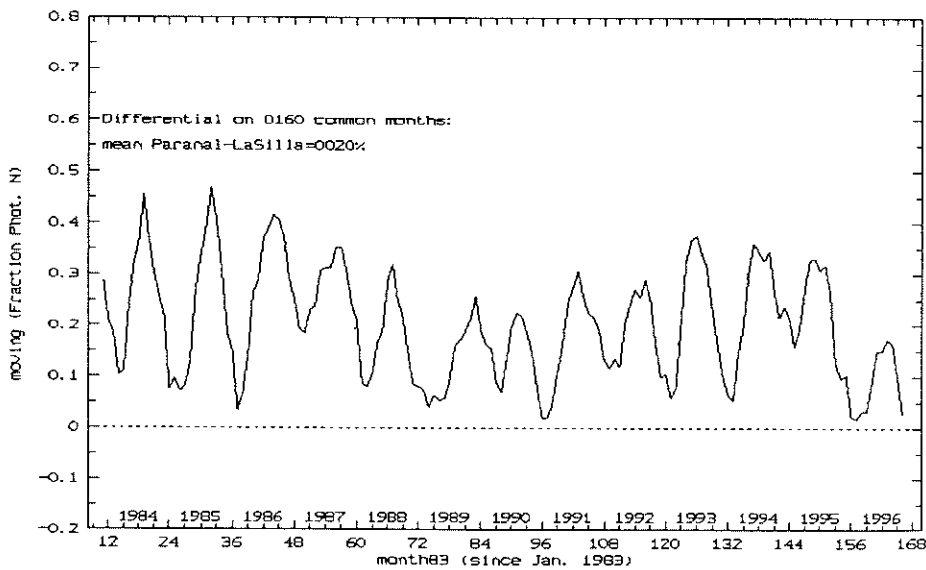


Figure 2: Monthly differential of photometric nights at Paranal and La Silla (filtered with a 5 month wide window) from 1983 to 1996

06, 12 and 18 UTC, with an horizontal resolution of about 60 km on 15 vertical pressure levels ¹. The variables at each grid point are wind, temperature, humidity, cloud fraction and water/ice content. The accuracy of global analyses is variable dependent and varies with the geographic location according to the availability of observational data to the assimilation procedure. Limited Area Models (LAM) can be implemented to reduce the grid size to 15 km over specific areas (mesoscale), their accuracy is however limited by the global analysis which they need for initialization.

Geostationary satellites (GOES, Meteosat) provide images of the earth surface every 3 hours at various wavelengths. For instance, the Meteosat 6.7 μm infrared channel relevant for water vapour has a pixel resolution of 10 km. Global Positioning System (GPS) Meteorology is a promising technique yet in development and water vapor assessment require light ground instrumentation (GPS receiver, surface temperature and pressure [Bevis 92]).

1.3 Feasibility Study

1.3.1 Methodology

In the frame of the development of a prediction scheme for the VLT observatory, the different techniques have been compared to ground based observations of precipitable water vapour made at Paranal over the past years.

Ground measurements are obtained every two hours at night with an infrared radiometer ([Morse 82]) looking at the zenith sky emissivity in two H₂O absorption bands. This instrument was used during the VLT site survey ([Ardeberg 90]) and calibrated for the altitude of La Silla by [Schulz 90].

The ongoing feasibility study by [Erasmus 96] compared Paranal ground measurements, Antofagasta radiosoundings, ECMWF analyses and Meteosat images with respect to precipitable water vapour.

1.3.2 Data Reduction

In the last three techniques, the mass of water (Kg) present in a column of 1 m² between the surface (pressure p_0) and the 100 mb (p_1) level is computed along:

$$PWV = -\frac{1}{g} \int_{p_0}^{p_1} w dp; \text{ Kg/m}^2 \text{ or mm} \quad (1)$$

where g is the acceleration due to gravity, w is the mixing ratio in Kg/Kg, and the pressure is expressed in N/m².

For radiosoundings and ECMWF reconstituted profiles, the mixing ratio at a given air pressure p and vapour pressure e is:

$$w = \frac{0.622e}{p - e}; \text{ Kg/Kg} \quad (2)$$

with $e = e_s \text{RH}/100$, RH is the relative humidity and e_s , the saturation vapour pressure expressed at temperature T (Celsius) by:

$$e_s = 6.1078 \exp \frac{17.27T}{237.3 + T} \quad (3)$$

¹1000, 925, 850, 700, 500, 400, 300, 250, 200, 150, 100, 70, 50, 30, 10 hPa

For satellite images, the vertically integrated mixing ratio w is derived from the upper tropospheric humidity (UTH) along:

$$w = \text{UTH } w_s \quad (4)$$

where w_s is the saturation mixing ratio obtained from meteorological tables assuming the temperature to be the annual 400 mb average in the area (derived from Antofagasta radiosonde analysis). The UTH in each satellite image pixel is derived from IR counts using calibration tables provided by the satellite agency ([Schmetz 88]) which itself use ECMWF temperature profiles to perform latitude dependent radiative transfer calculation (water absorbs earth IR emission and re-emit it).

1.3.3 Results

The sensitivity weighting function of the $6.7\mu\text{m}$ window extends from 600 to 200 mb and is thus well adapted to high altitude sites with a low water vapour content at ground level. A further assumption on the profile $w(p)$ has to be made to use equation (1) at lower altitudes and above 200 mb: [Erasmus 96] proposed to determine the average mode of the vertical distribution of w as a function of the season (derived from Antofagasta radiosonde analysis) and the best results were obtained when anchoring the lower end of these extrapolated profiles to actual relative humidity measurements made at the site itself.

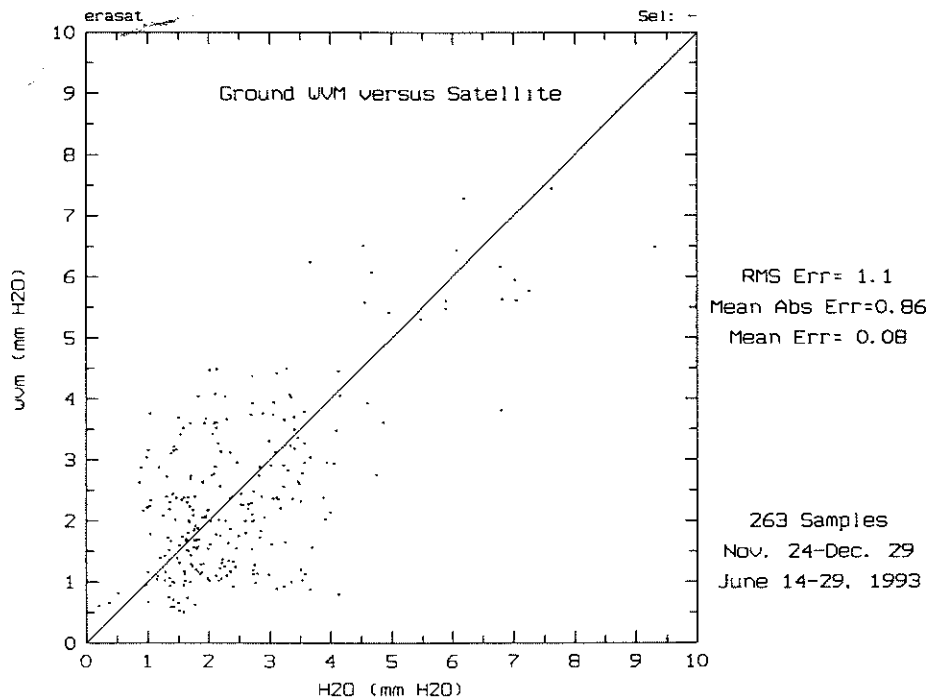


Figure 3: Regression plot of precipitable H₂O above Paranal estimated from satellite images (x axis) and from ground based measurements (y axis) for the period June 14-29, and November 24-December 29, 1993

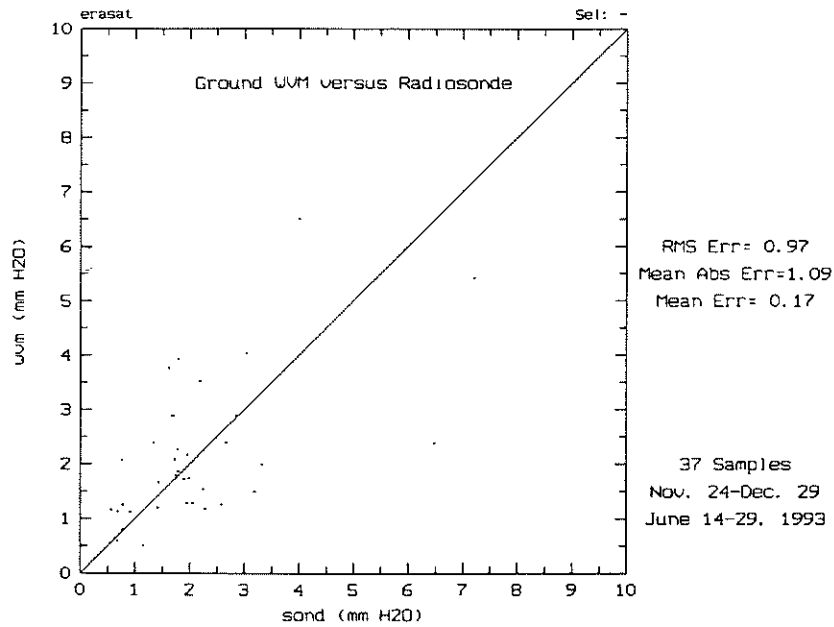


Figure 4: Regression plot of precipitable H2O above Paranal estimated from radiosoundings and from ground based measurements for the period June 14-29, and November 24-December 29, 1993

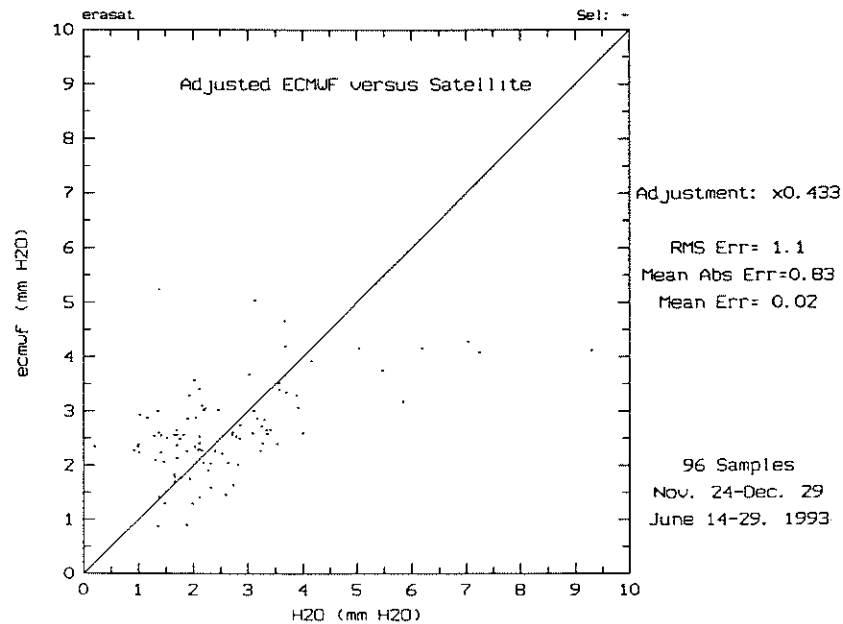


Figure 5: Regression plot of precipitable H2O above Paranal estimated from satellite images and from ECMWF global model profiles for the period June 14-29, and November 24-December 29, 1993

These results presented on Figure 3 show that the satellite provides a larger amount of data with an accuracy comparable to the Antofagasta radiosonde (Figure 4). From the latter only standard pressure levels are available, much better results would be obtained from on site radiosonde launches, but at a high cost.

Finally, Figure 5 shows the poorer performance of the global ECMWF model, in particular because of a saturation at high water vapour content. Moreover, the ECMWF data were arbitrarily adjusted by more than 50% to cancel the mean error versus satellite estimates.

1.4 Proposal

Meteosat-3 was positioned at 75W in June 1993 and stayed there until about October 1994. Then GOES-8 took over. Before June 1993 there was a period between 1990 and 1993 when there was only one US satellite (GOES-7) and this was located at 100W. The GOES-7 water vapor data is unreliable and poorly calibrated.

The strategy for a global H₂O survey in Northern Chile/Argentina would be to use the Meteosat-3 data from June 1993 to October 1994 and the GOES-8 data from October 1994 to the present. The result of the Erasmus study should first be confirmed for higher altitude sites by conducting a comparison with LSA site data as soon as available. A similar work should be done with NRAO and NRO ground based opacity measurements taken from Chajnantor (5050 m) and Rio Frio (4050 m) ([Holdaway 96]). As noted previously, it is to be expected that a satellite survey performs even better at 3500 m and above because of the smaller share of atmosphere lying outside the IR sensitivity window. When satisfactory results are obtained without the need for local anchoring measurements, a full mapping of the relevant area can be obtained for the past 4 years at a 10 km horizontal resolution.

The cost of such a study has been roughly estimated by A. Erasmus to 50.000 US\$ and includes the salary the PI (part time), one FTE (PHD/PostDoc), satellite data procurement and computing cost.

References

- [Ardeberg 90] A. Ardeberg, H. Lindgren, I. Lundström; *La Silla and Paranal: a comparison of photometric qualities* Astron. Astrophys., 230, 518, 1990.
- [Bevis 92] M. Bevis et al.; *GPS Meteorology: Remote Sensing of Atmospheric Water Vapor Using the Global Positioning System*; J. of Geophysical Research **97**, 15787-15801, Oct. 1992.
- [Erasmus 96] D.A. Erasmus, R. Peterson; *Feasibility Study and Development of Software Computer Code for Cloud Cover and Water Vapour Forecasts: Phase I*; ESO Report VLT-TRE-ERA-17440-1038, 1996; and *The Feasibility of Forecasting Cirrus Cloud Cover and Water Vapor Above Telescope Sites in Northern Chile*; PASP..108..208E - February 1997.

- [Grenon 90] M. Grenon; *The Northern Chile Climate and Its Evolution: A pluridisciplinary Approach to the VLT Site Selection*; The ESO Messenger **61**, 11-17, September 1990.
- [Holdaway 96] M.A. Holdaway et Al.; *Comparison of Rio Frio and Chajnantor site testing data* NRAO Millimeter Array Memo Series **152**, April 1996.
- [Morse 82] D. Morse, F. Gillet; *Water vapor monitor engineering report*; AURA Engineering report **73**; Oct. 1982, KPNO, Tucson Az.
- [Schulz 90] A. Schulz; *Precipitable Water Vapor Measurements on La Silla. A Calibration check*; MPI fuer Radioastronomie, Bonn, Division of Submillimeter Technology- Memorandum 121.
- [Schmetz 88] J. Schmetz, O.M. Turpeinen, V. Gärtner; *Upper Tropospheric Humidity Fields from Meteosat*; ESA Journal, **12**, 267-272, 1988.

Site Selection: Summary of Problems Encountered in Working at High Altitudes

R. Roach

Copenhagen Muscle Research Center
20 Tagensvej, RH 7652
2200 Kbh N, Denmark

Ascent above 2000 to 2500 meters terrestrial altitude is associated with an increasing risk of serious deficits in cognitive and motor tasks. Up to 4000 meters the deficits can be successfully countered by adaptive behavioral strategies, such as always following a checklist, double-checking one's work, working closely with a colleague to verify successful task completion. Above 4000-4500 meters these strategies are not sufficient to ensure adequate performance, indeed one may simply forget to complete a checklist procedure, or the impairment may be wide spread and thus a colleague's crosscheck may be as confused as the original work.

People have successfully adapted to 5200 meters and lived at that height for several months while completing complex and demanding research projects. But in every case the people involved were experienced high altitude specialists with known ability to adjust to the heights, generally young (20-35 years) and were not involved in frequent transport from low altitudes to high altitudes and back. Without question the successful completion of demanding physical or mental tasks is easier at 3000-3500 meters than at 5000 meters. Even with acclimatization which will allow people to work at 5000 meters with a low risk of developing serious illness, work will be a constant challenge at 5000 meters.

What causes the problems with thinking clearly that are uniformly seen at higher altitudes? It seems that it is simply the low oxygen environment as most changes are immediately reversible with oxygen administration. At very high altitudes, above 7500 meters, some permanent changes can occur that are not immediately reversed with oxygen breathing, at 5000-6000 meters no such changes are seen.

The degree of impairment at high altitude cannot, at present, be predicted from any sea level tests. We do think that how much one breathes at altitude, with more being better, does determine much of the response. Breathing during sleep may be a particularly weak link in the system, and is an important point to consider. Many people breathe irregularly while they sleep at high altitudes. During this irregular breathing their oxygen level may decrease to very low levels. It is likely that this then causes poor, interrupted sleep, and in addition to the low oxygen, can cause decreased mental performance due to sleep deprivation.

To live and work at a site at 5000 meters the best strategy is to build dormitory rooms that are supplied with increased oxygen content. This technology, using oxygen concentrators, has significantly advanced in the last five years and is now affordable, reliable and fairly easy to incorporate into existing structures. Each 1% increase in oxygen

percent in the inspired air lowers the altitude by 300 m. Thus, living at 5000 meters and breathing air with 6% additional oxygen (21% + 6%) would lower the effective altitude to 3800 meters. At 3800 meters the amount of irregular breathing will be less, and the oxygen levels during sleep will be significantly higher than at 5000 meters. A new and surprising finding is that on the day after sleeping in an oxygenated room at high altitude, workers had a higher oxygen level in their blood during the day. This means that sleeping at a lower effective altitude and then working at the actual altitude stimulates breathing and actually helps one cope better with the low oxygen during the day. Additional oxygen enrichment could be added to the control rooms. With use of a simple ante-room the oxygen levels inside dormitory and other oxygen-enriched rooms can be easily maintained. The cost for an 'oxygenator' to maintain a higher oxygen level in a two-person bedroom is approximately \$2000 USD. Economy of scale should bring this cost down considerably if one considers an oxygenator for an entire control room.

Using oxygen during physical work at 5000 meters will be useful only if the work is particularly demanding. Oxygen equipment itself is very heavy and many people will find it not worth the trouble for short, focused tasks. No risk occurs if someone goes from the oxygenated room, either in the dormitory or control rooms, into the ambient air. The advantage of only slightly increasing the oxygen levels inside, instead of trying to make them like sea level, is that workers become partially acclimatized to altitude and thus can cope with working in the un-oxygenated, ambient environment much better than someone exposed to that environment directly from sea level.

At 2500-3000 meters few problems will be noticed, though some individuals may be intolerant of even these altitudes. If it is possible to live and sleep at 2500 meters and commute to 5000 meters where the control rooms are oxygenated many people will be able to accommodate that level of low oxygen. It would be better, however, if the living/sleeping altitude were higher, say around 3000-3500 meters. Then the trip to 5000 meters would be much less taxing. In my opinion, consideration of human's physiological responses to altitude suggests that working at 3500 meters is preferable to 5000 meters.

Several options are available to help make the decision about the altitude of the study. The human performance concerns can be dealt with at either location, though it is not easy to make the altitude of 5000 meters as easy to work at as 3500 meters, especially for outside work where portable oxygen devices would need to be used. I do not recommend a separate study to answer these questions, it would be redundant with research previously done or currently underway and it would be costly. Two alternatives come to mind. In the summer of 1998 I am conducting a large medical research project in La Paz and on the nearby peak of Chacaltaya, Bolivia. La Paz is at about 3600 meters altitude and Chacaltaya is at about 5200 meters altitude. Some simple tests could be devised specific to the kinds of work anticipated at the LSA site. These tests could be conducted at sea level, 3500 meters and 5300 meters. The studies at both Bolivian locations would be long enough to give an idea of performance after one day, one week and one month (only at Chacaltaya that long). The costs would be reasonable, including travel, the study, and a report. A second possibility is to use existing data, summarized above, to compile a detailed report on the decrement in performance, both physical and cognitive, previously shown at the altitudes in question.

References

1. Cavaletti, G., and Tredici, G., Long-lasting neuropsychological changes after a single high altitude climb, *Acta Neurol Scand*, 87, 103 (1993).
2. Fowler, B., and Lindeis, A. L., The effects of hypoxia on auditory reaction time and P300 latency, *Aviat Space Environ Med*, 63, 976 (1992).
3. Hornbein, T. F., Long term effect of high altitude on brain function, *Intl J Sport Med*, 13, S43 (1992).
4. Kennedy, R. S., Dunlap, W. P., Banderet, L. E., Smith, M. G., and Houston, C. S., Cognitive performance deficits in a simulated climb of Mount Everest: Operation Everest II, *Aviat.Space Environ.Med*, 60, 99 (1989)
5. Regard, M., Landis, T., Casey, J., Maggiorini, M., B=E4rtsch, P., and Oelz, O., Cognitive changes at high altitude in healthy climbers and in climbers developing acute mountain sickness, *Aviat Space Environ Med*, 62, 291 (1991).
6. Townes, B. D., Hornbein, T. F., Schoene, R. B., Sarnquist, F. H., and Grant, I., Human cerebral function at extreme altitude, in *High Altitude and Man*, West, J. B., and Lahiri, S., Eds., American Physiological Society, Bethesda, MD, pp. 31 (1984).
7. West, J. B., Hackett, P. H., Maret, K. H., Milledge, J. S., Peters Jr, R. M., Pizzo, C. J., and Winslow, R. M., Human physiology on the summit of Mt. Everest, *Trans Assoc Am Physicians*, 95, 63 (1982).
8. West, J. B., Do climbs to extreme altitude cause brain damage? (Letter), *Lancet*, 2, 387 (1986).

Phase Calibration Strategies

edited by Stéphane Guilloteau¹ with inputs from the IRAM staff

¹ Institut de RadioAstronomie Millimétrique, 300 rue de la Piscine,
F-38406 Saint-Martin D'Hères, France

1 Calibration Strategies

In order to provide the highest angular resolution, the calibration technique should be able to remove atmospheric phase fluctuations on baseline lengths up to several kilometers, and at frequencies up to 350 GHz.

Several basic calibrations techniques can be easily identified

- Paired antennas in which the array is organized in close-by antenna pairs (e.g. 40-m separation), half of the array pointing towards a quasar while the remaining half observe the source
- Phase screen monitoring, which is a variant of the above, where a second set of smaller antennas is used to effectively "map" the phase over the site.
- Self-calibration which will only work on sufficiently strong sources.
- Fast switching in which phase referencing to a nearby quasar is performed sufficiently frequently to remove most atmospheric phase fluctuations.
- Phase compensation in which a total-power monitoring device on each antenna allows to retrieve the atmospheric pathlength to the required precision

The first method is very expensive in terms of sensitivity. The second will allow only relatively strong quasars to be used, which may be a severe limitation; it is very costly also since it requires a full set of dedicated antennas, receivers and correlator.

Self-calibration, despite all the success it had at cm wavelengths, has a too limited scope to be relied upon.

Fast switching imposes stringent constraints on the antenna drive system, since the cycle time should be short enough. Experiences and current knowledge on the atmospheric phase structure function indicates cycle time of order 10 sec are required. Although the likelihood to find a suitable quasar within 1-2 degrees from the observed source is important, the stress imposed on the antenna with such a scheme is

Phase compensation has been demonstrated with various degrees of accuracy at several places (IRAM, BIMA) and is being pursued at other observatories too (JCMT-CSO, OVRO). Each experience provides a different view.

2 Phase Compensation: State of the Art

2.1 IRAM

Recent experiments carried on the Plateau de Bure with the IRAM provide a new and quite promising view on this topic. These experiences are based on the monitoring of water vapor content through the total power output of the 1.3mm receivers. Because water vapor is by large the most important time variable dispersive constituent of the atmosphere, monitoring the fluctuations of the sky emissivity provides an almost direct measurement of the pathlength variations.

Observations with the IRAM interferometer have demonstrated the ability of such techniques to bring the atmospheric pathlength fluctuation from more than 1 mm down to about 50 to 70 microns, over timescales up to 10 minutes. This demonstrates that the accuracy of the method is at least 7 %.

The IRAM technique has currently two drawbacks. The receiver stability as a function of telescope elevation is not sufficient to ensure the continuity of the pathlength monitoring when switching from the calibrator to the source. Second, the method totally fails as soon as clouds appear.

2.2 BIMA

BIMA uses the 3mm receivers to predict the pathlength fluctuations. This sounding wavelength is much less sensitive to pathlength variations than the 1.3mm band. Accordingly, the accuracy is much lower than the IRAM result (about 0.3 mm), but the long term and elevation dependent stability of the receivers a-priori enables to recover the continuity between source and calibrator.

However, this is a difficult task because of varying ground-pick up as function of elevation. Detailed modelling of the antenna behaviour may be necessary to solve this problem.

2.3 OVRO

OVRO is developing a system based on the 22 GHz water vapor line. Although the intrinsic sensitivity is relatively low, thereby requiring extremely stable receivers. However, the system works in a differential mode, by using 3 filters: one centered of the line, and one on each side. Hence only the line signal is kept. Since the line is relatively narrow, the system may be able to work even under moderately cloudy conditions, because the cloud emission is reasonably achromatic over the required bandwidth.

2.4 CSO-JCMT

The system under development for the CSO-JCMT interferometer uses the same principle as the OVRO one, but the 183 GHz line of H₂O instead of the 22 GHz one. The line is strong, indeed so strong that it is actually saturated for most of the current astronomical sites. However, at Mauna-Kea and at the expected site for the LSA, the line becomes optically thin.

Cloud compensation will be less effective because the line is much broader, so that chromatic effects in the cloud emission may become non negligible.

2.5 Outer Scale of the Atmospheric Turbulence

Using the IRAM instrument, we have been able to determine one of the key missing parameters of the phase structure function: the pathlength fluctuations *at the outer scale of the turbulence*, just by monitoring the total power of one receiver. Three such measurements (expressed in terms of rms phase at 230 GHz) are displayed on Figure 1, in respectively excellent, average and poor conditions. Note that the measurement in excellent weather conditions is actually an upper limit to the tropospheric phase noise, because the measurement accuracy is limited by the intrinsic stability of the detection system.

Phase noise below 30° at 230 GHz on arbitrarily long baselines are thus possible on excellent days. This is sufficient to provide good quality images. Note that 3 mm observations would have a lower phase noise, and hence comparatively better imaging quality (though not significantly better seeing).

On more typical days, the atmospheric phase noise is still low enough to be corrected by the total power monitoring techniques, even without further progress in the atmospheric modeling. It is only on "poor days" that the model accuracy may be insufficient. However, such days should be extremely rare on the LSA site, as illustrated by the MMA site study at Cerro Chajnantor (even accounting for a possible degradation due to a lower altitude of the LSA site).

3 Recommendations for the LSA

3.1 Use of the Phase Compensation

The above results have demonstrated that with proper engineering, receivers which are stable enough to monitor the atmospheric pathlength can be built, and that the accuracy of the atmospheric modeling is sufficient over the 1-3 mm band to compensate for the atmospheric phase noise under most of the expected weather circumstances. Engineering will be easier if the sounding receiver is a dedicated one. However, because of the property of the phase structure function, the sounding direction can be several arcminutes from the observing direction.

Ensuring proper continuity of the pathlength prediction between the source and the calibrator is a difficult task. A fundamental limit of the phase compensation technique comes from differential ground pick-up variations as function of elevation for each antenna.

However, the situation for the LSA is quite different from that of current instruments. With the LSA sensitivity, the probability to find with 1 degree of the source a quasar sufficiently strong to allow calibration after 10 to 30 sec integration is extremely high, while for current instruments the typical distance to the calibrator is about 20 degrees. Hence the fundamental limit is much less important for the LSA. Experiences at IRAM should be performed to assess the validity of this statement.

Moreover, the proximity between the quasar and the source also allows to release the constraints on the long term stability of the receivers. since observations every 5 to 10 minutes become realistic.

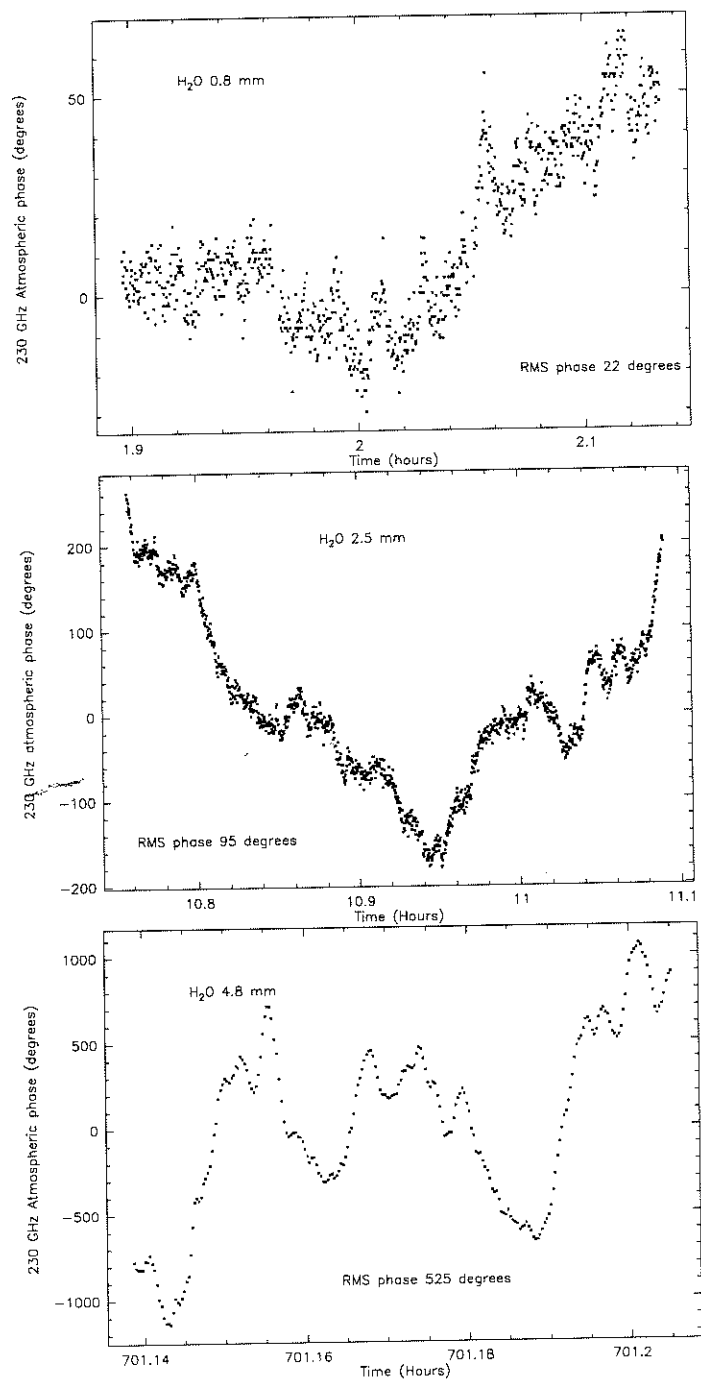


Figure 1: Total tropospheric phase excursion above one antenna derived from the total power fluctuations. Top: excellent conditions, Middle: normal weather, Bottom: poor weather. In all cases the outside temperature was below 0°C

3.2 Dual Frequency Observations

Because compact sources tend to have steep spectra, calibration is often best done at the longer wavelengths. If relatively frequent calibration must be performed, this will require either simultaneous observations at 2 frequencies, or fast switching between 2 receivers.

The term "fast" must be understood precisely: switching between receivers must be performed in a timescale short compared to the phase variations *after compensation for the atmospheric pathlength fluctuation*, if any. So if no pathlength compensation is used, switching back and forth between two receivers must be accomplished within 10 sec, while with pathlength compensation the cycle is only dictated by the "long term" stability of the monitoring receiver. However, in such a scheme, the relative calibration between both receivers is affected by the accuracy of the pathlength compensation device.

Simultaneous dual-frequency observations remove this error term, since the error on the relative phase and/or pathlength difference for both receivers is then only affected by thermal noise. This scheme is a priori preferable for high quality imaging. However, the required optics may introduce additional receiver noise.

A continued investigation of the advantages and inconvenients of the two methods is important during the LSA development.

3.3 Frequency of Phase Calibration

Atmospheric effects set apart, phase calibration also serves to correct for other instrumental effects, such as focal length changes, displacement of the nodal point of the telescopes, changes in the IF transport system length, etc... Changes in the IF system can in general be corrected by appropriate electronics, but those linked to the thermal behaviour of the antennas have to be calibrated out.

In current instruments, phase calibration is performed every half hour or so. A faster turn-around cycle would allow to relax some of the specifications concerning the thermal properties of the antenna. However, a faster cycle might imply stronger constraints on the antenna drive specification, to avoid excessive overhead time when slewing from source to calibrator. The duration of the calibration cycle also has impacts on the specifications of the phase monitoring device: this device must be stable to the desired accuracy over a timescale twice longer than the calibration cycle time.

It is suggested that a base value of 10 minutes be used for all specifications.

LSA Telescopes

Dietmar Plathner

I.R.A.M. Institut de Radioastronomie Millimétrique
300 rue de la Piscine
Domaine Universitaire de Grenoble
38406 St. Martin d'Hères
France

1 Introduction

The October 1995 report on the LSA (D. Downes et al.) specifies in its Chapter 5.1 (Antennas): "to minimize repairs and maintenance on a spread-out, remote, desert site, a major design goal should be reliability of all components. The antennas should be simple and robust, and well-designed to maintain their mm-quality surface without any active correction system."

These ideas combined with the demand for low-cost solutions have been taken as design goals for the work on the LSA telescopes presented here. The IRAM 15-m dishes were taken as reference as they combine a certain number of well-proven and low-cost structural elements with for the required precision reasonable overall dimensions.

2 General

The IRAM 15-m dishes are built according to the principal of homology and have to be corrected permanently for gravitational deformations by displacing the subreflector. The deformation of the main reflector is in the order of 1.5 mm at the outer rim.

To suppress the active correction system at the subreflector, these deformations have to be reduced to a fraction of the wavelength, i.e. to something less than 0.5 mm typically.

The back-up structure of the existing 15-m dishes is already composed of mostly lightweight struts of carbon fibre material with relatively high stiffness values (76% of that of steel). High modulus fibres would decrease the 1.5 mm deformation by something like 25% only, but would increase the price exponentially. Therefore structural modifications were looked into.

If one simplifies a cross-section through a reflector one could, in a first order approximation, imagine a horizontal homogenous beam supported in two points as shown in Fig. 1a. The geometrical relations are scaled to the situation found on the 15-m IRAM telescopes. The overhanging part with a length L represents something like a cantilever beam under its own load. Its deformations increase with L^4 . Thus if the deformations of the LSA should be 10 times less than for the existing telescopes, then $L_{LSA} = (L^4/10)^{-4}$. The change in deformation is shown in Fig. 1b taking the same scale.

This basic consideration was applied to the back-up structure of the IRAM 15-m dishes displacing the supports from ring 2 to ring 4 and the former deeper back-up structure was flattened (see Fig. 2) with the idea to get the elevation axis as close as possible to the vertex of the dish and in view of the low weight exercised by the small panel surface inside the support area.

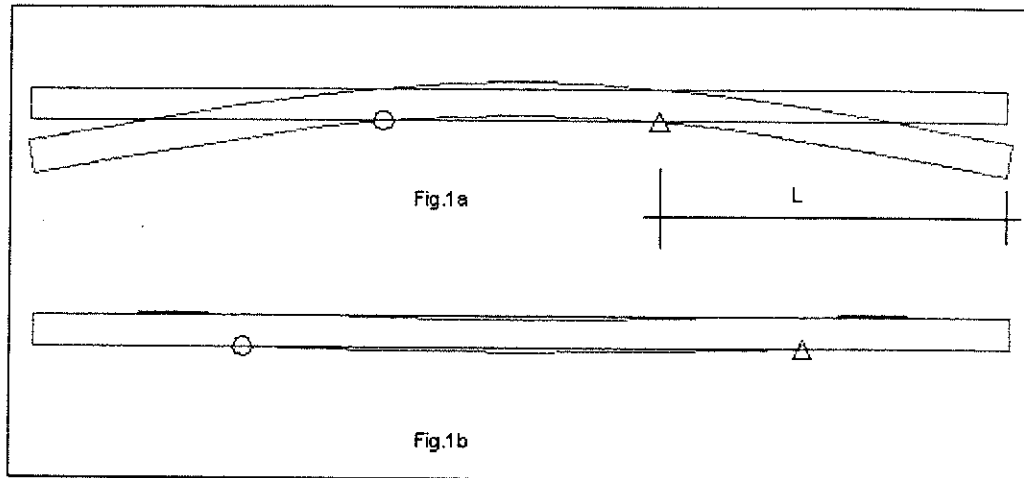


Fig. 1: Influence of support position on the deflection of a beam

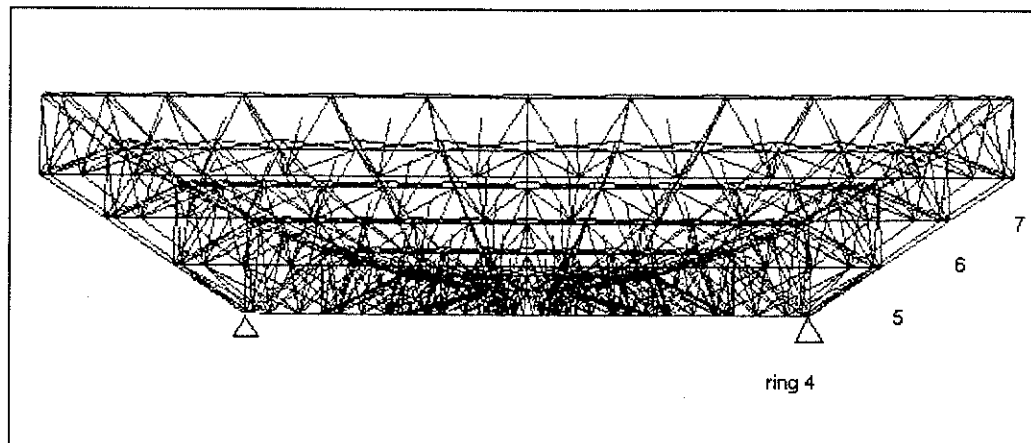


Fig. 2: Back-up structure

3 Design Specifications

The telescopes will be installed on a high altitude site (> 3000 m) in a remote desert region. This will define limit values for humidity, wind, temperature exposure, UV-radiation assembly requirements and maintainability. There will be a big number of telescopes (≥ 50) and they have to be transportable to change astronomical configurations, typically once per year, and they are exposed to the outside world as radomes or other protection would complicate the situation even more. Nevertheless they have to be designed to provide necessary precision and longevity for long lasting high quality mm-observations. Finally they should be affordable and be of an alt-az concept with Cassegrain optics.

In this early stage of developing the project it is not possible yet to establish a detailed list and define all parameters to make sure that these telescopes are valuable elements of the LSA interferometer.

Based on the above overall specifications and compared to the values defined for the IRAM 15-m telescopes (J. Delannoy, 1985) some aspects of the LSA telescopes have been studied.

4 Description of the Telescope Structures

An alt-azimuth configuration is described which integrates the ideas presented in Chapter 2 for reduced gravitational deformations into a structure which is based on more or less classical telescope design and materials. A computed image of the telescope is shown in Fig. 3. It illustrates also the particularity of this telescope which has a mechanical off-set between the horizontal elevation and the vertical azimuth axis.

4.1 Description of the 15-m Dishes

The dishes are composed of:

- a back-up structure equipped with
- a set of surface panels and
- a Cassegrain cage which is serving as a support structure.

The **back-up structure** is composed of a number of truss elements in which the struts are made from thermally stable carbon fibre tubes and the corresponding nodes from steel. The geometrical set-up is derived from the IRAM 15-m telescopes with the difference that there will be only 30 sectors instead of now 32. The whole structure will be surface protected, such that thermal influences from ambient are minimized and that the intense UV-radiation on the site cannot deteriorate the carbon fibre structures.

The **surface panels** are modelled as aluminium plates with mechanical data derived from the panels installed on the Plateau de Bure interferometer.

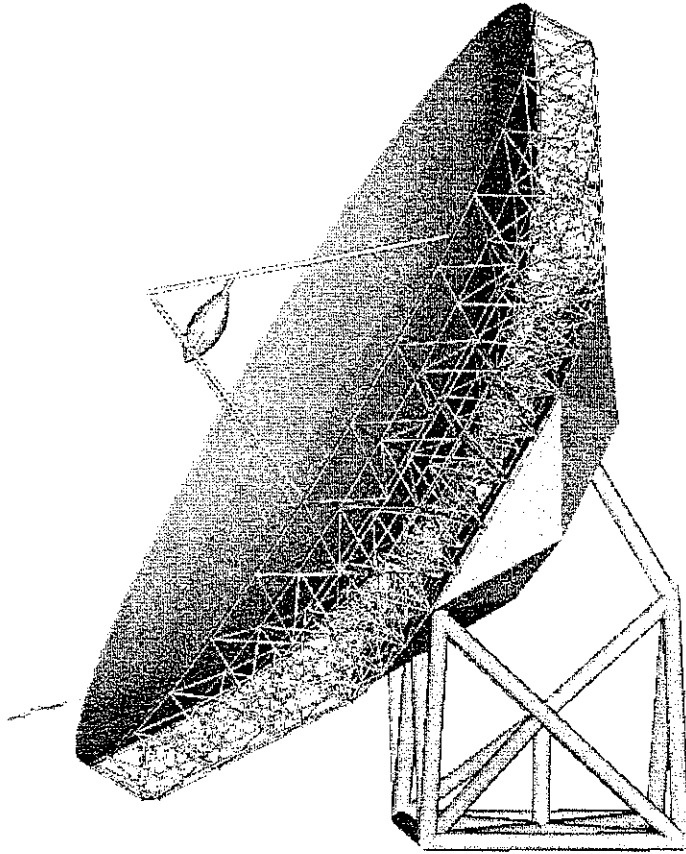


Fig. 3: Computed image of the LSA telescope

As already mentioned earlier, the back-up structure is supported in ring 4 of the truss configuration. Six of the 30 nodes of that ring are connected to **the Cassegrain cage** which is composed of a hexagonal box structure welded from steel plates. The Cassegrain cage is supported by the pedestal of the telescope

- in 3 points in the vertical (z) direction,
- in 2 points in the horizontal (y) direction and
- in 1 point in the other horizontal (x) direction.

The assembled configuration of the 15-m dish is shown as a perspective computer model in Fig. 4 looking from the back to an inclined structure.

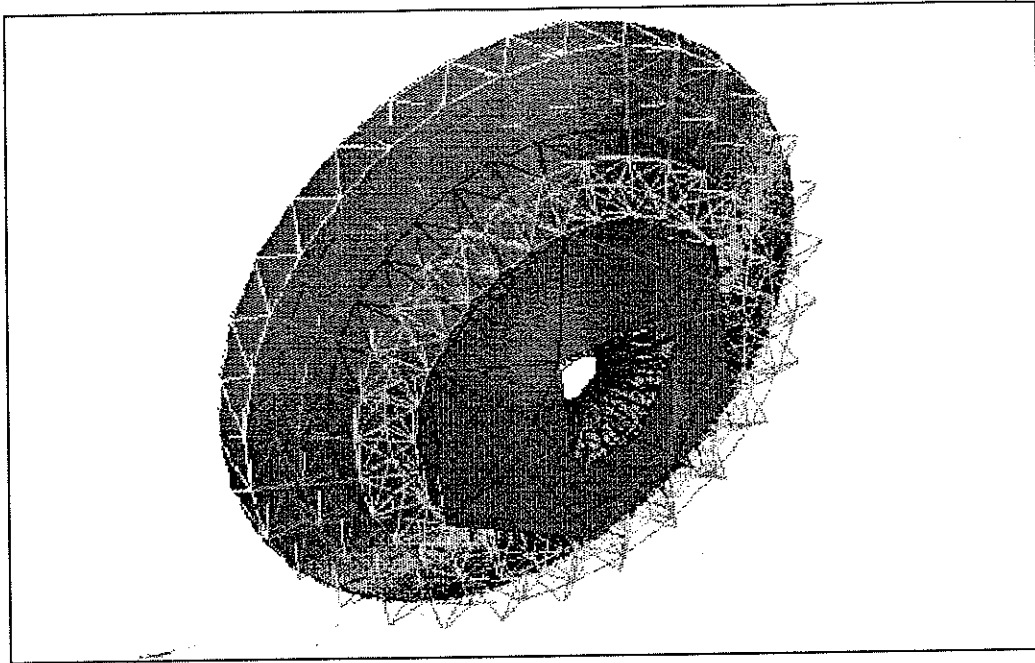


Fig. 4: 15-m Dish-assembly (seen from back)

4.2 Description of the Pedestal

The pedestal is again a truss structure composed of steel struts welded together as shown in the computer model in Fig. 5. Nodes 1 and 2 are equipped with spherical radial bearings which connect to the back-up structure and give support to the back-up structure in vertical (z) and horizontal (y) direction. To node 3 is fixed a thrust bearing giving support to the back-up structure in horizontal (x) direction. The last node (4) in the upper part of the pedestal is carrying a linear drive which is connected at the second end to the reflector and supporting it in z -direction.

Nodes 5-9 in the lower part of the pedestal provide the fixation to the ground and rotation about the vertical axis. The central node 5 carries a roller bearing blocking the x , y and z degree of freedom of the pedestal. Nodes 6 to 9 are equipped with motorized rollers running on a circular rail positioned horizontally.

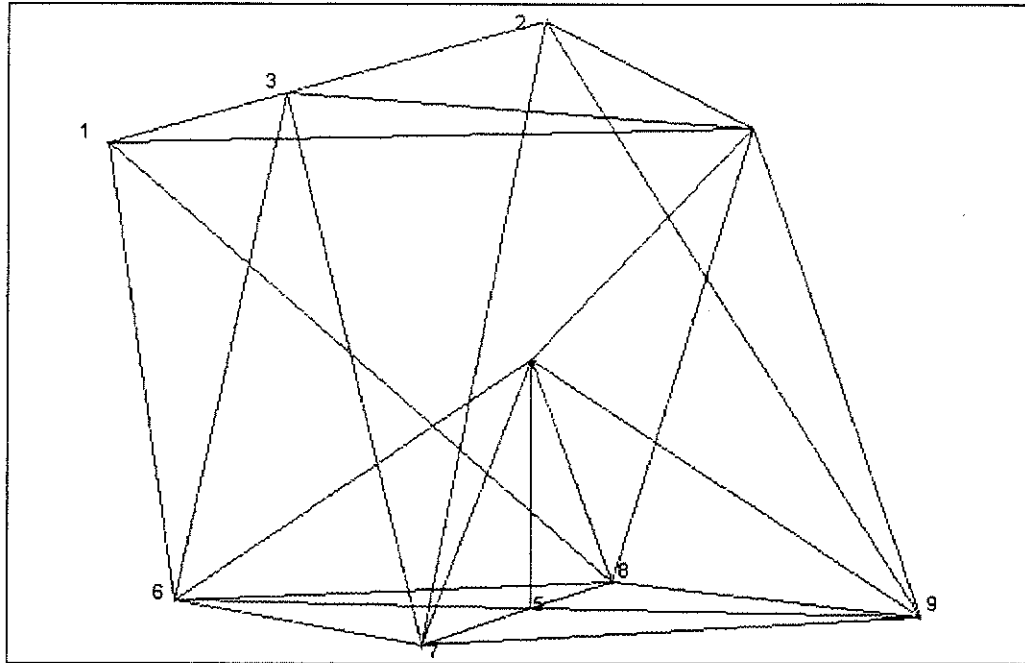


Fig. 5: Pedestal

4.3 The Axes

The bearings on nodes 1 to 3 of the pedestal are in line and define the elevation axis. The tilt motion of the reflector assembly about this axis is illustrated by Fig. 6. The off-set position of the elevation axis reduces considerably the dimensions of the pedestal which results in higher stiffness, low weight and finally lower cost. To further reduce the dimensions of the pedestal the tilt motion from 0 to 15 deg. elevation was suppressed for telescopes under operational conditions. If the horizon position should be needed for test purposes, it would be achieved on a particular foundation in the assembly zone.

A counterweight to balance the reflector structure about elevation axis is felt not to be needed as varying wind loads will impose stiffness requirements in the drives which can easily cope also with the unbalanced loads.

The position of the azimuth axis is defined by the central bearing on node 5 of the pedestal and the vertical direction given by the four rollers on nodes 6 to 9.

4.4 Drives

The tilt motion about elevation axis is achieved by the linear drive mentioned further above. Its nature is not yet defined, but it will probably be composed of a long distance

rough part and a short distance fine drive.

The rotation in azimuth is created by direct drives on the rollers in the four corners of the pedestal.

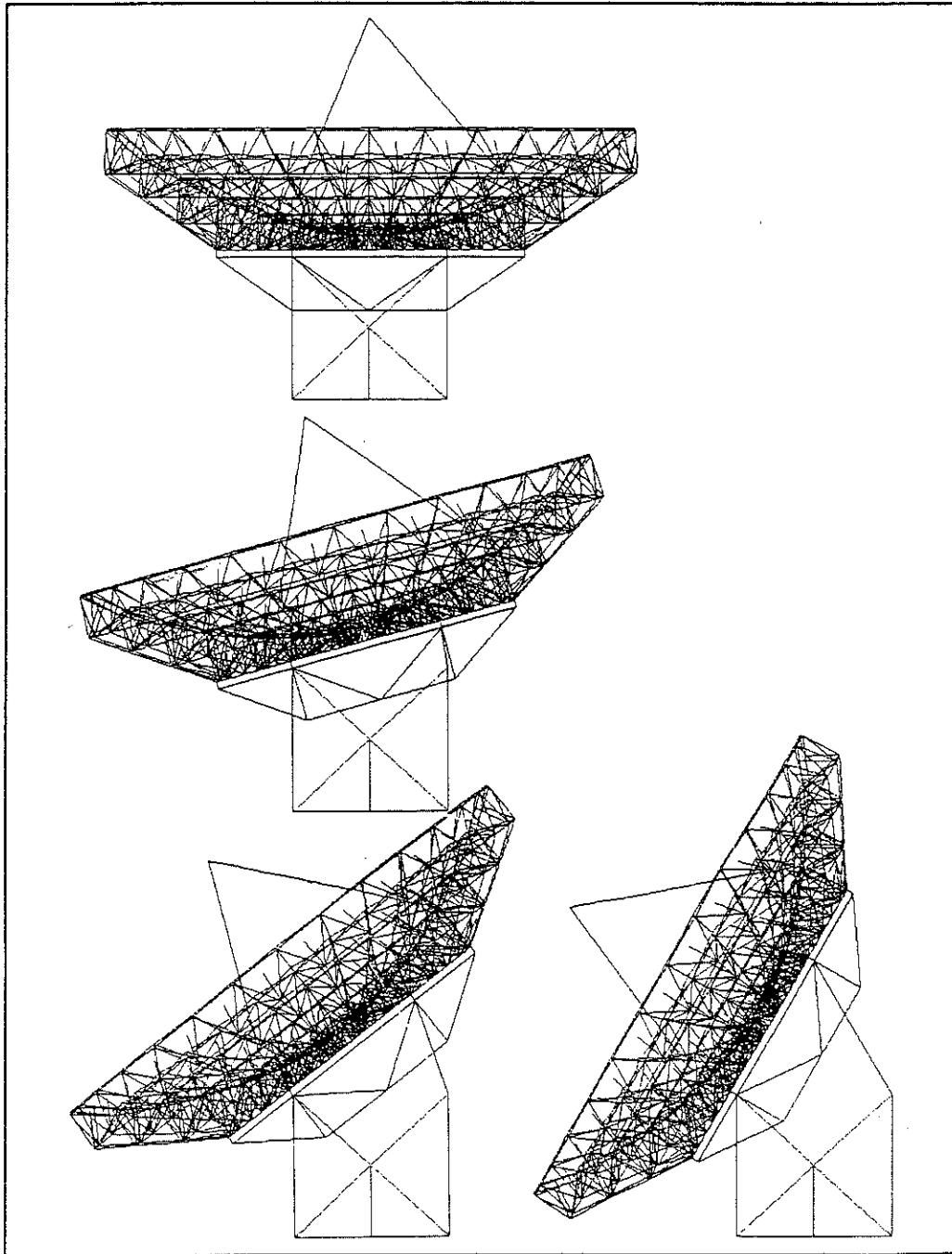


Fig. 6: Rotation about el. axis

4.5 Encoders and Limit Switches

Both axes of the telescopes will be equipped with absolute encoders enabling a coarse orientation of the telescope and providing possibilities for electronic limitation of the rotation about the two axes. This kind of limit switches is doubled by electro-mechanical devices for increased security.

The control of the telescope will be done by a master slave configuration using a laser measuring system as indicated in Fig. 7. This measuring system will be composed of the items necessary to measure two angles. The laser and interferometer parts are installed as indicated in the sketch on the ground and centered to the azimuth axis. The reflective angle targets are supported by the elevation axis. Both groups are mounted to servoed rotational supports respectively fixed to the ground and to the elevation axis and rotating about the corresponding axes. The two supports represent the master system which dictates the telescope motions. To keep the output of the angle measuring system to a zero value the telescope has to follow the master.

The advantage of the device is given by the fact that the reflector is positioned independently of structural deformations in the pedestal so that high precision pointing can be achieved.

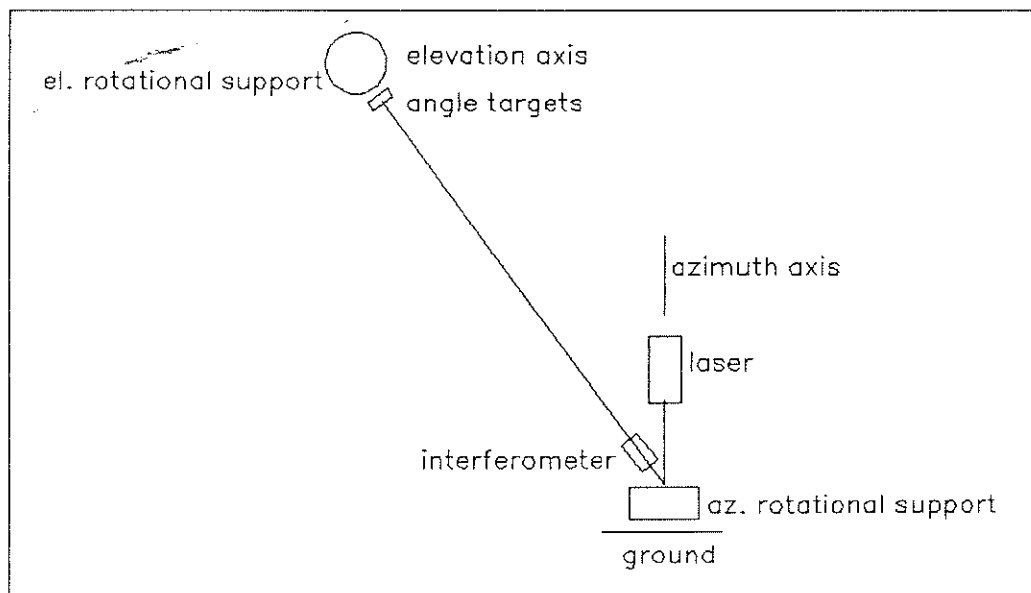


Fig. 7: Master-slave laser measuring system

4.6 Subreflector and Support

The subreflector will be made from aluminium with an anodized surface and will measure typically 1.5 m in diameter. It will be supported by a tripod configuration. The tripod is made from zero expansion carbon fibre tubes. The lower ends of the legs are connected to nodes of the back-up structure which match with three attachment points of the hexagonal Cassegrain cage support.

4.7 Transportability

The design of the LSA telescope is such that only the central bearing has to be unscrewed from the foundation and the cables disconnected to prepare the telescope to be transported.

The transport itself is done by a transporter on tires because the assembled telescope will have a total weight of typically 40 tons only. Good vibration damping will protect the bearings, drives and other precision equipment from shocks. Max. speed of the transporter should not exceed 5 kms/h. The transporter is equipped with a smooth and precise lifting and placing device to handle the telescopes with great care. The transporter can run on roughly prepared stone roads. For the time being it is assumed that it is used only on a flat plateau.

5 Computational Verifications

A 15-m dish was studied under gravity load to prove that deformations can be considerably reduced when applying the ideas mentioned in Chapter 2. This should lead to a fixed focus operation in the elevation range of 30 to 75 deg. Fitting to this dish configuration a truss structured pedestal is proposed and calculated under a simulated wind load of 10 m/s.

5.1 Finite Element Analysis of the Reflector Structure

For the analysis a model was prepared which encloses

- a back-up structure composed of struts
- the set of surface panels modelled as plates and
- the Cassegrain cage again in plate elements.

The model is shown in Fig. 3. For the calculations it was supported as described in Chapter 4.2.

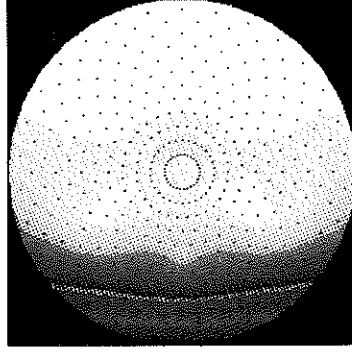
7 load cases were computed applying gravity and tilting the reflector assembly from horizon position to zenith in steps of 15 deg. The deformation analysis was done with a program from ALGOR/U.S.A.

With a program which was already used for the 15-m Plateau de Bure dishes (J. Delannoy, 96) the deformations of the surface nodes were transformed into maps showing the residuals of a weighted paraboloid fit and also the residuals relative to a reference surface in the mean of elevations 30, 45, 60 and 75 deg. (M. Bremer, 96).

The maps including those of the computed deformations are shown in Fig. 8 to 11 for the specified observation range in steps of 15 deg.

Files: teldef01.out with tede1345.out

Legend [μm]: min=-411.99, max= 68.64

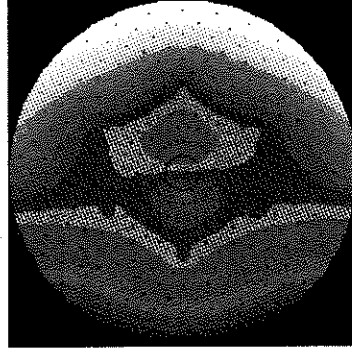


Gravitational Deformation
for Elevation = 45°

Δz Displacement
calculated with ALGOR

Files: teldef01.out with tede1345.out

Legend [μm]: min= -21.59, max= 36.84



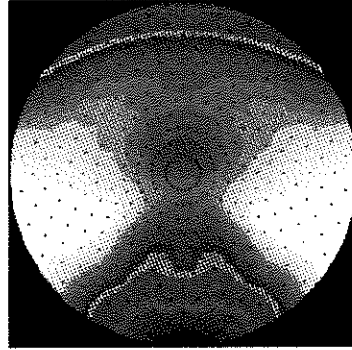
Gravitational Deformation
for Elevation = 45°

Residuals relative to a
Reference Surface:
Mean of Elevations:
30°, 45°, 60°, 75°

σ r.m.s. = 6.57 μm
Edge taper = 10 db

Files: teldef01.out with tede1345.out

Legend [μm]: min=-119.85, max= 94.77



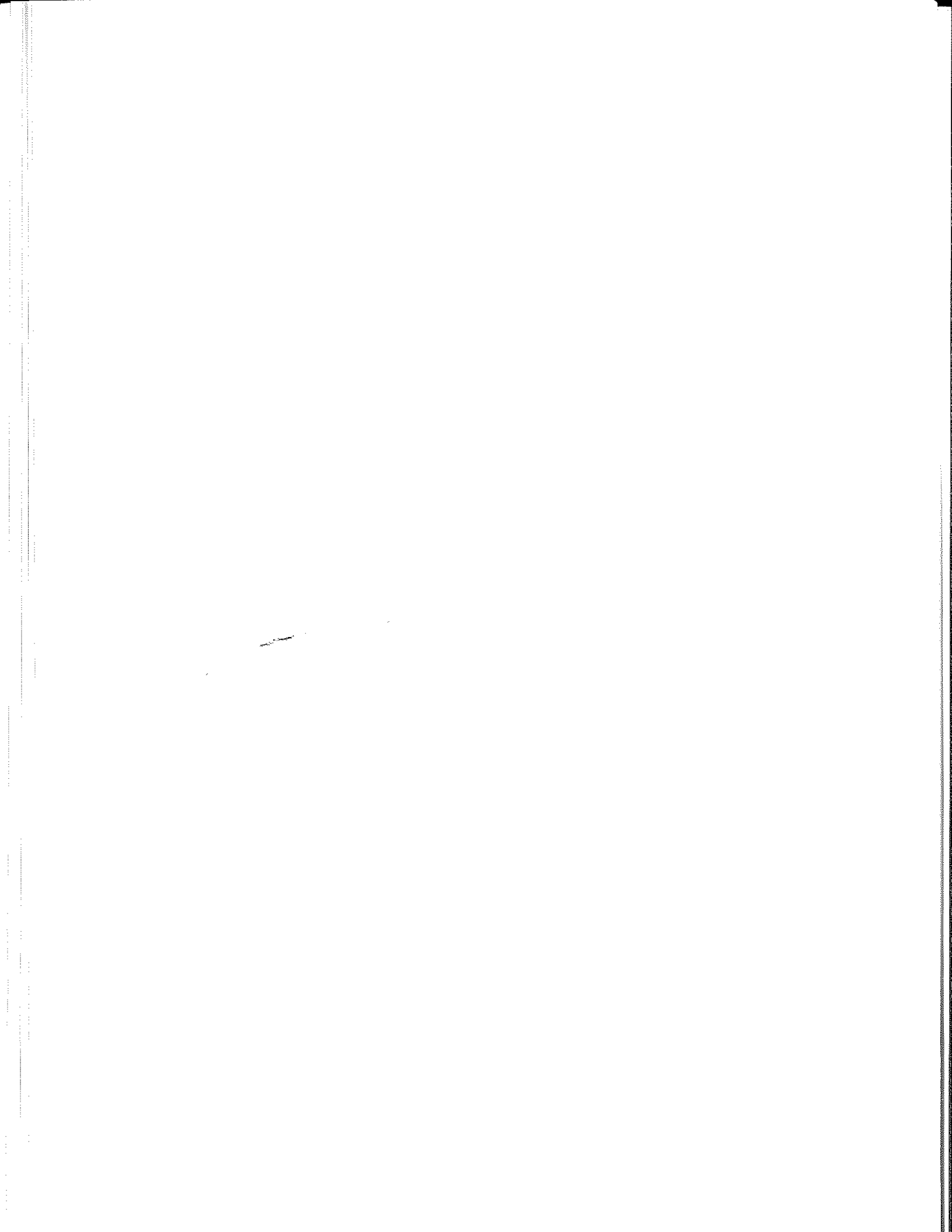
Gravitational Deformation
for Elevation = 45°

Residuals of a
Weighted Paraboloid Fit:
F = 4875.183 mm
Tilt x = -32.40"
Tilt y = -0.89"

σ r.m.s. = 28.56 μm
Edge taper = 10 db

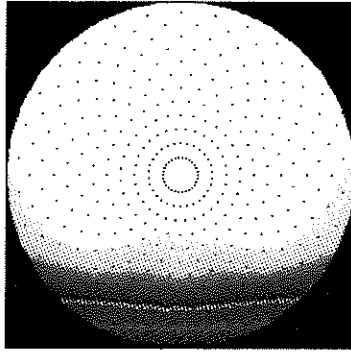
Translation apex X0, Y0, Z0 (mm): -0.048 1.485 -0.018

Fig. 9: Deformation and error maps for 45° elevation



Files: teldef01.out with tede1360.out

Legend [μm]: min=-396.34, max=-2.77

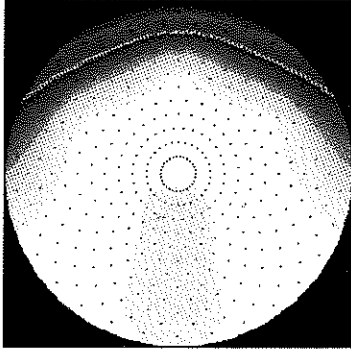


Gravitational Deformation
for Elevation = 60°

Δz Displacement
calculated with ALGOR

Files: teldef01.out with tede1360.out

Legend [μm]: min = -35.10, max = 0.66



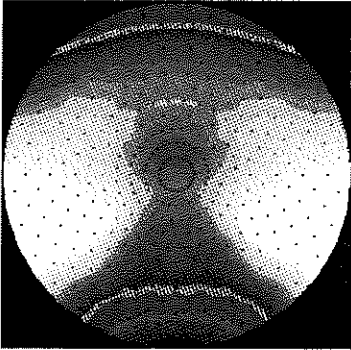
Gravitational Deformation
for Elevation = 60°

Residuals relative to a
Reference Surface:
Mean of Elevations:
30°, 45°, 60°, 75°

σ r.m.s. = 6.96 μm
Edge taper = 10 db

Files: teldef01.out with tede1360.out

Legend [μm]: min=-147.33, max= 92.63



Gravitational Deformation
for Elevation = 60°

Residuals of a
Weighted Paraboloid Fit:
F = 4875.222 mm
Tilt x = -22.16°
Tilt y = -0.64°

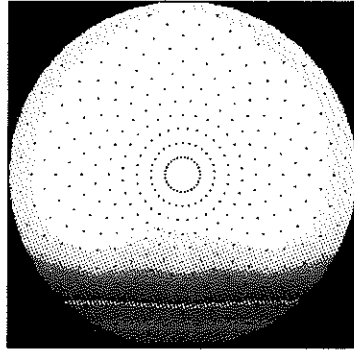
σ r.m.s. = 30.30 μm
Edge taper = 10 db

Translation apex X0, Y0, Z0 (mm): -0.033 0.978 -0.021

Fig. 10: Deformation and error maps for 60° elevation

Files: teldef01.out with tede1375.out

Legend [μm]: min=-354.66, max=-8.24

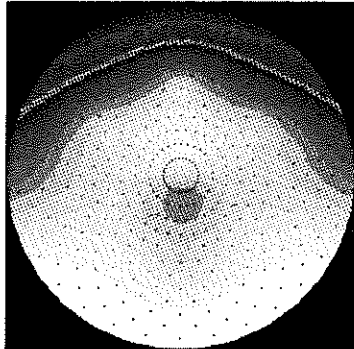


Gravitational Deformation
for Elevation = 75°

Az Displacement
calculated with ALGOR

Files: teldef01.out with tede1375.out

Legend [μm]: min=-105.92, max= 36.65



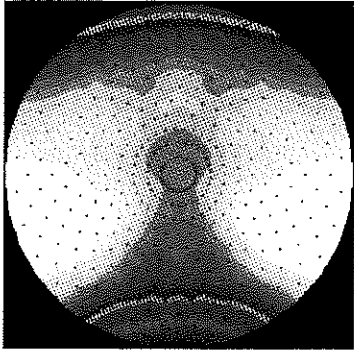
Gravitational Deformation
for Elevation = 75°

Residuals relative to a
Reference Surface:
Mean of Elevations:
30°, 45°, 60°, 75°

σ r.m.s. = 18.47 μm
Edge taper = 10 db

Files: teldef01.out with tede1375.out

Legend [μm]: min=-184.64, max= 86.06



Gravitational Deformation
for Elevation = 75°

Residuals of a
Weighted Paraboloid Fit:
F = 4875.246 mm
Tilt x = -10.60°
Tilt y = -0.36°

σ r.m.s. = 30.47 μm
Edge taper = 10 db

Translation apex X0, Y0, Z0 (mm): -0.019 0.413 -0.022

Fig. 11: Deformation and error maps for 75° elevation

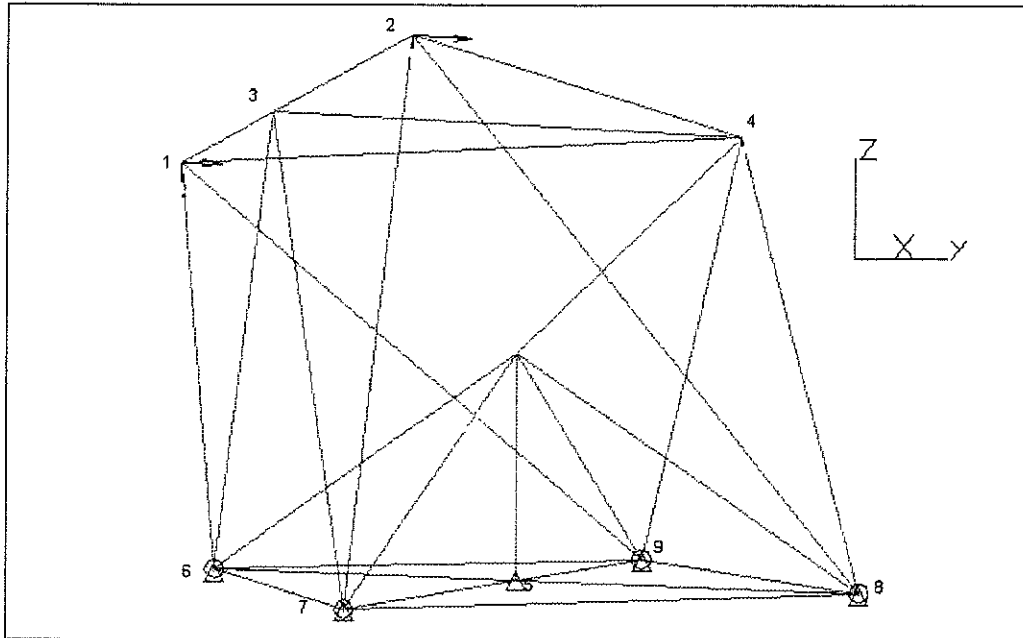


Fig. 12: Computer model of pedestal under simulated wind loads

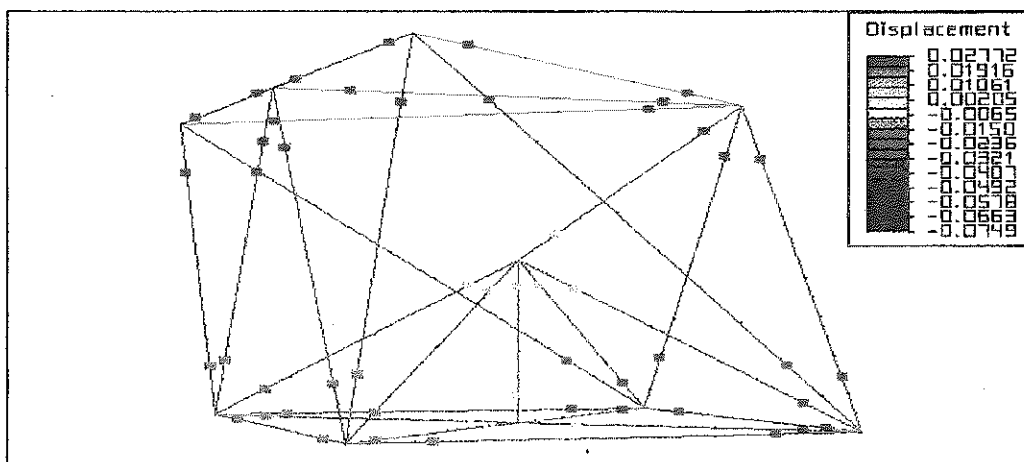


Fig. 13: Deformations in y-direction

From the maps for the z-displacements it can be seen that they are below 0.5 mm and therefore give hope to the specified fixed focus performance with the new reflector. And indeed the r.m.s. values of the residuals relative to the reference elevation of 52.5 deg. give $\sigma < 20\mu m$ which is quite an acceptable value (see maps in the middle of the figures).

The third maps in the figures indicate that the focus variation of the individually fitted paraboloids in the operational range varies by only $\Delta f = \pm 58\mu m$.

From the IRAM 15-m dishes it is known that the reflectors have nearly no thermal problems, due to their carbon fibre back-up structure. This means values of typically $\sigma < 7\mu m$ r.m.s. can be expected for the new dishes, but computational verification must still be done.

The wind load contribution has neither been studied yet; again from comparison with the IRAM dishes it should be less than $20\mu m$ r.m.s. due to the fact that

1. the wind speed is reduced to 10 m/s which gives at least a factor of 2 less for the wind load and
2. the back-up structure is considerably stiffer.

5.2 Computations on the Pedestal

For the computations the model of the pedestal was prepared like shown in Fig. 12:

- the model is blocked in the center in x, y, z-direction
- the four corners are resting on gap elements permitting vertical lift-off but blocking the model in neg. z-direction
- the four corners are blocked in x-direction
- the wind load is applied in horizontal y-direction on the corresponding upper nodes of the structure
- a preload is applied to the central bar which results in a 0.15 mm vertical displacement of the upper end of this element.

The windloads were calculated assuming the wind direction parallel to the optical axis of the dish (i.e. dish in horizon position) under a speed of $v = 10$ m/s. A load factor of $c = 2$ was applied. This resulted in a load of $F = 16800$ N which was applied in equal parts to the corresponding two nodes. The deformations in y and z directions are indicated in Fig. 13 and 14. They can be kept below 0.1 mm which is very important for the phase stability of the telescope.

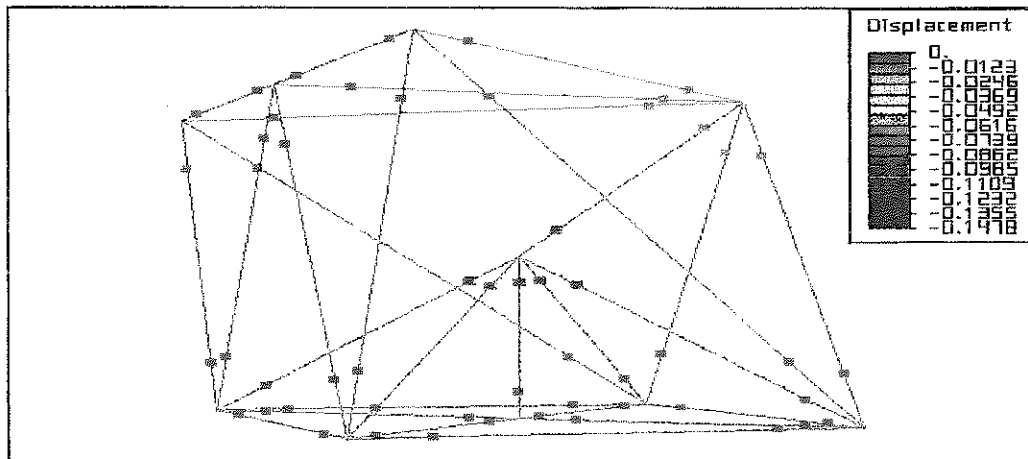


Fig. 14: Deformations in z-direction

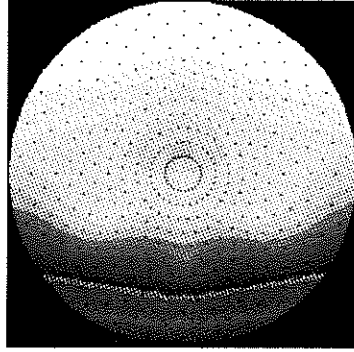
6 Conclusion

The first computational verifications on critical items of the LSA telescope performances show that it will be possible to build a simple and robust “work-horse” to be operated on a remote desert site. Applied materials and technologies are state of the art and proven to be long lasting. The design minimizes the number of components thus increasing the reliability, reducing maintenance and last but not least costs.

Further studies have to be done (see table below), particularly under thermal and wind loads but also to improve the general layout, overall performance and production aspects. The industrially available laser measuring system has to be adapted to the telescope structure. It will then allow to control the position of the dishes independently of deformations in the pedestal.

Files: teldef01.out with tede1330.out

Legend [μm]: min = -398.65, max = 135.72

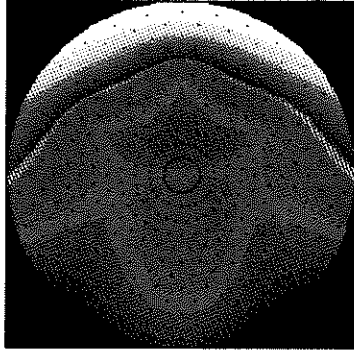


Gravitational Deformation
for Elevation = 30°

Az Displacement
calculated with ALGOR

Files: teldef01.out with tede1330.out

Legend [μm]: min = -13.98, max = 103.92



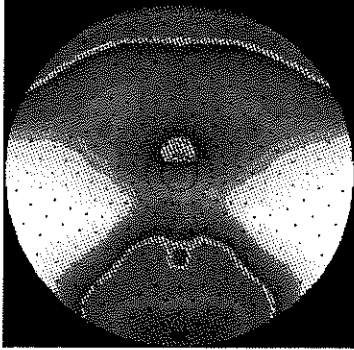
Gravitational Deformation
for Elevation = 30°

Residuals relative to a
Reference Surface:
Mean of Elevations:
30°, 45°, 60°, 75°

 σ r.m.s. = 18.92 μm
Edge taper = 10 db

Files: teldef01.out with tede1330.out

Legend [μm]: min = -94.85, max = 90.04



Gravitational Deformation
for Elevation = 30°

Residuals of a
Weighted Paraboloid Fit:
F = 4875.131 mm
Tilt x = -40.36°
Tilt y = -1.07°

 σ r.m.s. = 25.36 μm
Edge taper = 10 db

Translation apex X0, Y0, Z0 (mm): -0.055 1.888 -0.014

Fig. 8: Deformation and error maps for 30° elevation

ACTIVITIES ON LSA TELESCOPES (Phase 2)

N°	Item	Man Years	Costs (MFF)
01	Studies on the telescope structure <ul style="list-style-type: none"> • FEA (1.0 MY ; 0.5 MFF) • Design (2.0 MY ; 1.0 MFF) 	3.0	1.5
02	Studies on elevation actuator	0.5	0.4
03	Studies on azimuth drive system	0.5	0.4
04	Studies on metrology system	1.0	1.0
05	Definition of panel system	0.5	1.8
06	Definition of node-strut-system	0.5	1.3
07	Definition of surface measuring system	1.0	2.0
08	TOTAL	7.0	8.4

References

- Bremer, M., 1996, private communication
 Delannoy, J., 1985, in ESO-IRAM-ONSALA workshop on (sub)millimeter astronomy
 Delannoy, J., 1996, private communication
 Downes, D., 1985, LSA report

Millimetre Receiver Technology for a Large Array

James W. Lamb

IRAM, 300 rue de la Piscine, F-38406 Saint-Martin D'Hères, France

Abstract

The current state of receiver technology for millimetre wave receivers is reviewed with regard to the requirements of a large interferometric array. Optics, amplifiers, mixers, local oscillators and cryogenics are all considered. It is concluded that the technology exists today to construct receivers of high sensitivity, but technical developments should continue to improve reliability and useability.

1 Introduction

The possibility of making a large interferometer array rests on the ability to build large numbers of sensitive, reliable receivers at moderate cost. Current technology for receivers for single dish and small arrays is quite mature with sensitivities approaching the quantum limit (Carlstrom & Zmuidzinas 1996). Receivers today routinely use SIS mixers with niobium junctions as the first stages. Local oscillator (LO) sources are typically Gunn oscillators with frequency multipliers where necessary. In such a short article it is impossible to review all aspects of the Technology, and the References must be regarded as representative rather than exhaustive.

1.1 Requirements for Receivers

Some requirements for receivers are given below in Table I. For the purposes of this review these are indicative rather than definitive.

Table 1. Receiver requirements for a large millimetre array

Parameter	Specification
Frequency range	40–350 GHz
Noise temperature	$4h\nu/k$ (SSB)
IF Bandwidth	2 GHz
Polarisation	Dual-linear
Phase	Good stability, low noise
Reliability	“Good”
Cost	“Low”

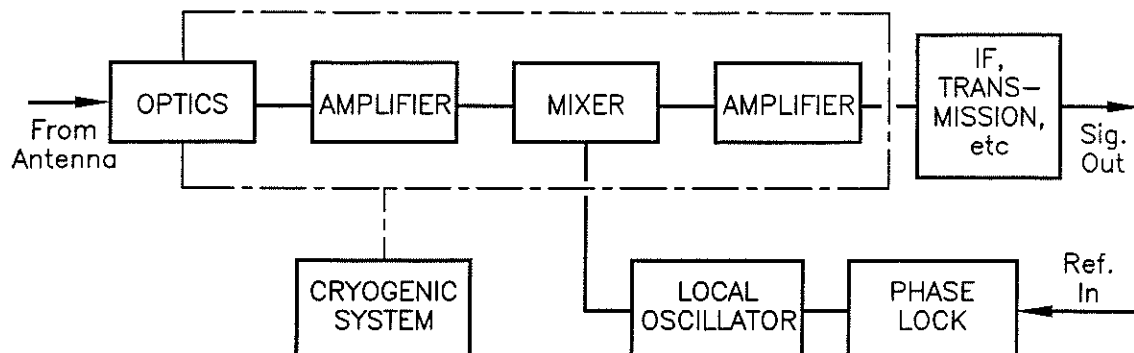


Figure 1: General block diagram of a heterodyne, showing the sections discussed in the text.

A phased introduction of frequency bands should be envisaged, but ultimately one could consider contiguous coverage of the whole millimetre band. It is reasonable not to exclude atmospheric absorption bands which could be rather narrow at a good site. A 30% bandwidth for each receiver would result in six bands from 65 to 400 GHz — dual-polarisation on 60 antennas would require 720 channels.

The importance of reliability can be seen by considering the result of failures in components. For example, assume each of N antennas has M backshort drive motors with an average time to failure of t_{mtbf} and that it takes a time t_{rep} to repair. For $t_{mtbf} = 3$ yr, $t_{rep} = 1$ day, $N = 60$, and $M = 12$ one expects a failed motor almost half of the time. Clearly the reliability of individual components should be extremely good.

1.2 General Receiver Scheme

Most receivers follow the block diagram given in Fig. 1. An optical system brings the signal from the antenna and perhaps performs other functions. At present few systems have input amplifiers and the first stage is usually a mixer. A phase-locked LO is required for the mixer to downconvert the signal to the intermediate frequency (IF) where it may be amplified and processed by later stages. Since all current low-noise receivers operate at cryogenic temperatures a refrigeration system capable of a temperature of 2–20 K, depending on the application, is required.

2 Optics

The minimum function of the optics is to couple the signal from the antenna into the mixer. Typically a feed horn is used and one or more lenses or focusing mirrors may also be required. More complicated devices are often used, including: grids, quarter/half-wave plates, Fabry Perots, Martin-Puplett Interferometers, and prisms. Although optical losses

may be quite small in the millimetre band they are still significant in comparison with very low-noise receivers. Several loss mechanisms should be considered. *Diffraction* losses result from the truncation of the optical beam. Clearances should be sufficiently large to make this negligible, and large apertures are particularly required near images of the sky, while smaller ones can be accepted near images of the telescope aperture. Surface accuracies of $\sim \lambda/100$ are needed. *Ohmic* losses in reflectors depend on conductivity, wavelength, and surface finish. At 300 GHz the loss may be 0.18% for Al, and 0.13% for Cu so some ohmic losses at room temperature are acceptable. *Dielectric* losses are proportional to frequency and depend on the material and preparation. Low-loss plastics attenuate by $\sim 0.5\% \text{ mm}^{-1}$, so cold losses may be acceptable for lenses.

3 Mixers

Mixers may be classified according to the nonlinear device (SIS, SIN, Josephson junction, hot-electron bolometer); structure (waveguide, planar); and function (double sideband, image rejecting, image separating). Only superconductors are considered here as there are no other devices with competitive sensitivities at these frequencies.

3.1 Devices

SIS mixers are currently the most sensitive in the millimetre range, and representative state-of-the-art performance is shown in Fig. 2, taken from Karpov (1994), Payne et al. (1994), and Kooi et al. (1995). The double sideband noise approaches $2h\nu/k$ so that the SSB noise is close to the $4h\nu/k$ goal. SIN mixers have the potential benefit that there are no perturbing Josephson currents, but because the non-linearity is less than for SIS devices the performance is currently three times worse (Karpov et al. 1995b). Josephson mixers rely on pair tunneling and require much smaller area junctions than SIS mixers. Lack of a significant shunting capacitance means that many harmonics are significant and the noise which is down-converted by the shunt resistance results in relatively poor noise performance (Taur 1980). Furthermore, there are regimes where chaotic behaviour may dominate. Hot electron bolometers (Gershenson et al. 1990; McGrath 1995) can have very short thermal time constants and therefore respond to the beat between an LO and signal to produce an IF output. As a relatively new device, the hot electron bolometer can be expected to improve. However, even theoretically, it is unlikely to be competitive with the SIS mixer at millimetre wavelengths. Noise temperatures of 450 K have been obtained at 100 GHz, with IF's up to 2 GHz (expected to approach 5 GHz)(Okunev et al. 1995).

Niobium is the preferred superconductor for millimetre wavelengths: it is rugged, well understood and its moderate transition temperature yields good results at 4.5 K. Progress has been made with niobium nitride, but the best SIS results are not as good as for niobium (Karpov et al. 1995a). The higher transition temperature is not a significant advantage, though the larger gap voltage could make the Josephson currents less important. "High- T_c " devices are still in early development.

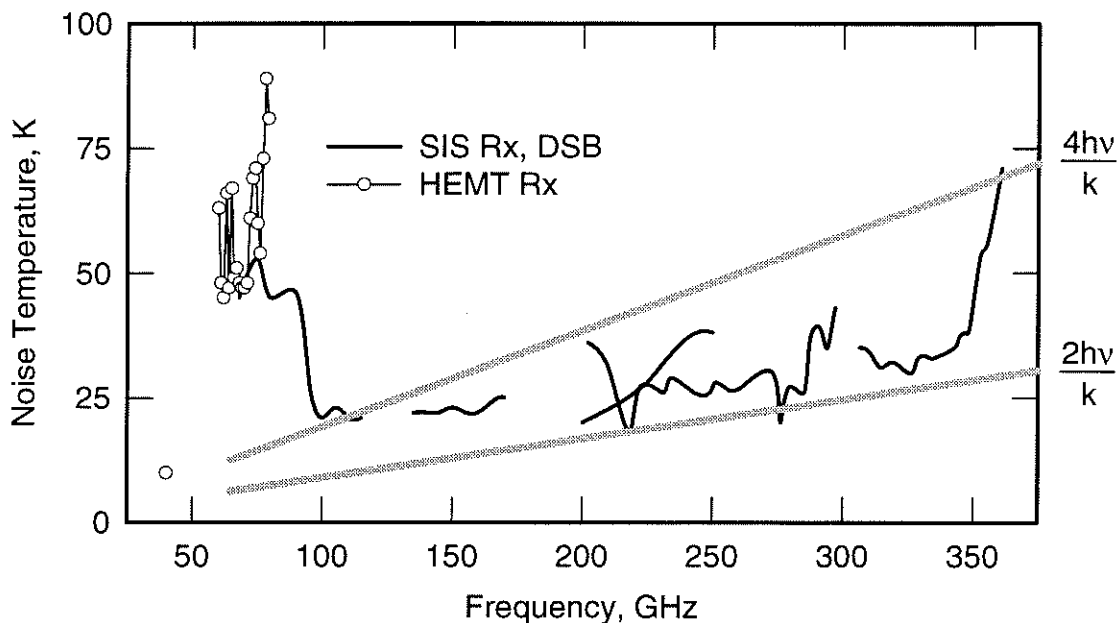


Figure 2: Representative noise temperatures for SIS and HEMT receivers. See text for references.

3.2 Structures

The best results in the millimetre band have been achieved with waveguide mixers. Corrugated horns are almost ideal, having good beam shapes, low cross-polarisation, and good match over bandwidths of 40% or more. As waveguide devices they have a cut-off frequency which helps to reject interference. Horns have successfully been made and tested for frequencies up to 3.1 THz (Ellison 1994).

Planar (“Quasioptical”) structures have appeared in several forms, including the bow-tie, log-periodic, log-spiral, double dipole and double-slot. Fabrication of planar devices is simpler than waveguide devices, but they need accurate lenses with anti-reflection coatings. Low noise temperatures have been reported, particularly at higher frequencies, but often the beam couples poorly to a telescope, and there may be cross-polarisation. Good patterns are reported for double-slot antennas (Zmuidzinas & LeDuc 1992) but main beam efficiency is $\sim 70\%$ (c.f., $\sim 99\%$ for a corrugated horn).

3.3 Functionality

The simplest mixers are fixed tuned double-sideband devices with bandwidths of $> 25\%$. Due to the lack of mechanical tuning the reliability is high, and frequency changes are rapid. Image rejection requires a quasioptical or waveguide filter. (In the future a mixer with a very broad bandwidth could be envisaged which could be intrinsically single-sideband. Tuning would then be done within the IF band).

Image rejecting mixers with one or two backshorts are well established. Rejection may degrade as IF bandwidths are increased, but for an interferometer only modest rejection is required — line confusion is avoided by LO phase switching. Moving backshorts will

have some reliability problems and there are also more likely to be problems with stability of the mixer.

An alternative to rejecting the image is to separate the signal from the image using two mixers. Some demonstrations of the concept have been made and 25 dB separation has been achieved over narrow bandwidths, although at the expense of doubling the mixer noise (Akeson et al. 1993). The main advantages are when the atmospheric and spillover noise are dominant, which may not be true on a good site.

4 Local Oscillators

Powers of order $100\mu\text{W}$ are required from LO sources. Although the power at the mixer is much lower there are significant losses for the phase-lock system, waveguides, and couplers. Injection without tuning implies that coupling of the order of -20 dB is required. To match receivers, bandwidths of $\sim 30\%$ are required. For an interferometer LO's need to be phase-locked and have low phase and amplitude noise.

4.1 Solid State vs Superconducting Oscillators

Solid state oscillators have a well developed technology with high power, low noise and narrow intrinsic linewidths. They usually operate at ambient temperature, but loss into a dewar may be as low as 1 dB. There are mechanically or electrically tuned oscillators, and appropriate multiplier technology which is well developed. Superconducting technology is less well established. Fundamental operation is possible over the millimetre band and the devices operate in the cryostat. Intrinsic linewidth is relatively large, and though they are electrically tuned suitable phase-locking has yet to be demonstrated.

4.2 Solid State Oscillators and Multipliers

Gunn oscillators, prevalent today, achieve fundamental operation to at least 170 GHz and second harmonic operation to 290 GHz with $300\mu\text{W}$ output power (Eisele & Haddad 1994). Phase-locking is relatively simple and the oscillator phase and amplitude noise do not contribute significantly to the system sensitivity (Padin et al. 1988). Significant tuning bandwidths may only be obtained with mechanical tuners. IMPATT oscillators are electrically tunable but generally too noisy to use. Progress has been made with TUNNETT devices, having 70 mW at 105 GHz, low phase-noise, and electrical tuning, although not yet with large continuous tuning bandwidth (Eisele & Haddad 1995). Transistor oscillators may be made up to 215 GHz with $\sim 1\mu\text{W}$ (Rebeiz 1994) higher powers may be expected in the future. Electrically tuned low phase-noise YIG oscillators tune from 26 - 40 GHz (Mede et al. 1996).

In concert with oscillator development, improvements have been seen in multipliers. Advances in varactor technology (materials, air-bridges, parameter optimisation) have brought better efficiency and reliability (Crowe 1995). Some benefits can be obtained from cryogenic cooling including higher power handling and improved efficiency (Erickson et al. 1992). Improvements in waveguide circuit design have produced good fixed-tuned performance.

An electronically-tuned LO system for a Schottky mixer array has been built by Erickson et al. (1992). It uses a YIG tuned FET from 29 – 38 GHz, followed by a power amplifier and varactor tripler. Although the oscillator is electrically tuned a mechanically tuned filter is required to reject the amplifier noise. With lower noise amplifiers and smaller LO coupling for SIS receivers this may be avoided.

4.3 Superconducting Oscillators

Josephson junction (JJ) array and flux-flow oscillators (FFO) are both under development for LO sources. JJ's generate power by Josephson oscillations, while FFO's depend on the rapid transit of flux quanta along an extended Josephson junction. Although significant power can be generated, spectral linewidths are relatively large (~ 0.1 MHz). Both devices are rather complex and will require significant development. For JJ oscillators, arrays of devices are required to achieve required power levels. Effective synchronisation of the devices is complex and competes with the tuning bandwidth (Booi 1995). Investigations continue on FFO's to determine the constraints on linewidth and other properties (Henne et al. 1995).

5 HEMT Amplifier Technology

The maximum frequency of a HEMT (high electron mobility transistor) works is a function of material and geometry. Noise temperature is roughly proportional to frequency: 1 K GHz^{-1} is typical, 0.5 K GHz^{-1} achieved and 0.25 K GHz^{-1} predicted. The lowest noise has been obtained with discrete transistors. Noise temperatures of 50 K at 75 GHz have been reported for an amplifier at 20 K (Posieszalski 1993), comparable to the performance of SIS receivers at frequencies approaching 100 GHz (Fig. 2). Monolithic amplifiers are attractive for large quantities, and integrated amplifiers at 77 – 110 GHz (Wang et al. 1993), and 130 – 150 GHz (Wang et al. 1995) have been fabricated. Limits of the present $0.1 \mu\text{m}$ gate technology are being approached and major technological steps are needed to reach higher frequencies. Although HEMT's may not replace SIS mixers as first stages in the near future, they may give wide bandwidths when used as IF amplifiers. Bradley (1995) has built an amplifier at 18 – 26 GHz with a noise temperature of ~ 7 K. Progress has been made in matching HEMT's to SIS mixers (Weinreb 1987; Padin et al. 1995).

6 Cryogenics

It seems almost certain that temperatures around 4 K will be required. Although hybrid dewars have been successfully used on small arrays (5 – 6 antennas, 2 channels (Blondel et al. 1995)), liquid cryogenics are impractical for a large interferometer array, and closed-cycle systems will be used. Joule-Thompson (JT) refrigerators have been in operation for many years with good reliability statistics. High capacities at 4 K are easily achieved with 2–3 W being common. Temperature stability of a couple of millikelvin can be obtained on timescales of up to several minutes or more. Such systems have been used on telescopes for several years for masers and, for a shorter period, SIS receivers (Woody et al. 1985; Payne et al. 1994).

More recently 2-stage or 3-stage Gifford-McMahon (GM) refrigerators have been developed using rare earth compounds for the heat exchanger. As with most GM refrigerators, the temperature is subject to variations over the displacer cycle, but it can be smoothed out by appropriate design. A 4-K GM refrigerator has been designed used for a millimeter receiver (Plambeck et al. 1992). No data are available yet on the long-term reliability or lifetime of these systems.

7 Conclusions

All the technology to build receivers for an array operating at millimetre wavelengths exists today. Sensitivities approach quantum limits, and frequency coverage for a single receiver may be $\sim 30\%$.

As a baseline model, the most likely design of receiver would have several channels in a 4 K dewar with a JT refrigerator. A simple optical path with a grid to separate the two polarisations and some mirrors to direct the beam into corrugated feed horns would be used. DSB waveguide SIS mixers would be followed by low noise wide-bandwidth (> 5 GHz) HEMT amplifiers. Solid state local oscillators at low frequencies (< 40 GHz) followed by fixed tuned multipliers and HEMT amplifiers could provide an electronically-tuned, low-noise, phase-locked source.

The challenge facing receiver builders is how to make the systems reliably and cheaply. A very significant engineering effort is required to take millimetre technology from the "custom" level to "production" volumes.

References

- [1] Akeson, R. L., Carlstrom, J. E., Woody, D. P., Kawamura, J., Kerr, A. K., Pan, S.-K., Wan, K (1993): Proc. Fourth Int. Symp. Space Terahertz Technology, LA, USA, 12-18
- [2] Blondel, J., Carter, M., Karpov, A. Lazareff, B. Mattiocco, F. (1995): Digest 20th Int. Conf. on Infrared and Millimeter Waves, Florida, USA, Dec. 1995
- [3] Booi, P. A. A. (1995): *High-Frequency Array Oscillators Based on Nb/Al-AlO_x/Nb Junctions*, Thesis, Universiteit Twente
- [4] Bradley, R. (1995): Private communication
- [5] Carlstrom, J. E., Zmudzinas, J. (1996): "Millimeter and Submillimeter Techniques", to appear in *Reviews of Radio Science 1993-1995* (OUP, Oxford)
- [6] Crowe, T. (1995): Third Int. Workshop on Terahertz Technology, Zermatt, Switzerland
- [7] Eisele, H. Haddad, G. I. (1994): Electron. Lett **30**, 1950-1951
- [8] Eisele, H. Haddad, G. I. (1995): IEEE Trans. Microwave Theor. Tech **43**, 210-212

- [9] Ellison, B. N., Oldfield, M. L., Matheson, D. N., Maddison, B. J., Mann, C. M. Smith, A. F. (1994): Internat. Seminar on Terahertz Electronics (Part II), Lille, France, June 13-14
- [10] Erickson, N. R., Goldsmith, P. F., Novak, G., Grosslein, R. M., Viscuso, P. J., Erickson, R. B., Preadmore, C. R. (1992): IEEE Trans. Microw. Theor. Tech. **40**, 1-11
- [11] Gershenzon, E. M., Golt'sman, G. N., Gogidze, I. G., Gusev, Y. P., Plantev, A. I., Karasik, B. S., Semenov, A. D. (1990): Superconductivity **3**, 1582-1597
- [12] Henne, P, Kohlstedt, H., Ustinov, A. V., (1995): Third Int. Workshop on Terahertz Technology, Zermatt, Switzerland
- [13] Karpov, A., Maier A., Blondel, J., Lazareff, B., Gundlach, K.-H., (1995a): Proc. Sixth Int. Symp. Space Terahertz Technology, Pasadena, USA, 344-354
- [14] Karpov, A., Maier A., Blondel, J., Lazareff, B., Gundlach, K.-H., (1995b): Int. J. IR and Millimeter Waves **16**, 1299-1316
- [15] Karpov, A (1994): Proc European SIS Users Meeting, Köln, Germany
- [16] Kooi, J. W., Chan, M., Bumble, B., LeDuc, H. G., Schaffer, Phillips, T. G. (1995): IntJ. IR and Millimeter Waves **16**
- [17] McGrath, W. R. (1995): Sixth Int. Sympos. Space Terahertz Technology, Pasadena, 216-227
- [18] Mede, F., Gleissner, J., Brennemann, A., Beyer, A. (1996): Microwave Eng. Europe, Jan, 29-33.
- [19] Okunev, O., Dzardranov A., Gol'tsman, G., Gershenzon, E. (1995): Proc. Sixth Int. Symp. Space Terahertz Technology, Pasadena, USA, 247-253
- [20] Padin, S., Woody, D., Scott, S. L. (1988): Radio Science **23**, 1067-1074
- [21] Padin, S. Woody, D. P., Stern, J. A., LeDuc, H. G., Blundell, R., Tong, C.-Y. E., Pospieszalski (1995): Proc. Sixth Int. Symp. Space Terahertz Technology, Pasadena, USA, 134-139
- [22] Payne, J. M., Lamb, J. W., Cochran J. G., Bailey, N. J. (1994): Proc. IEEE **82**, 811-823
- [23] Plambeck, R, Thatte, N., Sykes, P. (1992): Proc 7th Int. Cryocooler Conf., Santa Fe, NM, Nov. 1992
- [24] Pospieszalski, M. W. (1993): Proc 23rd EuMC
- [25] Rebeiz, G. (1994): IEEE Antennas Propagat. Magazine **36**, 36-38.
- [26] Taur, Y. (1980): IEEE Trans. Electron Devices **ED-27**, 1921-1928

- [27] Wang, H., Lai, R., Chen, S. T., Berenz, J. (1993): IEEE Antennas and Propagat. **3**, 381-382.
- [28] Wang, H., Lai, R. Lo, D. C. W., Streit, D. C., Liu, P. H., Dia, R. M., Pospieszalski, M. W, (1995): IEEE Microw. and Guided Wave Lett. **5**, 150-152
- [29] Weinreb, S. (1987): IEEE Trans. Microw. Theor. Tech. **MTT-3**, 1067-1069
- [30] Woody, D, Miller, R. E., Wengler, M. J. (1985): IEEE Trans. Microw. Theor. and Tech. **MTT-32**, 9095
- [31] Zmuidzinas, J., LeDuc, H. G. (1992): Trans. Microw. Theor. Tech. **40**, 1797-1804

(Note: this paper was reproduced from the original in "Science with Large Millimetre Arrays" (1996, Springer, Berlin; ed. P. Shaver), with the kind permission of Springer-Verlag.)

Receivers for the LSA

Bernard Lazareff

IRAM, 300 rue de la Piscine, F-38406 Saint-Martin D'Hères, France

Abstract

Various aspects of receiver design for a large array are reviewed under the aspects of sensitivity and reliability. Some critical issues are identified and estimates are proposed for the manpower and hardware funding needed in the design study phase. This contribution builds on the preceding report prepared by J. Lamb, and will therefore not repeat the points already addressed in that report.

1 Introduction

The LSA project's main goal is to achieve a major jump in sensitivity over current mm arrays. Sensitivity results from the combination of large collecting area and low system noise. There are ultimate limits to system noise due to the atmospheric background, and therefore there is no substitute for a large collecting area. However, one should make sure that the major financial effort needed to build 10000 m² of antennas is put to the best use. Therefore, receiver sensitivity is a key issue for the LSA.

With on the order of 50 antennas (and several receiver channels per antenna) operating on a remote high altitude site, reliability is maybe even more important than the ultimate improvement in performance.

I do not address receiver cost in this contribution because receivers are expected to be a non-negligible, but still modest fraction of the antenna-based costs.

2 Cryogenics

As mentioned in the report of J.Lamb, closed-cycle cryogenerators have been in operation in a number of observatories for several years. By the time the LSA project enters the detailed design phase, there should be some field experience with IRAM's cryocoolers at both sites. In the writer's opinion, for a project of the size of the LSA, that will strain the manpower resources of the astronomical community, cryogenics should rest on a commercial solution with an established reliability record. One should note that at present the largest volume commercial application for 4K cryocoolers is in medical scanners, with maglev only a potential market at the moment. It is recommended that a market review be conducted just before the detailed design phase. Besides technical specs like cooling power, temperature stability, vibration level, and reliability, the following practical aspects should be considered : maintenance intervals and costs, air cooling versus water cooling (at the envisaged operating altitude).

Notation	Value	Name	Notes
T_{rec}	20K	Rx noise, DSB tuned	
T_{recS}	28K	Rx noise, SSB tuned	(a)
T_{recW}	25K	Rx noise, 20GHz BW IF	(b)
T_{recQ}	40K	Rx noise, quadr. IRM	(c)
T_{recH}	100K	Rx noise, HEMT	(d)
F_{eff}	0.9	Forward coupling	(e)
T_{cab}	300K	spillover term. temp.	
τ	0.14	atm. opacity	(f)
T_{sky}	250τ	sky rad. temp.	
L_{DS}	0.025	dipl. loss signal path	(g)
L_{DI}	0.07	dipl. loss image path	(h)
T_{cold}	10K	cold image load	(i)

Table 1: Values of parameters adopted for comparing receiver models in the 1.3mm band. Notes : a) using empirical result that when a mixer is SSB tuned, its DSB noise increases by $\times 1.4$; b) assuming 10K increase in IF noise and 0dB mixer conversion loss; c) The mixer noise of a quadrature IRM is (ignoring losses) twice that of the individual mixers (but it is SSB!), this degradation may be pessimistic for receiver noise; d) Optimistic (?) estimate at less than 0.5K/GHz; e) see discussion of optics; f) 1mm PW, 45° elevation; g) three reflection, $1.5\times$ theoretical; h) as above, plus two mirrors and window; i) difficult to thermalize to 4K; h+i) the effective value for the cold load is supported by experimental values for the IRAM PdB receiver.

3 Signal Frontend

Five representative receiver models are evaluated below :

1. SIS mixer tuned SSB, 4GHz IF BW
2. wideband DSB SIS mixer, 4GHz IF BW, cold image dump via an optical diplexer
3. wideband DSB SIS mixer with 20GHz IF BW
4. quadrature image-rejecting SIS mixer
5. HEMT RF amplifier

In order to keep the discussion simple, we focus on just one atmospheric window : 1.3mm; atmospheric properties are evaluated at 240GHz.

We give in Table 1 the values of parameters adopted for the evaluation. Receiver temperatures values are *measured* DSB, independent of the actual response of the receiver; that is how noise values are most often quoted in the technical literature, i.e. the result of a Y-factor measurement.

The results are presented graphically on Fig. 1, expressed as SSB system temperature in the receiver reference plane, i.e. omitting the factor $e^\tau F_{eff}^{-1} = 1.28$. Table 2 gives the values of T_{sys} both in the receiver reference plane and outside the atmosphere on the T_A^* scale.

From the models analyzed in this section, one concludes that atmospheric radiation and spillover account for the majority of system noise in all cases; that SSB operation

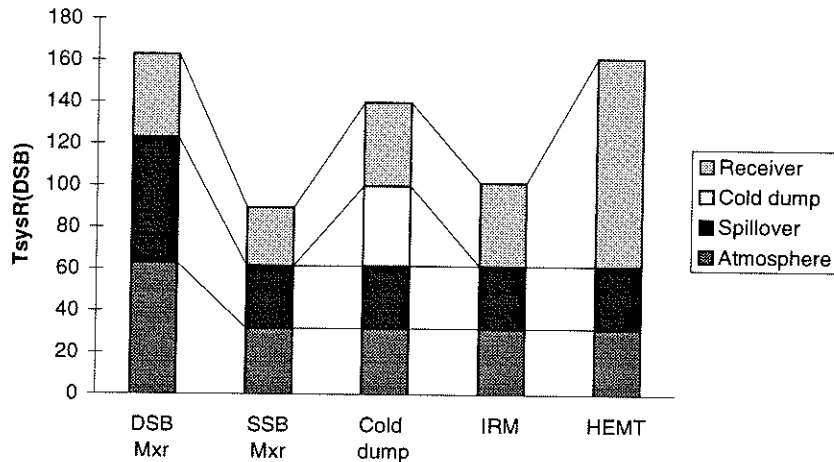


Figure 1: Breakdown of contributions to system noise for five receiver models

Model	T_{sysR}	T_A^*
DSB Mxr	163	208
SSB Mxr	89	114
Cold dump	140	179
IRM	101	129
HEMT	161	206

Table 2: System temperature in the receiver plane and outside the atmosphere for five receiver models

is highly desirable; and that a cold image dump does not give a substantial advantage over DSB operation. This leaves only tunable mixers and quadrature IRM's as attractive solutions for spectroscopic observations. One should note that high rejection of the image band is not necessary in the present context. We have not presented a model with an intermediate rejection in the above comparisons, because we do not know in detail how T_{rec} varies with rejection; one should keep in mind that most of the benefits of rejection of input noise in the image band are obtained with a modest rejection of the order of 6dB. Because they have no moving parts, quadrature IRM's would be the preferred over tunable mixers : we strongly recommend a development effort in that area.

Continuum observations present a different case: there the figure of merit is T_{sysDSB}/\sqrt{B} . Increasing the bandwidth may carry a penalty in receiver noise, because of the higher IF noise temperature. We show in Table 3 that the increase in bandwidth from 4 to 20GHz offsets even a doubling in receiver noise. If such a configuration would be found attractive for detection of dust emission in distant galaxies, and *if* the IF transmission and processing problems could be solved, one might consider a dedicated "wideband" receiver channel in the 1.3mm band which seems the most adequate for these observations.

T_{rec}	B	T_{sysDSB}	T_{sysDSE}/\sqrt{B}
20	4 GHz	81	41
40	20 GHz	101	23

Table 3: Comparison of two models for continuum detection; all other parameter values are taken from Table 1.

4 Local Oscillator Systems

Most LO systems now in operation for mm bands rely on Gunn oscillators and, above the 3mm band, varactor multipliers. Gunn oscillators have normally two mechanical adjustments. Some fixed-tuned multipliers have been demonstrated with bandwidths up to 25–30% (Millitech). Other “hidden” parts also have mechanical adjustments, e.g. variable attenuators. LO systems with no moving parts would *a priori* be more reliable. Two possibilities exist which still require substantial development :

1. Producing a beat between two submm/FIR lasers; however, because the effective frequency is a fraction of the frequency of either laser, this poses stringent requirements on the spectral purity of the lasers. Potentially, a single such system might produce LO power for all the frequency bands of the instrument. If gas lasers are used, the associated plumbing’s reliability has to be verified.
2. YIG-tuned microwave oscillator followed by a chain of solid-state multipliers, either active (HEMT) or passive (varactor fixed-tuned).

5 Phase Compensation Receiver

Compensation of atmospheric phase is essential for good quality imaging at long baselines. More modelling, development, and experimenting is necessary to determine the best operating frequency(-ies) near 180GHz.

6 Optics

The optical layout is tightly coupled on one hand, to the cryostat design, and on the other hand, to the scientific and overall system drivers for the project : choice of frequency bands, which bands observed simultaneously, etc. . .

In the best of the receiver models examined above, spillover accounts for roughly 1/3 of the system noise. Prevalent wisdom is that for an interferometer, the optimum edge taper is 10–12dB. Spillover can easily be improved by under-illumination, but at the expense of aperture efficiency. Studies of illumination optimization by shaped optics have been made (Paine 1994, Lamb 1994). These studies should be reviewed, and maybe followed upon, with the goal of optimizing A_{eff}/T_{sys} , based upon expected values of T_{rec} . However, only modest gains can be expected.

7 Recommended Work for the Design Study Phase

7.1 Cryogenics

No development work. Collect reliability data from actual users of commercial equipment (may require cooperation from manufacturer to provide references). Explore solutions for periodic maintenance : contract or train in-house personnel ? Even if maintenance manpower is in-house, parts have to be bought from manufacturer : negotiate price of parts for periodic maintenance not only before cryogenerators are bought, but before the design is committed to a particular brand/model. See other points mentioned in Sect. 2.

Another point is maybe premature at this stage, but is mentioned for the record. Early enough into the project, and certainly before the construction and even prototyping phase, reliable and *traceable* supplies for critical materials should be established. This concerns, e.g. high purity copper characterized for thermal conductivity at low temperature, dielectrics characterized for RF and IR attenuation, as well as machinability.

engineer 6mm@50% + 20kFF travel

7.2 Signal Frontend

1. Development work on quadrature IRM's. Goals : reasonable noise (below 50K) and rejection (6dB or better). **Rx engineer 3my@75% + Rx technician 2my@50% + SIS technician 2my@50% + masks 60kFF + workshop 2my@25%**
2. Development and testing of tunable mixer designed for high reliability. **Rx engineer 2my@50% + Rx technician 2my@50% + workshop 2my@25%**

The above estimates assume that the development group is appended to an existing institute that allows access to heavy equipment (e.g. network analyzer) which is absolutely necessary but is used only a small fraction of the time. Available local expertise is also assumed to be available. The manpower and equipment estimates would be much higher if the development group would be built from scratch.

Broad (anything more than 1GHz) IF bands probably requires integration of (part of) the IF amplifier into the mixer. Part of this work could be done in parallel with either of the above work packages. In either case, add **IF engineer 2my@50% + travel 20kFF**.

Work in mm-wave HEMTs should be pursued to reap benefits from possible device improvements in the future. Possibly work in Bonn or Yebes could be encouraged and/or supported with wafer purchases. **500kFF**. All mm-wave laboratory equipment is assumed to exist. If LSA-related development work is set up in an independent workgroup, on the order of 500kFF should be added for equipment.

7.3 Local Oscillator Systems

1. laser systems fact-finding : find out about ongoing work at NRAO **engineer 2mm + travel 10kFF**
2. laser systems development : **engineer 2my@100% + technician 2my@100% + equipment 1000kFF (??)**
3. solid state system without moving parts **engineer 2my@75% + technician 2my@25% + parts 400kFF**

7.4 Phase Compensation Receiver

1. fact-finding on existing developments at other observatories **scientist or engineer 2mm + travel 15kFF**
2. modelling of possible systems (atm opacity, required system stability) **engineer 4mm@100% + scientist 4mm@100%**
3. development, construction, and testing (on existing telescope) of one pair of prototype receivers **engineer 2my@100% + technician 2my@100% + 800kFF**

7.5 Optics and Cryostat Layout

1. cryostat & optics layout **engineer 18mm@100%**
2. shaped optics for optimized illumination **engineer 6mm@50%**

Transmission of Interferometer Signals in the Future

M. Torres

IRAM, 300 rue de la Piscine, F-38406 Saint-Martin D'Hères, France

The IF bandwidths to be treated in modern interferometers will evolve to 2 to 8 GHz contiguous band per receiver, and at least 2, perhaps 4, simultaneous receivers per antenna. On another hand, baseline lengths will change drastically, up to 4 to 20 kms. Under such conditions, signal transport systems will become one of the most critical points in the interferometers. We point out that the same questions arise for the mid-term evolution of instruments like the Plateau de Bure array, as well as for future large scale projects.

We may separate the problems in two categories: **Downlink** (from the antenna to the central building) and **Uplink**.

1 Downlink

Assuming full two-bit sampling to avoid excessive digitization losses, the information rate to be transmitted from each antenna is of order 8 to 32 Gbit/s. We actually know how to transport 10 Gbit/s using a single-mode fiber. This rate may be quadrupled using the WDM (optical filter). This is already compatible with our needs, suggesting that the rate problem will become minor in the future, especially since all the telecom industry works in this direction.

On another hand, the synchronisation problem of the data flow coming from the N antennas must be studied in detail. At 10 Gbit/s, the bit length is only 2 cm, i.e. 10^{-6} times the longest baseline lengths (20 km). An active loop will probably be necessary to control the fiber length variations, with a loop timescale of up to several minutes.

Such a system is of same nature than the geometric delay lines, and should probably be merged with it. It is economically likely to be located in the antenna, and integrated in the global frequency synthesis system.

2 Uplink

The reference frequency (and phase) allowing to build the first LO frequency must be carried out to the antenna. The required stability (1 degree at 100 GHz) which must be preserved between two calibration periods corresponds to 0.03 picoseconds, or $0.3 \cdot 10^{-9}$ compared to a transmission time of 100 microseconds. The current fiber stabilities are quite insufficient to match this requirement. Here, we cannot rely on the indirect help from the telecom industry, which has no necessity to control the transmission times to better than a few microseconds. Moreover, we also need to generate locally the second local oscillator and the sampling clocks with known phases.

3 Proposition

All the above problems are interdependants and call for a global solution around the fiber optics and frequency synthesis. To initialize the process, we propose three steps:

1. Construction of a "Survey Report".

This report should collect an comprehensive inventory of the knowledge available in the various observatories.

2. Construction of a "Working Model".

Based upon the survey report, a possible frequency plan should be designed, and global concept for the IF system proposed. The model should be examined in detail, either by a review panel, or in a specialized workshop. This "working model" should also be iterated with the receiver conception.

3. Construction of a "Test System".

Once the "Working Model" is accepted, a test system should be constructed to provide a detailed study of the critical points and to prove the validity and feasibility of the "Working Model" concept.

The estimated manpower and financial needs are

- 1) 6 months (1/2 time position), plus a few missions.
- 2) 6 months (1/2 time position) + 6 months (full time for an opto-electronic engineer), plus workshop cost.
- 3) 18 months (full time engineer position), plus laboratory equipment and components (about 1 MFF).

Easy dialog with the receiver design group is desirable during step 2.

Correlator Developments for (sub)Millimeter Telescopes

A. van Ardenne , A. Bos

Netherlands Foundation for Research in Astronomy, P.O.Box 2, 7990AA Dwingeloo,
The Netherlands

Abstract. The next generation correlators require an order of magnitude more processing power than the ones that are under construction today. Some of the key technological aspects are reviewed here, and the need for an R&D program is emphasised.

1 Introduction

The next generation correlators for the millimeter wave interferometers projected in the next decade, require at least an order of magnitude higher data handling capability when compared with today's instruments. The design experience gained with today's correlators and those under construction for lower frequency radiointerferometry, will undoubtedly constitute the starting point for their design. Straightforward extrapolations will however not provide the required performance for the novel instruments needed in (sub)millimeter astronomy. Hence other, yet fairly unexploited areas of technical R&D need to be addressed. These include high speed sampling techniques, the level of circuit integration and the possible need to apply optical techniques both external (in the case of digitized Intermediate Frequencies) as internal (inside the correlator) signal distribution.

Another concern which may impact the design, relates to the need to properly calibrating and correcting the atmospheric phase uncertainties for which more detailed input to the design is necessary. The correlator configuration and its supporting software, should allow for sufficient flexibility to cope with these effects.

2 Objectives

The next generation of (sub)millimeter radiotelescopes will generally consist of many-element arrays with the major characteristics summarized in Table 1.

The challenge for these large new arrays is to develop the correlator hardware and software capable to handle, control and process signals from a (say) 50-element interferometer for a multitude of astronomical needs. These include eg. a wideband/low resolution and smallerband/high resolution mode while making all four Stokes polarization parameters available in the calibrated and correlated output. This functional requirement is similar with those for existing albeit smaller interferometers at lower radio frequencies. In terms of processing

Table 1. Summary of existing and planned facilities

	European			U.S.		Japan	
	IRAM	LSA	BIMA	OVRO	CMA	MMA	LMA
Telescopes	5(6)x15m	50x16m	9x6m	6(10)x10.4m	OVRO +BIMA	40x8m	50x10m
Coll. area (m^2)	880	10.000	255	510	800	2000	3900
Baseline (km)	0.5(1.5)	5-10(100)	<1	<1	1	3(10)	10
Nr of baselines	10	1225	36	15	105	780	1225
Frequ (GHz)	80-260	40-230	80-115	80-115	80-230	40-360	100-500
occasional	330-360	330-450	210-260	210-260	330-360	>360	600-900
Altitude (m)	2552	>3000	1043	1216	~3000	>4000	>4000
Oper. ($year$)	current	>2005	current	current	~2000	~2005	2006

power ("bit operations per second"), there exists at least an order of magnitude difference due to the larger number of interferometers and the wider bandwidth.

The overall design should be configurable to cope with the different observing requirements i.e. wide bandwidth, choice of interferometers vis a vis baselines, spectral resolution eg. continuum vs. line and the bit correlation scheme. It should be flexible enough for functional extensions due to changing requirements (eg. extension of observing modes). These objectives are much related to the hard- and software architectures and of properly designed interfaces eg. to cope with the different data speeds and volumes. The primary set of different configuration modes are yet to be decided.

Furthermore, the design should be cost-effective, reliable and allow for ease of maintenance e.g. with regard to adequate monitoring and tests and ease of repair.

A starting point for target specifications of a potential correlator design, is given in Table 2. This is based on input from Downes (1995) and subsequent discussions.

Table 2: Target specifications assuming 50 telescopes. Configuration and calibration modes are not yet clear.

Total untuned (IF) bandwidth	4 – 8 GHz/pol/tel
Number of subbands (say: p)	TBD
Number of IF inputs	$p \times 50 \times 2$
Number of baselines	1225
Frequ resolution per polarisation	100 – 50 MHz (continuum mode) 500 – 25 kHz (spectral mode) in 10 MHz
Number of complex points per subband	TBD

Total number of complex channels	$\approx 10^7$ (depending on architecture)
Polarisation	4 Stokes parameters (I,Q,U,V)
Configuration	TBD
Other functions	Phase switching (e.g. for sideband separation, crosstalk and offsets) Gating (e.g. beamswitching, blanking) Adding (compound interferometer)

It is unclear how to implement appropriate calibration schemes in order to cope with the variable atmospheric conditions. These variations occur from telescope to telescope (see Hills (1996)) as well as over any single telescope aperture, the radiofrequency equivalent of 'seeing' cells. Beamswitching and blanking, per band and/or per telescope are probably necessary as means to minimize these effects. In this respect, more advanced calibration schemes apart from the common ones i.e. amplitude and phase-closure and redundancy, for example by using multiple beams taking advantage of the near-field of the troposphere and even image-plane correlators, should be given some thought.

As also suggested in Escoffier (1995), it is worth considering a dedicated continuum correlator as this is the main driver for the highest speeds needed while requiring relatively simple operations on the data. In this case attention should be given to the so-called smearing effect due to the non-compensated delay across the band.

For spectral line observations, a correlating scheme with minimal loss should be considered. For example, a three bits per channel correlation results in only a few percent sensitivity loss as compared to the ideal (analog) case. This must be weighted against the expense resulting from the added complexity.

3 Architecture

The architectural design of the correlator hard- and software is affected by interrelated aspects which are increasingly less easy to separate from the overall system design. Some optimization on a high level is therefore required. As a separate issue on a high design level, experience with present day instrumentation indicate that build-in flexibility is a matter to be considered seriously from the beginning.

Channelization of the total band vs. highspeed sampling and digitization eg. at the telescopes, is an important aspect to be considered for the hardware design. Channelization yield a robust yet very flexible design. For example, the design results in independently tunable frequency settings and filters per channel. The approach is rather straightforward with minimum design risks and requires the minimum correlation power. The need for many channels will allow a high level of functional integration probably "at the expense" of taking less advantage from the more rapid developments in the digital micro-electronics area including intelligent DSP's. A potential difficulty is the band to band alignment for wideband observations. The requirement for wideband Intermediate Frequencies

are making it attractive that digitization is done at the individual telescopes. This has the immediate implication of the accurate distribution of the sampling clock. Incorporation of the fine-delay is to be considered in that case. This being solved then has the advantage that the signal distribution can be done relatively simple eg. through stable fibre-optic links. In the case of high speed sampling and apart from the required developments to result in reliable sampling and clock distribution schemes, all digital implementations may prove to be very attractive. An assessment has been done in the context of the MMA studies (see Escoffier (1995)).

The matter of sampling relates to the number of levels (1-bit versus multibit) correlation. From the point of view of sensitivity, the sensitivity loss of 57% (i.e. $\pi/2$) for a simpler 1-bit system is most pronounced for spectral observation. In case of a 2-bit system, this loss can already be reduced to a more acceptable level of less than 15%.

Another aspect deals with the interrelation between architectural design and the actual implementation. In actuality this is an interconnectivity matter defining the integration level versus modularity and flexibility.

Other factors related to the detailed design are to be found in the areas of Single-Side-Band versus Double-Side-Band IF-to-baseband conversion i.e. Real vs Complex correlation, the matter of using Fourier Transform techniques prior to correlation or the other way around (ie. XF vs. FX correlators, see Bos (1993)) and the question where and how to perform the delay compensation and fringe rotation to reduce the natural fringes.

With all these factors in mind, the development of a systematic approach at the system design level will prove to be an extremely useful optimization tool.

The supporting software mostly relates to Test and Configuration software the architectural design of which is connected to the hardware architectural design. Matters to be addressed relate to the level of integration, the embedded processing eg. FFT's or other algorithms, control and test software interfaces, the interface to external, off-line software and by the appropriate datahandling. Today's design relies on software engineering approaches using a staged object-oriented design techniques with explicit classes for the user interfaces and the mode of observation (see De Vos (1995)).

4 Technology assessment

The product of the maximum desirable bandwidth times the number of interferometers constituting the array i.e. $B.N(N-1)/2$, serves as a simple complexity measure of the correlator capacity. For the LSA, this product is about 5000 Giga(word) Operations/sec which should be compared with the 19.2 G Oper./sec of the new Westerbork correlator now under construction or the 5.4 G Oper./sec of the VLA correlator. This measure does not take into account the specific bitcorrelation scheme (ie. number of bits), the clockspeed nor the maximum number of real or complex channels given a certain instantaneous (IF)-bandwidth. The approximate correlator capacity for an XF-correlator with

the performance of Table 2, indicates a capacity which is 1-2 orders of magnitude larger than the new correlator back-end presently under construction for Westerbork and the Smithsonian Millimeter Array. To put this in perspective, the actual number of Gigabit operations per second for radioastronomical correlators over the last decades show a 1000 times capacity increase over the last 20 years. The future requirement in say, 2005-2010 is beyond the PetaOperations/Second but close to a straightforward extrapolation of these figures. Not too surprisingly, microelectronics developments in cost, power consumption and the number of transistors per chip ("Moore's Law") show similar developments over these decades. These are positive indications that our aim is ambitious but realistic.

Before making final choices, there are several areas of attention which need to be addressed:

Firstly, high speed A/D-converters are for example being developed for possible use in a new (multibeam) autocorrelator at the JCMT. For interferometry with different requirements, attention should in particular be given to the phase characteristics of these samplers. For its realization, developments in the military domain may be of use combined with a dedicated effort to suit our purpose. High speed sampling also have impact on processing elements after A/D conversion which need to be addressed as well including the engineering consequences. As a rule, it can be expected that sampling at lower speed not only reduces engineering risks due to the lower speeds involved but also of cost. The latter is due to a potentially higher level of integration in less demanding technology as well as a reduction of processing power in proportion to the number of filter channels.

Also, a high level of functional integration is likely to be necessary both for engineering and cost effectiveness. This approach should be balanced by the reduction in flexibility. Areas where integration may be particularly attractive are in the IF- and A/D-channels. The feasibility depends on their number and the required filtering but the design of IC's in these areas is not excluded and should be detailed further. Also, mixed mode designs in which both analog and digital functions are combined on a single IC are, helpful.

Most recent correlator designs already use IC's with some level of customization, i.e. 'customised intelligent' DSPs. These are presently characterized by 100k gates consisting of 1 Million transistors operating at up to 125 MHz clockspeed. Development trends in microelectronics will result in gate array designs 5-10 this size. Recent experience indicate that full custom designs in the all digital functions are probably difficult and should be replaced by gate array designs which industry supports. Low power, low voltage e.g. 2 Volt CMOS electronics both reduce the consumption of power locally while making the engineering challenge appreciable.

The further developments of supporting software and design, test and verification tools, enhance design capabilities and will be extremely helpful to realize the LSA's of modern times.

There are several areas where the role of optics in relation to the correlator, could be advantageous:

- Distribution of digitized "astro" signals from each telescope to the central

control area including clock distribution, depending on the architecture.

- Networks supporting monitoring and control functions.
- Signal(re)distribution inside the correlator.
- Optical processing functions. This is presumably the most speculative domain with a long lead time to actual application. Nevertheless, highly sophisticated functions are available in other applications.

Not mentioned is the use of optical delay lines as a possibility. Although in principal possible, it seems that the use of dynamic storage in small memory buffers in digital logic, is easy and technologically consistent with other aspects of the design and hence is recommended.

Furthermore, it is not too wild a guess that the Object Oriented software technology now in development in the 'on'-line as well as in the 'off'-line packages under development, will have significant impact on the design of the software architectural approach in new correlators. The same applies with respect to an OSI-layered approach in the real time environment. This approach offers many advantages including reliability, supportability and flexibility.

There is a need to formalize and describe the impact of instrumental and atmospheric effects on each astrosignal as it passes through the telescope and other instruments including the correlator. This generic formalism is now being incorporated in the international AIPS++ effort coordinated through the NRAO in the US. Further studies and developments in these areas will prove to be useful to the the LSA effort.

5 Engineering challenges

Apart from the challenge to set up the appropriate level of R&D and to make this a manageable project, technical challenges remain both in the implementation and realization itself. In this context and apart from the cost issue which need to be addressed further, there are constraints related to:

- Structural design matters eg. power management and thermal control and time and clock distribution. Also, the level of integration will put constraints on manageable levels of crosstalk and EMI-shielding needs.
- Reliability and servicability/maintainability
- Monitoring and tests and finally the means and methods ie. the supporting development tools and engineer design methods exercising a system level design view.

6 Conclusions

Correlators for new millimeter arrays require an order of magnitude more processing power than those for existing applications and those under construction. With the results of a properly designed R&D-program partly based on today's collected experience, it seems feasible to design and build such an instrument within the forthcoming decade. Such R&D-program should primarily be aimed

at given insight in the baseline architecture needed for an LSA-correlator, the desired technologies, the development effort and the costing envelope.

References

- Downes, D. (ed) (Oct 1995): *LSA: Large Southern Array Project Report*
Hills, R.T. (1996): (This Workshop)
Escoffier, R. (1995): *A possible MMA correlator design* (Memo to the MMA system design group, May 5, 1995)
Bos, A. (1993): *The EVN/NFRA correlator: design considerations*. (NFRA ITR 202)
Vos, C.M. de (1993): *Towards a Telescope Management System for the WSRT*. (NFRA Report TMS1.v3)

(Note: this paper was reproduced from the original in "Science with Large Millimetre Arrays" (1996, Springer, Berlin; ed. P. Shaver), with the kind permission of Springer-Verlag.)

LSA-Correlator Study: Starting Point for a Dedicated Workprogram

A. van Ardenne, A. Bos

Netherlands Foundation for Research in Astronomy,
P.O. Box 2, 7990 AA Dwingeloo, The Netherlands

1 Research Areas for the Next Generation of mm-Wave Telescopes

There are a number of areas which need further exploration in order to conclude on the architectural and functional design versus cost and timescales of the correlator for the next generation of Large (Sub)millimeter Array of Telescopes.

Figure 1 shows a generic functional diagram of a correlator for a synthesis instrument, serving as a baseline reference in this document. The technical feasibility for the LSA-correlator has been briefly addressed in [1] and it has been made clear that at least the following issues need to be topic of further research:

(I) System Design and Correlator Architectures

Aspects of this study are:

- (a). Present correlation schemes ie. F-X vs X-F and alternative new schemes. Matters to be adressed are complex vs. real correlation, how to implement the delay system.
- (b). Dedicated Wideband (high speed, widechannel, single bit?) correlator versus spectral-line correlator with wideband capability vs. a flexible spectrometer.
- (c). Fringingstopping per antenna or per interferometer
- (d). Other correlation schemes eg. pertaining to multibit schemes to minimize correlation losses for spectral line work and the use of alternative arithmetics (eg. residue arithmetic). Apart from the reduced correlation loss in a multibit scheme may also improve to be beneficial to the calibration capability.

(II) (High Speed) Sampling versus Correlator Architecture

- (a). Hybrid correlator architecture vis a vis wideband sampling. Implications for data processing.
- (b). Sampling at the individual telescopes, rather than at the central control building would impact the architectural and design. See Figure 2 for a schematic functional lay-out possibility in these two cases.

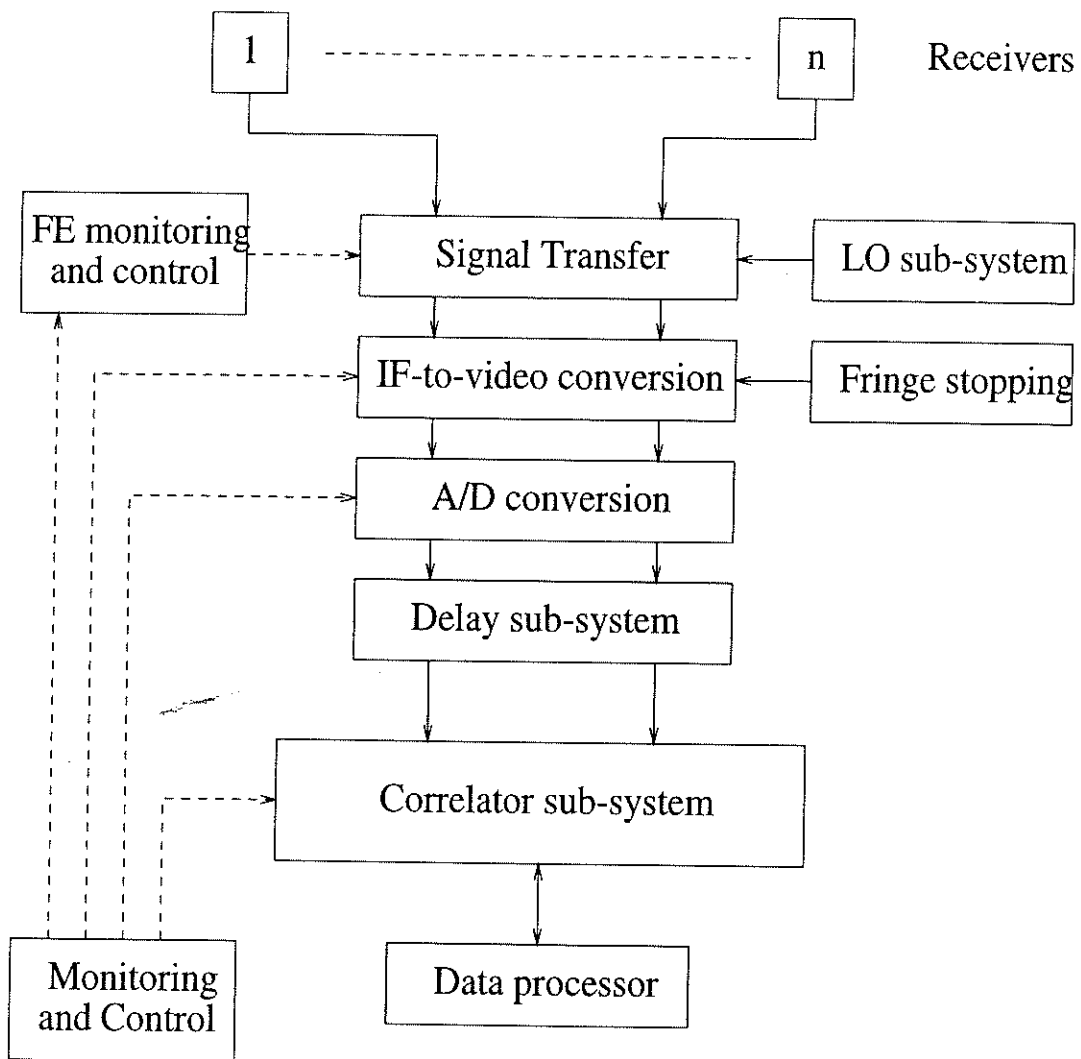


Figure 1: A generic functional diagram of a correlator for a synthesis instrument, serving as a baseline reference in this document.

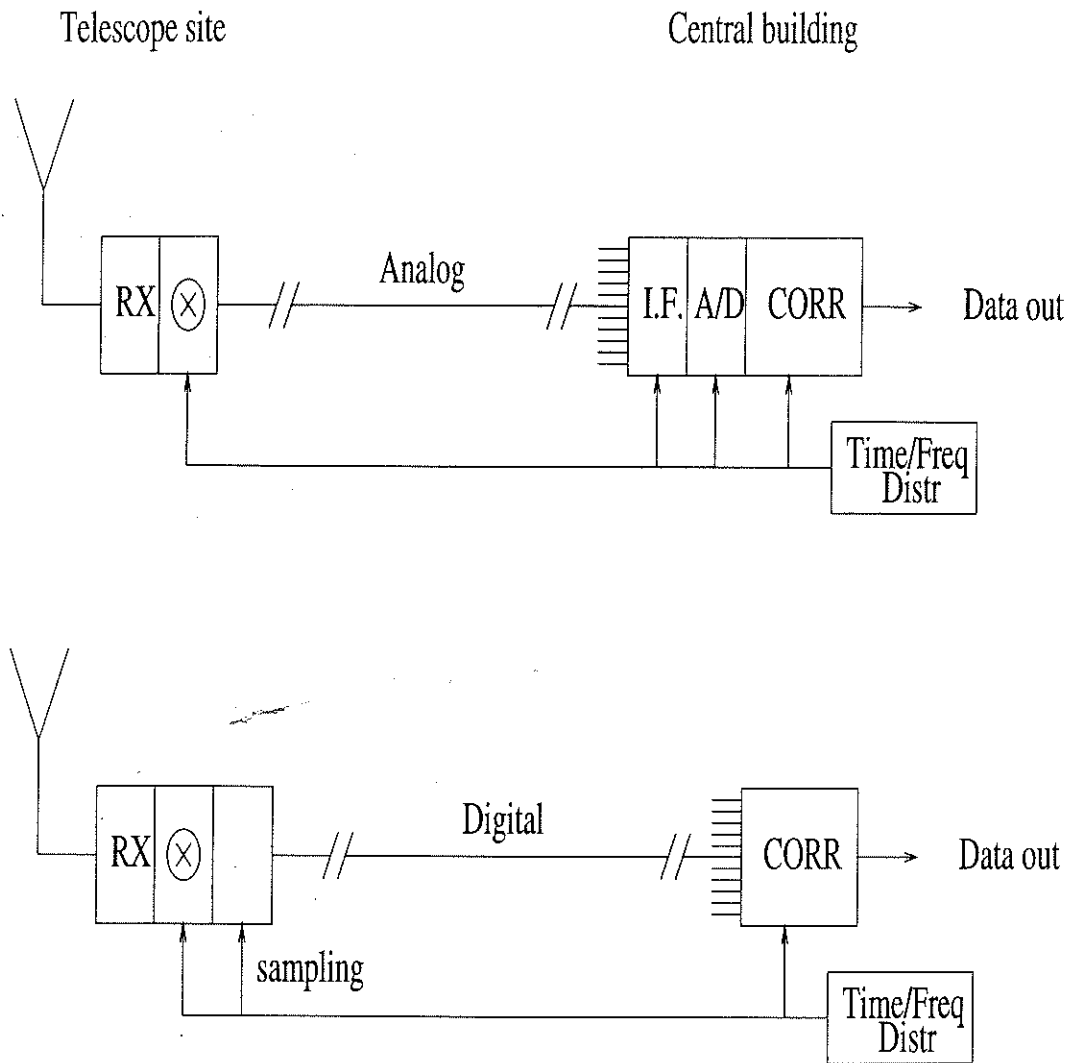


Figure 2: Two schematic functional lay-out possibilities.

! E V Y t 7

A ct

- (c). This study issue together with the choice of analog cables versus digital signal transport versus the role of optical fibers (which also are capable of transporting analog signals), is not a-priori a trivial matter.

(III) Implementation versus Available Technologies

- (a). Analog and digital IC's where, what and how? Present day micro-electronics technologies give excellent potential to functionally integrate with the aim to reduce end-to-end (building) costs and lower maintenance costs.
- (b). Interconnects and the role of optics. The issue at hand is the use of optics in the correlator interconnect and the overall network configuration.

(IV) Other Aspects

- (a). Calibration (eg. system temperatures, atmosphere, polarization) vs. stability
- (b). The number of telescopes per year versus optimal configuration in the building process. This issue will affect the design and implementation of the correlator.

2 Approach

The study can be done along the following sequence of approach ie. study phases:

- (a). Inventory of problem areas and identification and selection of relevant technologies
- (b). Feasibility study of the different possible approaches and the selection of the most appropriate ic. optimal one.

It is estimated that these matters can be addressed fruitfully with the aim to generate first conclusions on realistic implementation schemes and a functional system design by two high level workers under the guidance of (a) senior and acknowledged person(s) given study periods of 2-2.5 years/person.

3 Costs

The forementioned approach will require about 150 kECU/yr and 100 kECU/yr total, on instrumental and development cost including travel and the ability to do actual hard- and software development. The precise amount of salaries is dependent on the calculation method but this envelope cost figure includes an approximate 30% cost overhead.

Salaries:

Workers (2 fte)	90	kECU
Supervision & management (0.3 fte)	25	kECU
Overhead (30%)	35	kECU
Subtotal:	150	kECU

Hard & Software:

Test & Instrumentation set-up	60	kECU
Components etc.	40	kECU
Subtotal:	100	kECU

This estimate needs to be discussed before more detailed conclusions can be drawn on the distribution of the costing per study phase.

4 Target Specifications and Costing Envelope

It is assumed that the target specification from Table 1 in [1] is the starting point for the study with regard to functional performance. A cost envelope of the whole physical-electronics package of order 75 MECU should be taken as a preliminary costing envelope (see [2]).

Assume therefore:

(i) Receivers: Dev. (7 MECU) + Production (50×0.65 MECU)	39.5	MECU
(ii) IF & interconnects: Dev. (2 MECU) + Production (11 MECU)	13	MECU
(iii) Software & mon/control (incl. dev.)	3	MECU
(iv) Correlating backend Dev. (2.5 MECU) + Prod. (10 MECU)	12.5	MECU
(v) Imaging and analysis tools (incl. dev.)	2	MECU
(vi) Contingency	5	MECU
Total:	75	MECU

It is estimated that the costing of item (iv) based on today's technology would require an amount of about 30 MECU. Hence, the challenge is clearly not only on the technical merits with regard to the astronomical application but also on cost reducing issues like functional integration and design for production.

5 Relations to Other Areas

Clearly, the focus areas mentioned above, are closely connected to other areas as they are essentially touching on system design specifications and functional design aspects. Hence, it is recommended that all aspects are viewed from the system level through close contacts to other study elements. For example as the more obvious with the IF-study, the receiver design and the data collection/processing and configuration and control software.

SA:
GE
RN
AY

ort
997

IFRA
object

See figure 3, which depicts the approach of an integrated system design (ie. hard- and software architectural design).

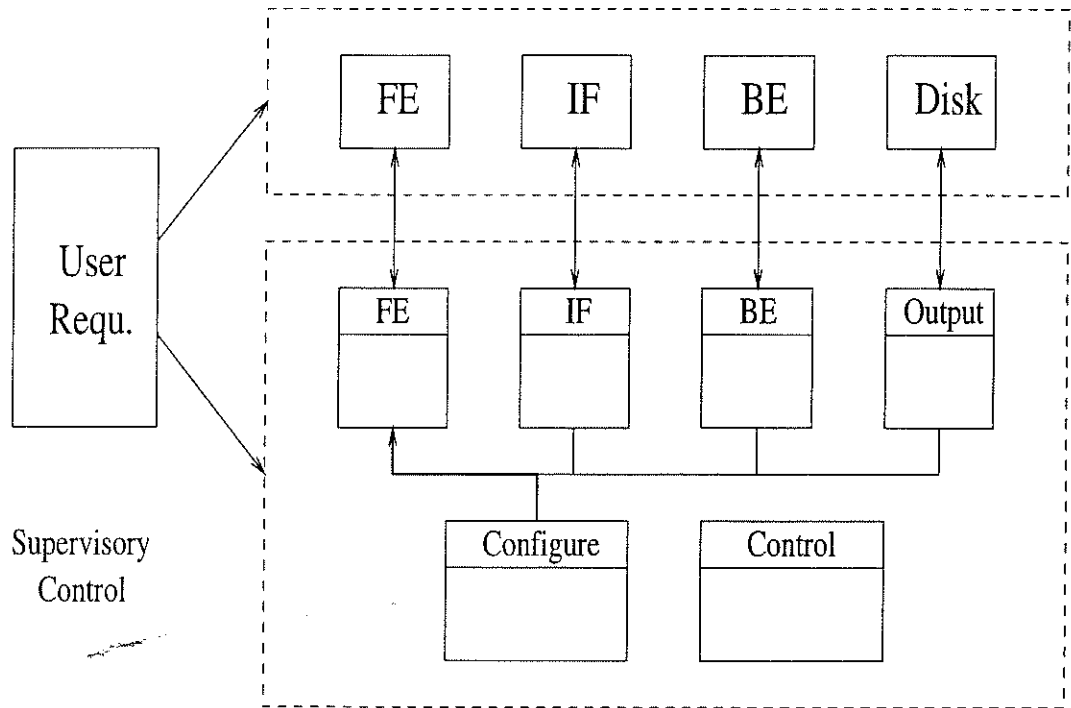


Figure 3: An integrated system design (i.e. hard- and software architectural design).

References

- [1] A. van Ardenne, A. Bos; Correlator Developments for (sub)Millimeter Telescopes in Proc. ESO Astroph. Symp. 1995 (ed. P. Shaver) 395-401
- [2] D. Downes et al.; LSA: Large Southern Array study report, Oct. '95